LBL-14881
UC-28 c.2

Lawrence Berkeley Laboratory
UNIVERSITY OF CALIFORNIA

Accelerator & Fusion Research Division

RECEIVED
LAWRENCE
BERKELEY LABORATORY

MAR 21 1983

LIBRARY AND
DOCUMENTS SECTION

HIGH INTENSITY URANIUM BEAMS FROM THE SUPERHILAC AND THE BEVATRON: FINAL REPORT

Bevalac Staff

March 1982

TWO-WEEK LOAN COPY

This is a Library Circulating Copy which may be borrowed for two weeks. For a personal retention copy, call Tech. Info. Division, Ext. 6782.

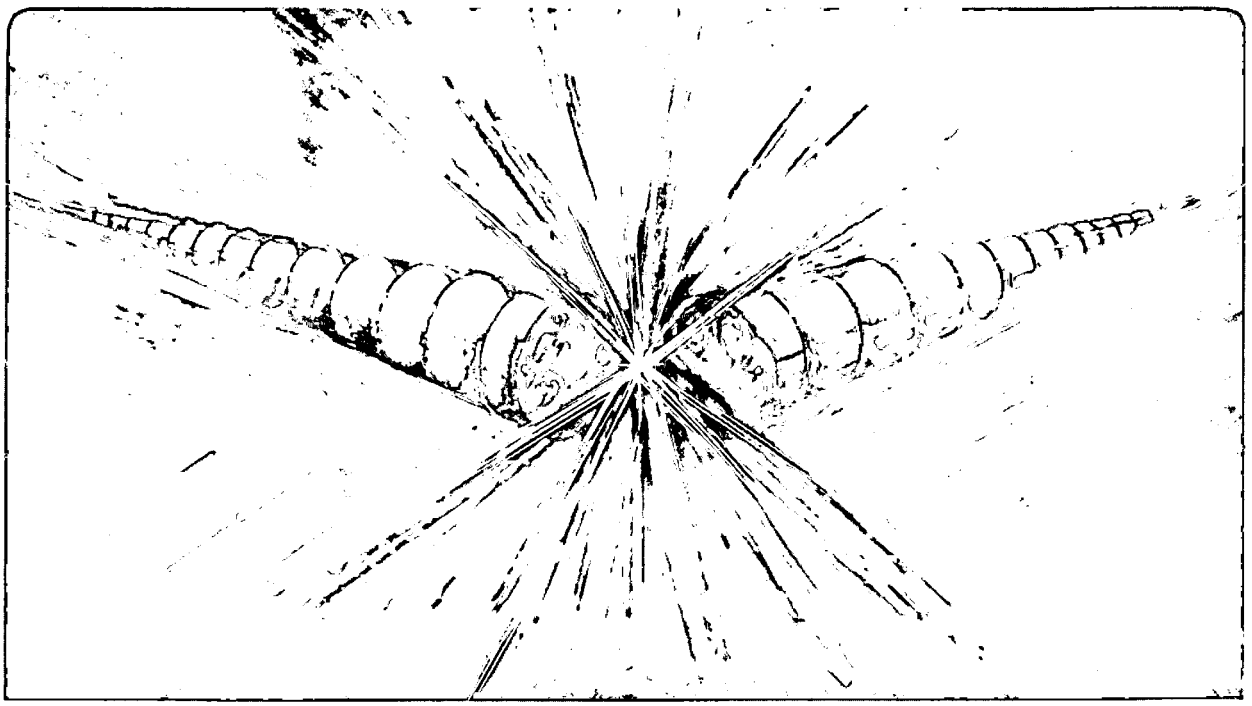

LBL-14881 c.2

Prepared for the U.S. Department of Energy under Contract DE-AC03-76SF00098

DISCLAIMER

This document was prepared as an account of work sponsored by the United States Government. While this document is believed to contain correct information, neither the United States Government nor any agency thereof, nor the Regents of the University of California, nor any of their employees, makes any warranty, express or implied, or assumes any legal responsibility for the accuracy, completeness, or usefulness of any information, apparatus, product, or process disclosed, or represents that its use would not infringe privately owned rights. Reference herein to any specific commercial product, process, or service by its trade name, trademark, manufacturer, or otherwise, does not necessarily constitute or imply its endorsement, recommendation, or favoring by the United States Government or any agency thereof, or the Regents of the University of California. The views and opinions of authors expressed herein do not necessarily state or reflect those of the United States Government or any agency thereof or the Regents of the University of California.

LBL-14881*

High Intensity Uranium Beams

From the SuperHILAC and the Bevatron:

FINAL REPORT†

March 1982

Bevalac Staff
Accelerator and Fusion Research Division
Lawrence Berkeley Laboratory
University of California

*This work was supported by the Director, Office of Energy Research, Office of High Energy and Nuclear Physics, Nuclear Science Division, U.S. Dept. of Energy under Contract No. DE-AC03-76SF00098.

†Preliminary Design Report and Technical Description, PUB-5014 Rev., November 1979.

TABLE OF CONTENTS

		Page
A.	Introduction	1
	A1 History of Project	1
	A2 Project Objectives	1
	A3 Former Capabilities	1
	A4 Performance Specifications with New Capabilities	2
	A5 Special Facilities	2
	A5.1 SuperHILAC High Mass Injector	2
	A5.2 Bevalac Transfer Line	2
	A5.3 Bevatron High Vacuum Improvements	3
	A6 Conventional Facilities	3
	A7 Time Scale	4
B.	SuperHILAC High Mass Injector	5
	B1 General Description	5
	B2 Cockcroft-Walton Pre-Injector	5
	B2.1 Cockcroft-Walton Power Supply	8
	B2.2 Ion Source	10
	B2.3 High Voltage Terminal House	13
	B2.4 Terminal House Utilities	13
	B2.5 Accelerating Column	15
	B3 Injection Beam Line and Isotope Analysis	16
	B3.1 Quadrupole Magnets and Power Supplies	16
	B3.2 Dipole Magnets and Power Supplies	18
	B3.3 Trim Magnets and Power Supplies	20
	B3.4 Buncher	20
	B3.5 Stripper	21
	B3.6 Vacuum System	21
	B4 Low Velocity Linear Accelerator	23
	B4.1 Wideröe Linac Tank	24
	B4.2 Support Stubs and Inner Conductor	26
	B4.3 Drift Tubes	28

Page

B4.4 Drift Tube Quadrupoles and Power Supplies 29
B4.5 Cooling System 34
B4.6 Vacuum System 35
B4.7 rf System 36
B5 SuperHILAC and Control Center Modifications 41
B5.1 Computer/Operator Control 43
B5.1.1 DMM 43
B5.1.2 Operator Console 46
B5.1.3 Portable Console 51
B5.1.4 System Status 51
B5.2 Instrumentation, Controls, and Interlocks 51

C. SuperHILAC Building Additions 52
C1 Introduction 52
C2 Scope 52
C2.1 Architectural 52
C2.2 Structural 53
C2.3 Required Mechanical Utilities 53
C2.4 Heating and Cooling 53
C2.5 Fire Sprinklers 54
C2.6 Electrical 54

D. Bevalac Transfer Line 55
D1 Magnets 55
D2 Power Supplies and Instrumentation 56

E. Bevatron Vacuum Improvement 58
E1 Vacuum Goal 58
E2 Design Approach 60
E3 System Description 62
E3.1 Quadrant Modifications 62
E3.1.1 Quadrant Liners 62
E3.1.2 Quadrant Installation 72

Page

E3.2 Beam Instrumentation 73
E3.2.1 Beam Induction Probes 73
E3.2.2 Finger Probes 75
E3.2.3 Vertical Clippers 75
E3.2.4 Inflector Cup 77
E3.2.5 Back Cup 77
E3.2.6 Multi-wire Chambers 78
E3.2.7 Fixed Scrapers 78
E3.2.8 Beam Electronics and Control 79
E3.3 Tangent Tank Modifications 80
E3.3.1 East Tangent Modifications 80
E3.3.2 South Tangent Modifications 82
E3.3.3 West Tangent Modifications 85
E3.3.4 North Tangent Modifications 88
E3.3.5 Tangent Installation 90
E3.4 Vacuum Pumping and Cryogenics 90
E3.4.1 Tangent Cryopump 91
E3.4.2 Injection Cryotrap 96
E3.4.3 Auxiliary Pumping 96
E3.4.4 Distribution Boxes 98
E3.4.5 Helium Refrigeration 99
E3.4.6 Cryogenic Transfer Lines 99
E3.4.7 Vacuum/Cryo Electronics and Controls 99
E3.4.8 Vacuum/Cryo Installation 100
E3.5 Injection 100
E3.5.1 BL18MH (1HM7) Inflection Magnet 100
E3.5.2 Electrostatic Inflector 101
E3.6 Extraction 102
E3.6.1 Perturbation/Spiller Magnet 102
E3.6.2 Perturbation/Spiller Magnet Support 105
E3.6.3 M1 Extraction Septum Magnet 106
E3.6.4 M1 Extraction Septum Magnet Support 107
E3.6.5 M2 Extraction Septum Magnet 108
E3.6.6 M2 Extraction Septum Magnet Support 108

Page

E4 Calculated System Performance 110

E4.1 Estimated Cryogenic Performance 110

E4.2 Estimated Vacuum Performance 112

E4.3 Ion Beam Considerations 112

E4.3.1 Primary-Ion Gas Desorption 112

E4.3.2 Secondary-Ion Gas Desorption 115

E5 Initial Performance Results 115

E5.1 Vacuum Results 115

E5.2 Cryogenic Results 116

E5.3 Ion Beam Results 116

E5.4 Conclusions 117

ILLUSTRATION INDEX

Figure	Description	Page
B-1	Elevation view of SuperHILAC injector area	6
B-2	Plan view of SuperHILAC injector area	6
B-3	Cockcroft-Walton rectifier	9
B-4	Generating voltmeter	9
B-5a	Cockcroft-Walton front view	11
B-5b	Cockcroft-Walton rear view showing spark gaps	11
B-6	Elevation view of ABEL source, closed position	14
B-7	Source shown in open position	14
B-8	Accelerating column	17
B-9	Charge state distribution for ^{208}Pb ions	22
B-10	Wideröe linac	25
B-11	Drift tube quadrupole magnet	32
B-12	Drift tube installation	33
B-13	Block diagram of rf system with instrumentation	37
B-14	Main rf amplifier block diagram	38
B-15	Wideröe accelerator and final rf amplifier	39
B-16	Frequency regulator block diagram	40
B-17	Schematic of system architecture	42
B-18	Schematic of DMM configuration	44
B-19	Operator console	45
B-20	Closeup of touch panel CRT	47
B-21	Schematic of video mixing of analog signals	48
B-22	Closeup view of graphics display	49
B-23	Portable console being used in Cockcroft-Walton terminal	50
D-1	Schematic of Bevalac transfer line	57

Figure	Description	Page
E-1	Graph of beam survival versus pressure	59
E-2	New liner within old vacuum chamber	61
E-3	Quadrant cross section	63
E-4	Enlarged quadrant cross section	63
E-5	Liner model	64
E-6	Quadrant liner details	64
E-7	Circuit board etched pattern	65
E-8	Quadrant liner assembly check	67
E-9	Quadrant liner ID numbers	68
E-10	Quadrant module 21	69
E-11	Module 35 longitudinal section	70
E-12	Beam instrumentation map	74
E-13	Finger probe assembly	76
E-14	East tangent region	81
E-15	Tangent liner ceiling hatch cross section	83
E-16	South tangent region	84
E-17	West tangent region	86
E-18	North tangent region	89
E-19	Elementary cryogenic circuits	92
E-20	Helium cryogenic system schematic	93
E-21	Liquid nitrogen cryogenic system schematic	94
E-22	Chevron diagram for tangent cryopumps	95
E-23	Perturbation/spiller magnet cross section	104
E-24	M1 septum magnet shaft cryogenic seal	108

A. INTRODUCTION

A1 HISTORY OF THE PROJECT

LBL has been the leader in the production of relativistic heavy ion beams. In 1971 nitrogen ions were successfully accelerated in the Bevatron. With the completion of the transfer line linking the SuperHILAC and the Bevatron, the Bevalac Heavy Ion Facility became operational in the summer of 1974. Since then, the Bevalac has forged into totally new physical realms by producing high energy beams of carbon, oxygen, nitrogen, neon, argon, and most recently, iron. At the same time, complete computer control has been achieved at the Super-HILAC, making it possible to accelerate two distinct ion beams, with one as heavy as lead, and to time share them not only among SuperHILAC users but also with the Bevalac. The result is that important scientific research programs--which range from nuclear physics and nuclear chemistry to biomedical studies and cosmic ray research--can proceed simultaneously at the SuperHILAC and the Bevalac, which are both operated as National Research Facilities.

A2 PROJECT OBJECTIVES

Experimental results with relativistic heavy ion beams have spurred world-wide interest in studying interactions with even higher mass beams at energies from several MeV to a few GeV per amu. The modifications entailed in this project, consisting of a new injector for the SuperHILAC, an upgraded transfer line to the Bevalac, and an ultra high vacuum at the Bevatron, present a unique opportunity for achieving both relativistic beams of all mass numbers and high intensity, intermediate energy beams between 35 and 200 MeV/amu.

A3 FORMER CAPABILITIES

The SuperHILAC formerly accelerated ions up to mass 208 (lead) to a maximum energy of 8.5 MeV/amu, but with low intensity (2 particle nanoamperes) at this upper end of its capability. Higher intensity beams (2 particle microamperes) were delivered at mass 40 and below.

The Bevalac's former capability extended to mass 56 ions (iron) at energies up to 2.1 GeV/amu. Intensities ranged from 5×10^9 particles per second (2×10^{10} particles per pulse) for carbon ion beams, to 1×10^5 particles per pulse for iron beams.

A4 PERFORMANCE SPECIFICATIONS WITH NEW CAPABILITIES

With the modifications of this project completed, the SuperHILAC can accelerate all ions through uranium with intensities increased by a factor of 100 for the heavier ions. The Bevalac can utilize these SuperHILAC beams, and accelerate them to the maximum Bevatron operating field which, in the case of uranium, will yield beams of 1.0 GeV/amu with intensities as high as 10^8 particles per second. Lighter ions will have maximum energies up to 2.1 GeV/amu and intensities constrained only by the space charge limit of the machine.

A5 SPECIAL FACILITIES

Improvements in three areas were required to accomplish these three goals.

A5.1 SuperHILAC High Mass Injector

A pre-accelerator, Wideröe linac, and beam transport lines were the principal elements of the new (third) injector. The pre-accelerator featured an air-insulated Cockcroft-Walton power supply to facilitate quick ion source changes. The Wideröe linac accelerates the low velocity, low charge state, very heavy ions for acceptance into the SuperHILAC. A gas vapor stripper at the exit of the Wideröe strips ions to the charge state required by the SuperHILAC. Complete time sharing of three beams can be accomplished readily with the existing computer control system and the addition of the third operator control station in the control room.

A5.2 Bevalac Transfer Line

To accommodate the heaviest full-energy exit-stripped particles produced by the SuperHILAC, the existing transfer line was upgraded and the last dipole magnet in the transfer line was replaced. In addition, the inflector magnet,

IHM7, was modified for high vacuum compatibility as described in the next sections.

A5.3 Bevatron High Vacuum Improvements

The Bevatron's initial vacuum of 10^{-7} Torr was to be improved to an ultra-high vacuum of 10^{-10} Torr to permit acceleration of very heavy ions in a variety of charge states while minimizing loss of ions due to charge-exchange interactions with residual gas atoms. A completely new, cryogenically-cooled liner (cold bore) was built and installed within the entire circumference of the Bevatron. In the quadrant (curved) sections, the vacuum chamber consisted of a progressively-cooled triple-walled box of copper-clad printed circuit board material, NEMA G-10. The outer box rests in the existing Bevatron vacuum of $\sim 10^{-7}$ Torr, the second box is cooled to liquid nitrogen (LN) temperature (77°K), and the innermost surface is cooled by helium to 12°K. The three layers are separated by superinsulation. The superiority of this design arises from its enormous pumping speed--the walls of the inner chambers all act as pumps--and the fact that in the lowest temperature chamber, where beam is circulating, there is almost no outgassing.

The liners of the tangent tanks are cooled to LN temperature both to improve pumping speeds and reduce gas load, and to minimize radiative heating of the 12°K helium-cooled box in the curved tanks.

The rf accelerating electrode, the internal beam instrumentation, and the inflection magnet system were all rebuilt to be compatible with the ultra-high vacuum.

A6 CONVENTIONAL FACILITIES

The new conventional facilities needed for the project were minimal. About 1700 square feet of space was needed at the SuperHILAC for the Cockcroft-Walton injector enclosure, the beam transport lines, and the power supplies. These areas are primarily concrete and steel structures. The conventional facilities also include additional power and cooling water distribution for the equipment, and associated heating, lighting, and fire protection systems.

A7 TIME SCALE

Construction time for this project was approximately 30 months.

B. SUPERHILAC HIGH MASS INJECTOR

B1 GENERAL DESCRIPTION

The two injectors formerly used at the SuperHILAC were a 750-kV air-insulated Cockcroft-Walton (EVE) and a 2.5-MV pressurized HV multiplier (ADAM). The EVE injector can deliver adequate intensities of ions up to mass 40 (argon). The ADAM injector can accelerate ions with lower charge-to-mass ratios, and they can produce beams of heavier ions. The intensity of these beams decreases as the mass number increases, with the lowest practical intensity being achieved with lead beams.

Experience with the two existing injectors provided substantial help in defining the general requirements for a new injector which would provide ample beams above mass 40. The requirements for acceptance by the first tank of the SuperHILAC are a particle velocity $\beta = 0.0154$ (corresponding to an energy of 113 keV/amu) and a charge-to-mass ratio of 0.046 or larger. Present ion source performance dictates an air-insulated Cockcroft-Walton as a pre-accelerator because of its easy accessibility and its good overall reliability. The low charge state ions then receive further acceleration and, if necessary, subsequent stripping to the required charge state before injection into the SuperHILAC. A low-beta linac of the Wideröe type has been built to perform this acceleration. The injector system described in the following sections, and summarized in the table below, consists of a Cockcroft-Walton pre-injector, injection beam lines and isotope analysis, a low-velocity linear accelerator, and SuperHILAC control center modifications (see Figs. B-1 and B-2).

B2 COCKCROFT-WALTON PRE-INJECTOR

The pre-injector portion of the new injector facility consists of a Cockcroft-Walton (C-W) high voltage power supply, the ion source, the high voltage terminal, and the accelerating column.

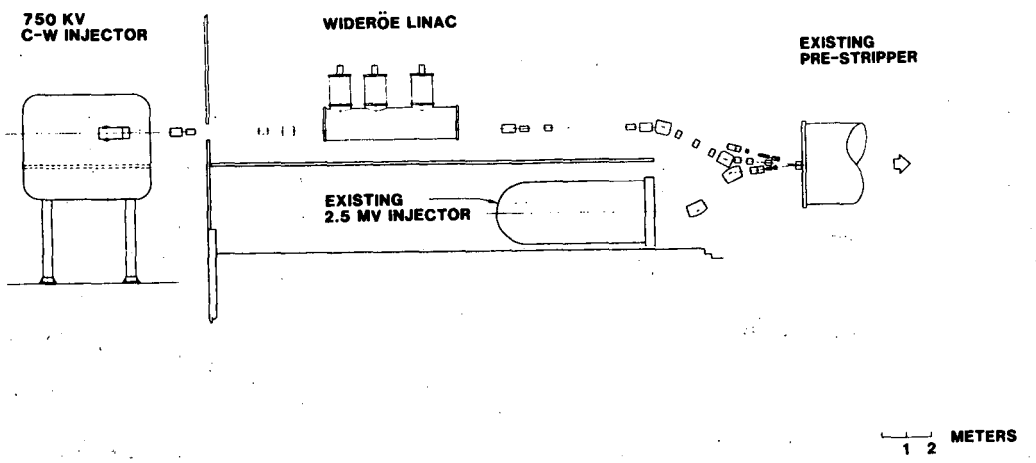

Figure B-1. Elevation view of SuperHILAC injector area (XBL 7910-12105A).

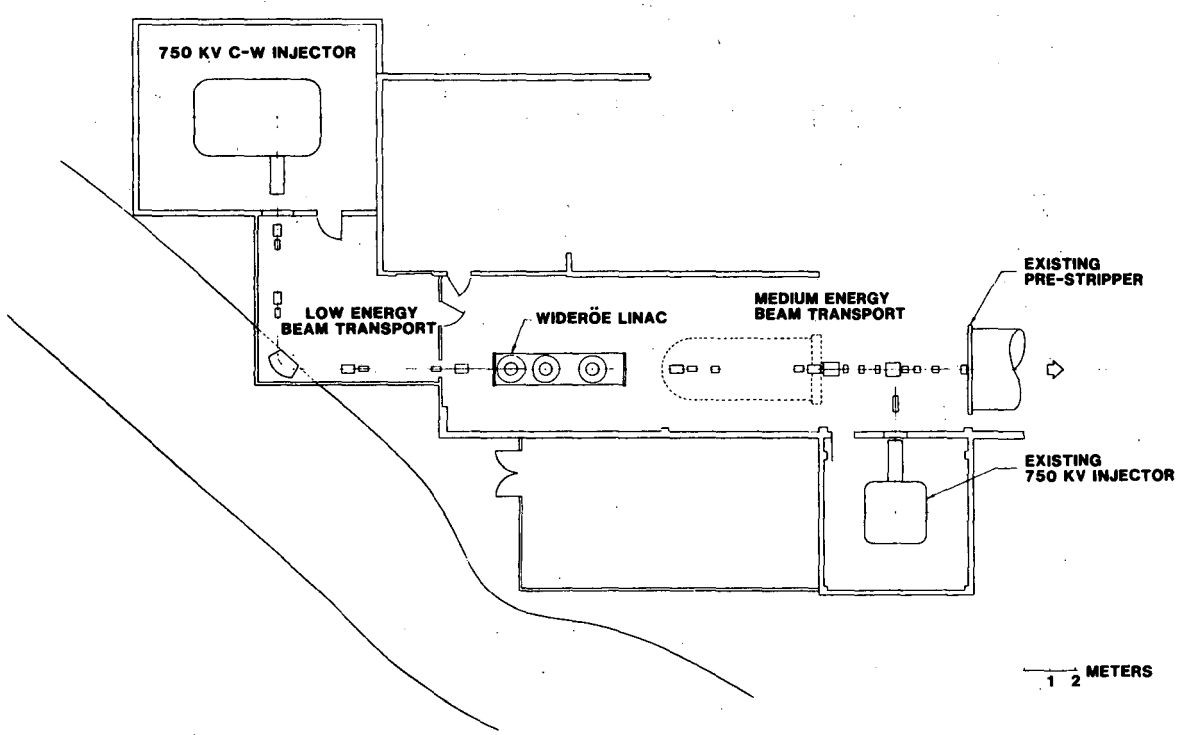

Figure B-2. Plan view of SuperHILAC injector area (XBL 7910-12105A).

TABLE B-1: PARAMETERS OF THIRD INJECTOR

Cockcroft-Walton Pre-Accelerator:	
Terminal voltage, $^{238}U^{5+}$	750 kV
Peak current	15 mA
Regulation	1×10^{-3}
Power available, terminal	100 kVA
Terminal volume	60 m^3
Ion Source:	
Type	Radial Extraction PIG
^{238}U charge state	5+
^{238}U flux	4 mA peak (5+)
Extractor voltage	30 kV
Duty factor	33 percent
Wideröe Structure:	
Length	5.17 m
Input energy	15.8 keV/amu
Output energy	113 keV/amu
rf power requirement	100 kW peak rf
Stripper:	
Type	Fluorocarbon vapor
Efficiency	12 percent for U^{11+}
SuperHILAC Output:	
U^{40+}	2 particle μA peak

B2.1 Cockcroft-Walton Power Supply

The high voltage power supply for the pre-accelerator is a half-wave cascade voltage multiplier. The recently installed Cockcroft-Walton power supply under the EVE injector terminal served as a prototype for the device which was constructed for the SuperHILAC third injector.

The power supply consists of ten decks and is driven by an air core transformer at the bottom of the power supply stack. Except for monitoring circuits, all associated electronics are located outside the high voltage enclosure.

The voltage required from the (C-W) power supply to accelerate $^{238}U^{5+}$ is 750 kV. This voltage can be achieved by the EVE C-W with some difficulty. By increasing the distance between power supply components, enlarging the radius of curved surfaces, and adding one more deck, 750 kV is reliably achieved by the new power supply.

The four legs that support the C-W components are composed of sections of solid PVC rod 13 cm in diameter. Between each rod is an aluminum ring 20 cm in diameter and 5 cm thick. The vertical separation between each ring is 23 cm, yielding a maximum operating gradient of 4 kV/cm along the surface of the plastic.

The rectifier modules are connected to the rings with 7.6-cm diameter balls. Rods connected to the rings support the capacitors. Stainless steel solution bowls were fitted over the capacitor connections to shield the mounting apparatus. The capacitor damping resistors are connected to the rings with balls also. The resistors limit capacitor current during a spark-down.

A spark gap assembly stands in the middle of the C-W stack. Spark gap electrodes are arranged so that each rectifier module is protected by a horizontal gap, and each capacitor/resistor network is shunted by a vertical gap. The gaps are set to spark at 100 kV.

To safely ground the C-W and short each capacitor, four grounding bars pivoted at the C-W base are attached to each capacitor connecting rod.

There are 20 rectifier modules in the C-W. Each module is composed of 25 10-kV silicon rectifiers, type CLR10. The rectifiers are wound in a helix over a plastic mandrel and terminated on each end with 50-ohm ceramic power

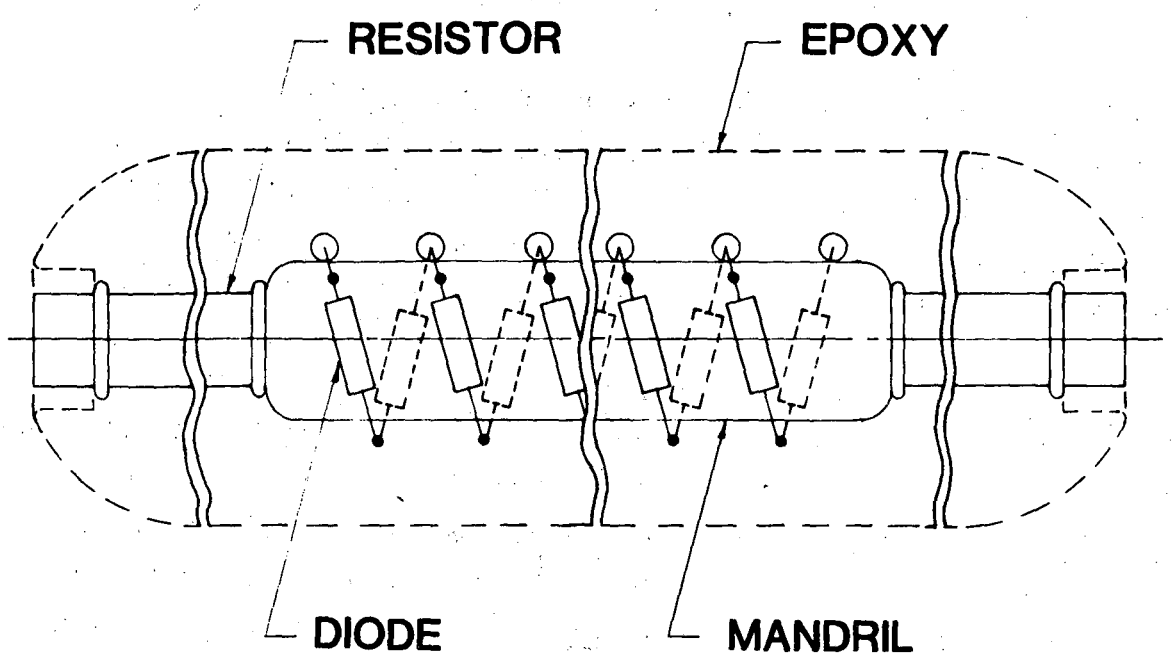

Figure B-3. Cockcroft-Walton rectifier (XBL 813-8400).

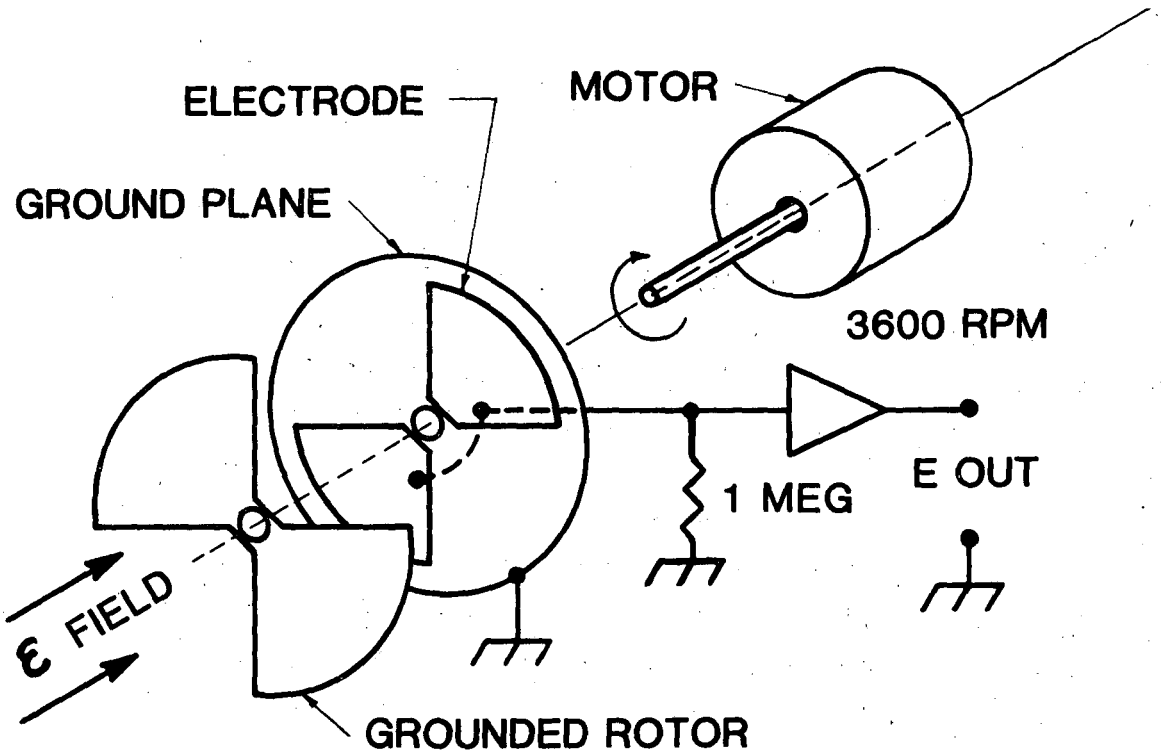

Figure B-4. Generating voltmeter (XBL 813-8401).

resistors. The resistor-rectifier assembly is cast in a dense, thermally-conductive epoxy (Fig. B-3).

Two generating voltmeters (GVM) mounted in a wall of the pre-injector enclosure measure the voltage gradient between the high voltage terminal and the wall. One GVM is used for high voltage monitoring. The other provides feedback for voltage regulation in the DC to 50 Hz bandwidth. A capacitive pickoff plate mounted near the GVM's is used for higher frequency feedback signals.

A GVM consists of a 3600-RPM split-phase small motor, a 20-cm diameter printed circuit board, a two-blade aluminum rotor, and a 1-Megohm load resistor (Fig. B-4). The printed circuit board is etched in the shape of the rotor to yield two isolated electrodes, which are connected to the resistor, while the remainder of the board is a ground plane. The rotor is positioned close to the board so as to periodically cover the electrode. The motor shaft is grounded by a brush assembly. At a gradient of 5 kV/cm, this GVM yields about 10 μa peak to peak. The GVM's are placed in a corona-free area away from the pre-injector accelerating column.

The Cockcroft-Walton power supply assembly is shown as installed in two views (Fig. B-5).

B2.2 Ion Source

There is provision for two ion sources of different types in the Super-HILAC third injector. They will not be operated simultaneously. Both sources use a common analyzing magnet and extractor power supply. Additional specialized equipment is associated with each source.

A Pasyuk source will be used mainly for the production of solid-material ion beams, but also for gaseous ions. It will operate reliably from 10-percent to at least 30-percent duty factor. The design of this source originates from the UNILAC version of the Pasyuk Penning source now in use at GSI. This basic source is often called a PIG source, since it was originally developed from the Penning Ionization Gauge (Penning, 1937). In this case, ions are extracted from a radial slit in the anode. The anode bore is long, and is fully immersed in a uniform longitudinal magnetic field.

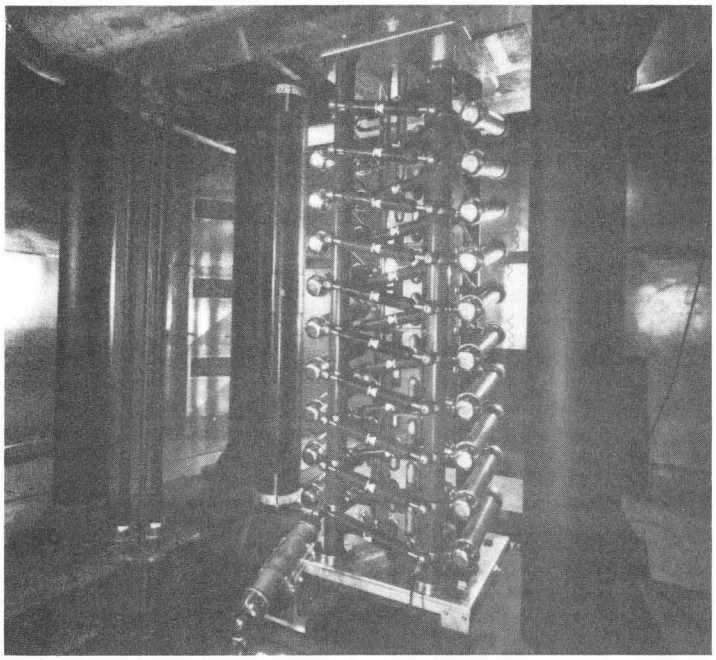

Figure B-5a. Cockcroft-Walton front view (CBB 811-856).

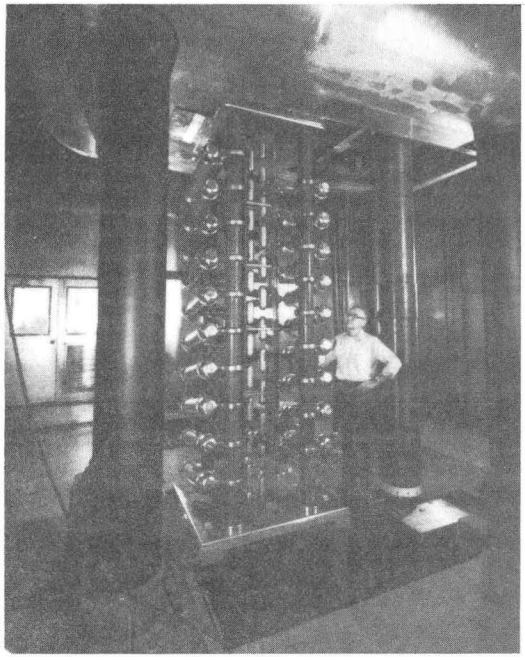

Figure B-5b. Cockcroft-Walton rear view showing spark gaps (CBB 811-854).

The arc supply is pulsed and rated at 10 A with an output voltage of 2 kV. Additional supplies for filament heating (80 amps, 6 V), electron heating (2 A, 1500 V), and sputtering (2 A pulsed, 1000 V) are utilized during normal operation. The extraction supply and magnet will be discussed below.

Solid-metal ion production is most efficient when the vapor pressure of the material and the operating temperature of the source are such as to support a vapor pressure in the sub-micron range. The best performance to date is with gold. Nearly 1 pmA of Au^{5+} has been demonstrated with an acceptable normalized emittance of .05 cm-mrad. Other elements have also been used with comparable beam intensities.

The analyzing magnet for the source bends the beam ~135° in order to eliminate unwanted and very intense beams of lower charge state ions. The magnet gap is 17.7 cm and the design field level is 6 kG. The magnet is approximately one cubic meter in volume, weighs four tons, and dissipates 20 kW. A well-regulated supply is used (~350 amperes, 5×10^{-4} regulation). Magnetic quadrupoles and steering magnets were also installed in the transport section between the analyzing magnet and the column entrance.

The extractor supply is used for elevating source and power supplies above terminal ground. It has 30-kV capability, 75-mA average (250-mA peak) current, with a stability of 5×10^{-4} or better over a 7-ms pulse length. Regulation recovery time is less than 10 μs with a 100-ms interrupt period (adjustable) following a load short. The supply can be pulsed at 36 pps.

Vacuum is provided by two 1-W CTI-72 cryopumps under each of the two beam lines, and a 10-W CTI-1020 pump with cup valve located near the PIG ion beam center of radius. Pumping speeds of 1500 liter/sec with air were measured. A typical operating pressure of 10 μTorr is recorded with xenon, the most frequently used support gas.

The following power distribution is typical for ion source equipment in the high voltage terminal:

Magnet	20 kW
Source	20 kW
Extractor	5 kW
Quadrupoles	10 kW
Electronics	2 kW
Vacuum	8 kW
	65 kW

The ion source is shown in Figs. B-6 and B-7.

B2.3 High Voltage Terminal House

The high voltage terminal house was designed for routine operation at 750 kV. By selecting clearances of 2.1-m minimum dimension from the terminal house to the ground walls, using 3.3-m-long graded column support legs, and rounding the corners of the terminal house to a 0.6-m radius, this design voltage is achievable using ambient air as the insulating gas. The overall terminal dimensions are 3-m by 5-m by 4-m high. The metal skin is aluminum sheet stretched over a steel skeleton framework. The house is divided by an intermediate deck separating the source, power supplies, electronics, and the easily accessible upper area from a utilities basement area that is about 1.4-m high. This lower area houses the large mechanical equipment, heavy alternators, and generators, power distribution equipment, large transformers, and other large components requiring infrequent service.

The terminal house and support structure are designed for a total load of 16,000 kg. There are four 35-cm OD vertical support columns (legs) made of filament-wound fiberglass-epoxy tubes with a 1.25-cm wall thickness. The legs are 3.3 m long, and are individually graded with a resistive coating to provide a current drain per column of about 1 to 10 μA with 750 kV on the terminal.

An elevator work platform was installed to provide convenient access and work space around all sides of the high voltage terminal house. The platform is designed to carry a 1,500-kg load and has a lift speed of 2.5 m/minute. It spans the 2.1-m space between the terminal house and ground plane walls, and forms the lower floor ground plane when it is retracted to its lowered position for high voltage operation.

B2.4 Terminal House Utilities

Power requirements for the terminal house power supplies (ion source, quadrupole, bending magnet, etc.) are mentioned in Section B2.2.

Power is supplied to the terminal by an insulated vertical drive shaft consisting of a 35-cm OD filament-wound epoxy tube with a 1.25-cm wall thickness. A 200-hp, 1800-rpm motor is located in a pit in the floor beneath the terminal house, and the drive shaft transmits the power to two generators in the high

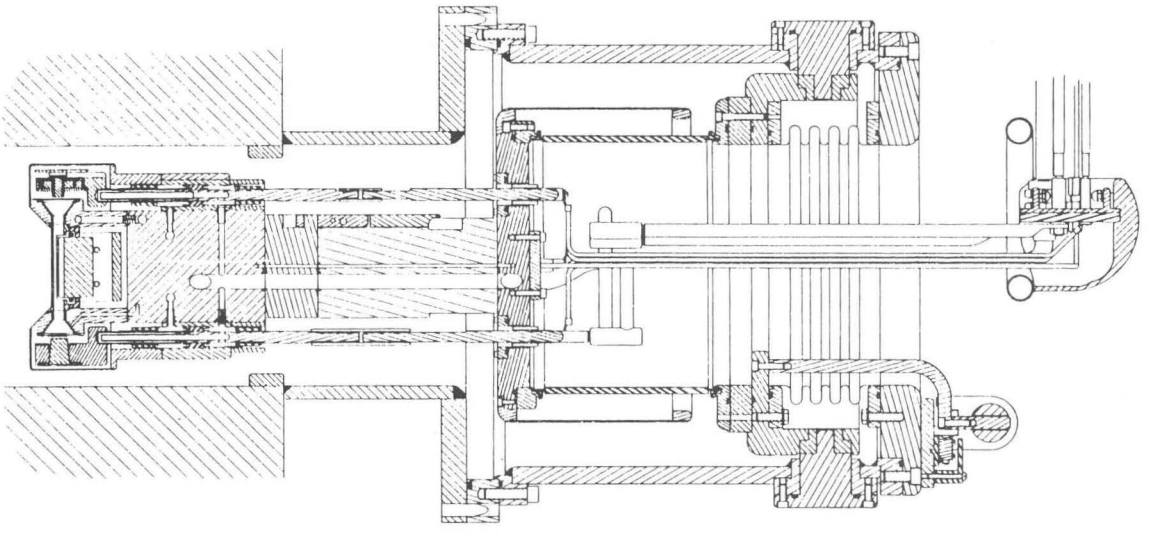

Figure B-6. Elevation view of ABEL source, closed position (XBL 812-166).

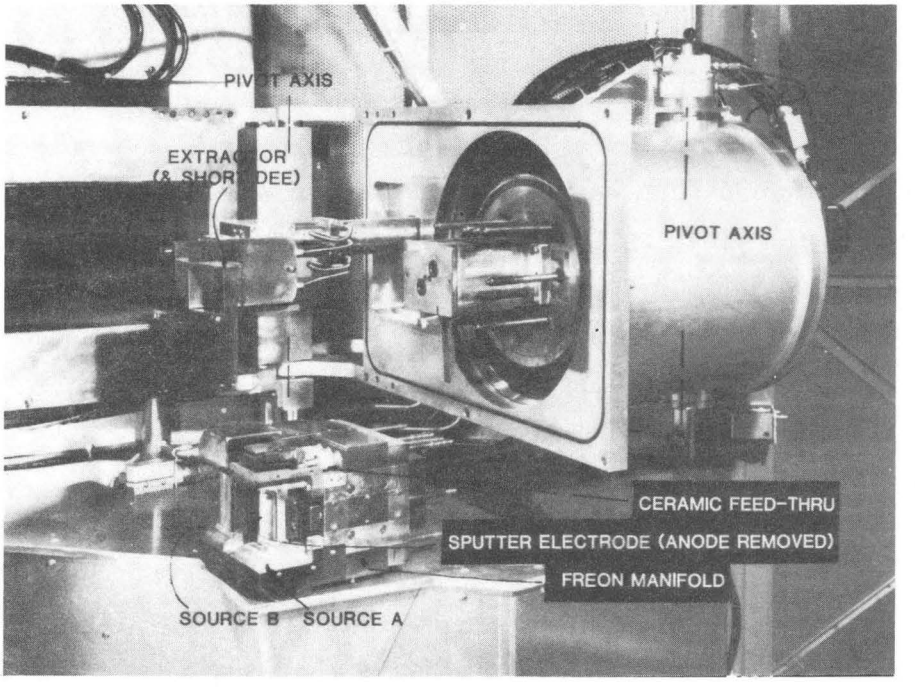

Figure B-7. Source shown in open position. The dual head assembly is shown with one gas cap removed (XBB 811-884A).

voltage terminal (a 60-Hz generator, rated at 75 kVA, and a 400-Hz unit, rated at 25 kVA). Both the motor and the two generators have vertical axes.

The cooling system was patterned after the unit in our present injector. Freon-113 is used as an insulating coolant, and it pumped from ground potential to high voltage through 6-cm diameter insulating plastic tubes (Teflon). The pump, storage tank, heat exchanger, controls, etc., are all located outside the injector enclosure for convenient access. Flow rates of 30 to 40 gpm with a pressure differential of 40 to 50 psi have been adequate for all terminal house cooling needs.

The vacuum systems for the ion source chamber magnet and accelerating column utilize cryogenic pumping. Mechanical roughing pumps required for the system are located in the house basement utility area.

B2.5 Accelerating Column

Ions leaving the source are charge-state analyzed by the source magnet and are then accelerated by the high-voltage column. The accelerating potential is provided by the Cockcroft-Walton power supply normally operated in the 500 to 750 kV range. The accelerating column assembly consists of three high-voltage accelerating modules, a plastic shroud to contain an insulating gas, and the various support assemblies.

The accelerating modules are a commercial product, a special design by NEC also used in the ADAM injector. Three of these modules are stacked together with 4-cm spacers between each of the three sections. Each of the spacers contains a 4-cm diameter aperture whose purpose is to reduce electron and ion backstreaming. This spacer was made of a refractory material to prevent damage from beam misalignment. The column modules were graded by a chain of resistors with a current drain of 1 mA at 750 kV. The voltage difference between each ring is set by the resistor string. At the ends of the module assembly, an additional guard ring was used to reduce the external electric field to a safe value.

To hold 750 kV across three modules, the column assembly must be contained in a SF_6 atmosphere at ambient pressure. The SF_6 is contained within a clear plastic shroud, 1 m square and 2.1 m long, the terminal-to-wall spacing. Each side wall of the shroud is completely removable to allow full access to the

accelerating modules. The shroud is SF_6-tight, with a cooled, filtered recirculation system to remove heat.

The three accelerating modules are held under compression within the shroud between two spun-aluminum nose cones and a compression bellows. No additional support struts or electrical conductors are present in the SF_6 region. Evacuated pipes transport the beam to and from the column. The entrance beam line is 8 cm in diameter. The exit beam line is 8 cm in diameter and has a magnetic quadrupole doublet located 1 m downstream of the column exit. The installed column is shown in Fig. B-8.

B3 INJECTION BEAM LINE AND ISOTOPE ANALYSIS

The injection beam line consists of two sections. The first section provides transport between the Cockcroft-Walton pre-injector and the Wideröe linac, and provides for complete isotope separation by magnetic analysis. This line is comprised of four sets of quadrupole doublets, horizontal and vertical steering magnet pairs, a 90° analyzing magnet, various beam probes and instrumentation, and a buncher. The second transport section joins the Wideroe and SuperHILAC pre-stripper linacs, and is comprised of quadrupole doublets and singlets, trim magnets, vertical bending magnets, and a fluorocarbon vapor stripper.

B3.1 Quadrupole Magnets and Power Supplies

A total of six sets of quadrupole doublets and six singlets (eighteen magnets) are used in the beam transport lines. Four sets of doublets are used in the low-energy section to match the ion beam from the pre-accelerator to the Wideröe linac, and two doublets and six singlets are used in the medium-energy line from the Wideroe to the pre-stripper. Fifteen quadrupole elements were the same design as those units already in use throughout the SuperHILAC. These quadrupoles are compact, high gradient magnets that have been very efficient and reliable in service. The design parameters are listed below for each element:

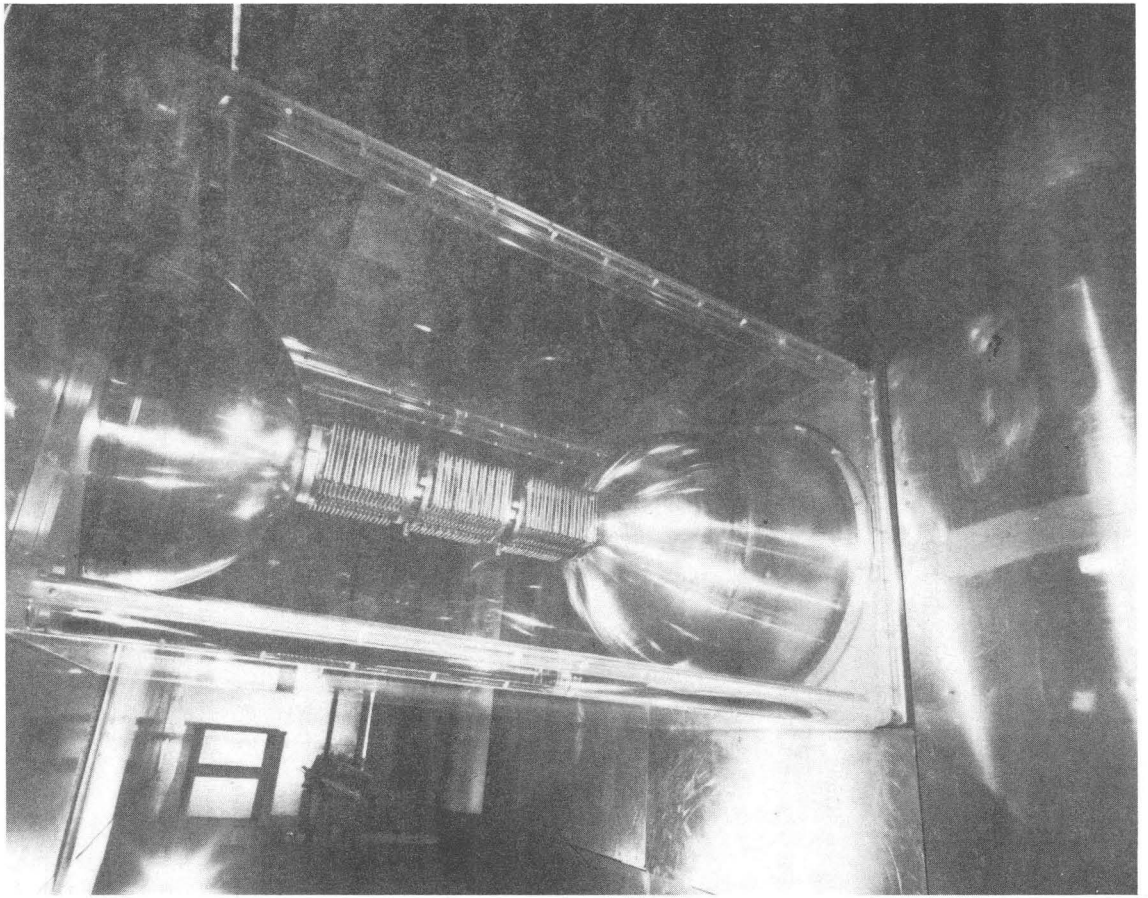

Figure B-8. Accelerating column (CBB 814-3094).

Magnet Bore, ID:	6.3 cm
Magnet OD:	30 cm
Pole Length:	15 cm
Overall Length:	23 cm
$B'L_{eff}$:	42 kG
Current:	225 A
Voltage:	20 V
Power:	4.5 kW
Cooling:	2 gpm (water)

There were three special quadrupoles used as singlets at the entrance to the prestripper linac. These are Freon flood-cooled, and were patterned after the Wideröe linac drift tube quadrupole design. These 20-cm OD units (versus 30-cm OD for the above units) were required in the heavily congested area where the three injector beam lines merge. The following list of parameters apply to these latter magnetic elements:

Magnet Bore, ID:	6.3 cm
Magnet OD:	20 cm
Pole Length:	16 cm
Overall Length:	25 cm
$B'L_{eff}$:	22 kG
Current:	210 A
Voltage:	11 V
Power:	2.3 kW
Cooling:	2.0 gpm (Freon 113)

We used the 240-A (5-kW) commercial power supply units that have become standard throughout the SuperHILAC for all beam line quadrupole elements.

B3.2 Dipole Magnets and Power Supplies

Three primary bending magnets are used in the injection transport line. The first, a 90° bend, turns the beam from the Cockcroft-Walton pre-injector to the Wideröe axis. As the ion beam is bent through the 90° angle, the isotopes are spread out and a single isotope may be selected with a mass discrim-

ination of 1 part in 300. The other two dipole magnets are in the line between the Wideröe and the pre-stripper tank and provide the vertical displacement required at the pre-stripper entrance. These magnets are of a compact tape-wound-coil construction that has been successfully developed at LBL. The three new power supplies were identical in design and were similar to four other power supplies already built and in use elsewhere in the SuperHILAC.

Design parameters for the first magnet, the 90° analysis dipole, are shown below.

Beam rigidity, BR:	8.6 kG-m, 338.5 kG-in
Gap:	3.8 cm clear, 4.1 cm to poletips
Width:	13 cm
B_o:	15.0 kG.
ρ:	57.4 cm
L_{eff}:	90.1 cm
Current:	450 A
N:	125 turns
Voltage:	~29 V
Edge Angle α:	30°
Cooling:	~4 gpm (water) at 40 psi differential pressure

The next two bending magnets are used to bring the beam line vertically downward to the proper angle (+5°) and elevation for the pulsed switching magnet at the pre-stripper entrance. The bend angles required are ~30° and 25° respectively for the two magnets, and typical parameters are as follows:

Beam rigidity, BR:	10.5 kG-m, 413 kG-in (stripped)
Gap:	3.8 cm clear
Width:	7.6 cm minimum
B_o:	12-15 kG
Current:	435 A
Voltage:	20 V

B3.3 Trim Magnets and Power Supplies

A series of horizontal and vertical trim or alignment magnets is also provided in the injection beam line to permit small steering corrections to be applied to the beam. These units are DC magnets that are run from bipolar power supplies. They are identical to units presently being used in the experimental area. A trim magnet set consists of one horizontal and vertical magnet contained in a common yoke with overall dimensions of 23 cm by 23 cm by 38 cm long.

The magnet pair is 46 cm long overall, and is run only with ambient air cooling. The parameters are summarized below:

Steel:	Gap:	6.6 cm
	Pole length:	15 cm
	Effective magnetic length:	20 cm
	B_o:	817 gauss
	$B_o L_{eff}$:	16.3 kg-cm
Coil:	Current:	6.1 A
	Voltage:	18 V
	Power:	110 W
	Temperature rise:	60°C (air cooled)
	Conductor:	No. 13 Awg. square copper wire
	Number of turns:	720 turns/coil

B3.4 Buncher

The double-gap buncher, located upstream of the entrance to the Wideroe, is operated at 23.4 MHz. This device causes an energy spread of about 1.5 percent to be added to the beam.

The buncher uses a lump-constant inductor loaded by a drift tube at the ungrounded end. There are two 0.5-cm gaps, spaced by 3.7 cm. The beam radius at the buncher is ~2 cm, requiring that the buncher aperture be at least 5 cm in diameter. At any diameter greater than about 2 cm, the non-linear effects due to the fringing field are large, so the gaps were gridded with thin tungsten bars. These bars dissipate 10 to 20 W at maximum beam intensity, and are radiation cooled.

The voltage on the drift tube is 5 to 15 kV. An insulator located near the drift tube supports the structure and provides vacuum feedthrough.

The buncher is water-cooled on the inner conductor and drift tube. The maximum temperature rise at any point is less than 5°C, resulting in negligible gap misalignment due to thermal expansion of the structure.

B3.5 Stripper

The stripper following the Wideröe raises the mean charge state of the beam so that acceleration can continue in the first tank of the SuperHILAC. The beam is analyzed in the transport line following the stripper to select the charge state required. The stripper material is a fluorocarbon vapor of high molecular weight at a pressure of about 1 Torr evaporated from a reservoir of liquid. This type of stripper imposes no limit on the beam power and is a low maintenance item. Carbon foils, usually used as strippers, are not generally practical here as they must be very thin in order to reduce the energy and angular spread of the beam, and are thereby delicate and easily destroyed by beam. Figure B-9 compares the charge state distribution of lead ions stripped by air, fluorocarbon vapor, and a carbon foil.

The vapor stripper consists of a reservoir of Fomblin Y-Vac-25/9 liquid electrically heated to no more than 200°C by a resistance heater. At the top of the reservoir, a water-cooled surface, thermally isolated from the reservoir, condenses the vapor back into the heated bath. To reduce the migration of liquid along the supports of the stripper assembly, a portion of the support was also cooled. LN baffles were also located near the entrance and exit ports of the stripper to condense some of the escaping vapor, reducing the load on the vacuum system.

The aperture diameter of the stripper is ~4 cm. A beam scraper was located upstream of the stripper to protect it from misaligned beam or beam halo.

B3.6 Vacuum System

The vacuum pumping stations for the injection beam lines are identical to those already being used throughout the SuperHILAC experimental area; the standard unit consists of a 10-cm vacuum gate valve (VRC model 94576-106, 13.5-cm diameter port), a 10-cm diffusion pump (T-M Vacuum Products model 441), and a backing mechanical pump (Welch model 1397B). The mechanical pump also

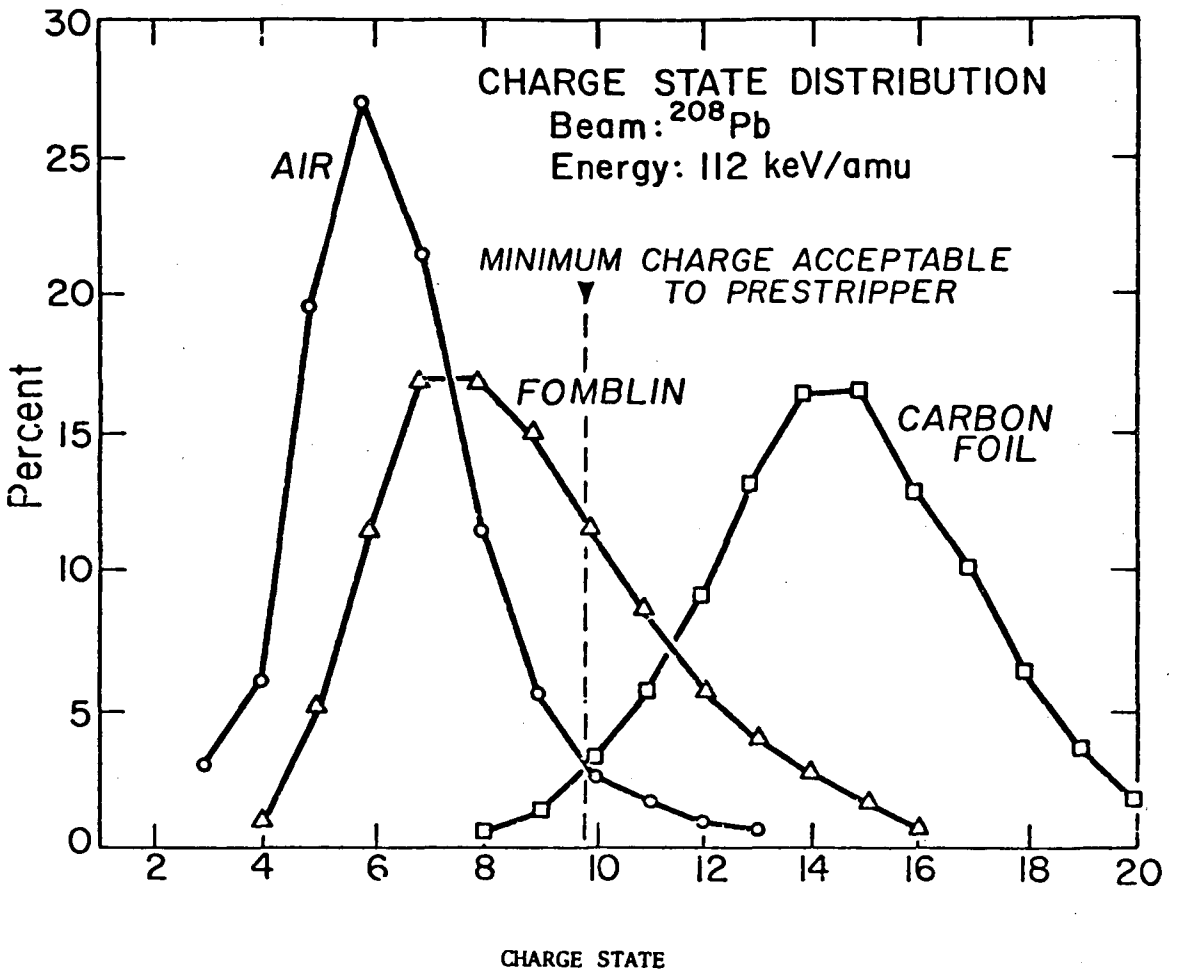

Figure B-9. Charge state distribution for ^{208}Pb ions at 112 keV/amu stripped by air, fluorocarbon vapor (Fomblin), and a carbon foil. Fomblin strips 12 percent of the beam to the minimum 10+ charge state required by the prestripper, and is not limited by high beam intensity as is the carbon foil (XBL 785-862).

serves as the roughing pump for the system. The diffusion pump features a built-in optically-dense cooled baffle and rapid heat/cool cycles due to a totally immersed ribbon heater element design. The 10-cm model has a rated pumping speed of 680 liters/sec.

The fabricated control boxes include an operator push button panel, panel gauges, and interlock status indicators. These standardized boxes are located at each pumping station for convenient operator usage. There are a total of seven separate pumping stations provided in the injection beam lines. In addition to the diffusion pump stations, several beam line LN traps were used to locally improve the pumping speed for water vapor and other condensibles.

The average pressure in the beam lines is normally in the middle 10^{-7}-Torr range. Although most beam line components are fabricated of stainless steel or aluminum, and careful fabrication and cleanliness procedures are carried out, the use of a large number of elastomer gaskets and sliding shaft seals for probes and instrumentation devices creates a large gas load which limits the base pressure. Pressures in this range have proven adequate for the transport lines.

The seven primary beam line pumping systems are separated along the injection line by large port beam line gate valves. These valves (VRC Model 94579-101 with modified flanges and bolt patterns) have a 8.5-cm diameter clear port. Control and interlock boxes are installed on each valve to permit clear indication of open or closed position as well as to provide a control switch to either operate the valve under local (manual) or computer control.

B4 LOW VELOCITY LINEAR ACCELERATOR

The principal requirement of the injector system accelerator is that it accelerate U^{5+} from a kinetic energy of 15.8 keV/amu to 113 keV/amu.

The Wideröe is a π-mode structure that in recent designs used elsewhere includes focusing quadrupoles in the drift tubes. Versions of Wideröe linacs are currently in operation at Manchester, at Orsay, and now at the UNILAC in Darmstadt. The UNILAC design solved the difficult problem of quadrupole alignment by placing the quadrupoles only in the even-numbered drift tubes mounted directly on the tank wall. The odd-numbered drift tubes are mounted on an inner support which is driven to high rf voltage.

In the Wideröe structure for very low velocity particles, the spacing between drift-tube gaps, $\beta\lambda/2$, becomes so small as to make quadrupoles unrealistically thin. However, the longitudinal phase advance from gap to gap can be any odd multiple of π, and a π-3π sequence of alternating gap-to-gap lengths produces a satisfactory solution to the drift-tube length problem.

In a π-3π machine, where the quadrupole length is $\beta\lambda$, the required gradient is less than 15 kG/cm for an operating frequency below 30 MHz. Accordingly, we selected 23.4 MHz as the operating frequency, which is the third subharmonic of the SuperHILAC. The frequency of the UNILAC Wideröe is 27.12 MHz, with about the same input particle velocity.

B4.1 Wideröe Linac Tank

The Wideröe linac tank is 5.17 meters long with a 134 cm inside diameter, and contains a total of 35 drift tubes, including two half drift tubes on the end walls. The sixteen long outer drift tubes are fastened to the outer wall of the tank and contain quadrupole magnets in a FODO sequence to permit focusing the beam during acceleration. The seventeen short inner drift tubes, mounted on the inner coaxial conductor, do not contain quadrupoles. Fig. B-10 shows a section view of the Wideröe linac.

The tank was fabricated from 1.25-cm nominal thickness, 10-percent copper-clad mild steel plate. The clad steel plates were rolled to the desired diameter and seam-welded with steel and copper welds. Steel end flanges were then welded to the copper-clad steel tank cylinder. The steel end walls, which are bolted to the tank, are copper-plated on the inside face for good rf conductivity. Sealing between the tank and end walls uses O-rings for vacuum and metal rings for rf contact. The tank has three flanged stub ports in addition to various pumpout and instrument ports. Tank wall cooling is by means of aluminum extrusion tubes compressed around the tank perimeter.

The Wideröe tank is supported on two structural beams mounted beneath the existing injector deck, and lies above and to the rear of the ADAM injector pressure vessel. The beam line in the tank (center of drift tubes) is 1.2 m above the injector deck. In order to provide sufficient clearance above the ADAM pressure vessel, the stub lines of the Wideröe linac were pointed up instead of down as at GSI.

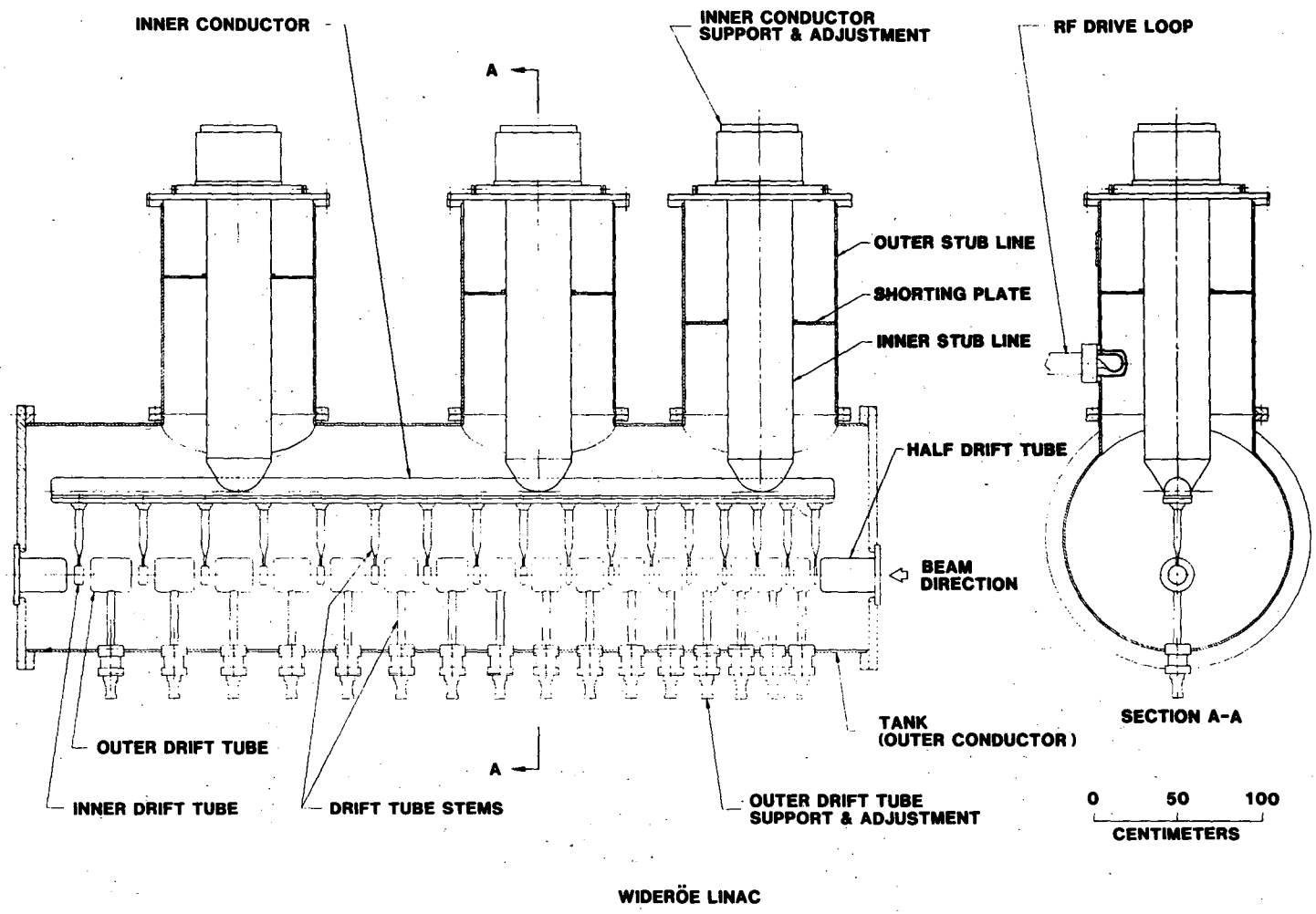

Figure B-10. Wideröe linac (XBL 7910-12107).

Four support legs bolted to both end flanges distribute the load of 12,000 kG of the fully assembled Wideröe linac. The support legs are adjustable in both the vertical and lateral directions to provide alignment for the tank. The drift tubes were aligned individually.

Wideröe Parameters

Structure	
Input energy	15.8 keV/amu
Output energy	113 keV/amu
rf power requirement	120 kW peak
Frequency	23.4 MHz
Line voltage	100 to 250 kV
Sequence	π-3π
Length	5.17 m
Diameter	1.34 m
Number of stubs	3
Number of drift tubes	35
Focusing	
Number of quads	16
Sequence	FODO
dB/dr	11.0 to 4.8 kG/cm
Accelerating Gaps	
Gap/Length	2.41 to 4.47 cm
Gap field	55 to 65 kV/cm
Aperture radius	0.8 to 1.5 cm
Transit time factor	0.65 to 0.85
Stable phase	-30°

B4.2 Support Stubs and Inner Conductor

The Wideröe tank has three inner and outer stub lines with three movable shorting plates.

The outer stub lines are 122-cm long and have an inside diameter of 90 cm. They were fabricated from 1.25-cm nominal thickness, 10-percent copper-clad mild steel plate rolled to the desired diameter and seam-welded with steel and copper welds. The steel end flanges were welded to the copper-clad steel stub cylinder. The outer stub lines were bolted to the stub ports in the tank wall and sealed by O-rings and metal rf rings.

The steel top flange bolted to the outer stub line provides mechanical support for the inner stub line and the shorting plate. Each outer stub line has a port in the wall for a tuning loop. The middle outer stub line also contains the rf driver loop. Additional portholes are located on the stub wall for cooling feedthroughs and hand access for adjusting the position of the shorting plate.

Stub wall cooling is by aluminum extrusion tubes compressed around the stub perimeter, similar to the tank-wall cooling method.

The inner stub lines are ~2.0 m long and have an outside diameter of 39.11 cm. The stub lines were constructed of steel tubes which were copper-plated on the outside. Steel flanges were welded to both ends of the copper-plated tube. The wall of the inner stub line is cooled by water-flooding the concentric space between the wall tube and an inner cooling tube.

The inner conductor, on which the short inner drift tubes are mounted, was fabricated in three sections and then fastened together with two connecting spools. The total length is 4.69 m.

Each section was constructed of two concentric steel tubes, either round or rectangular, with an effective outside diameter of 15.9 cm. The tubes were cut on the bottom side along their length and then welded to a rectangular steel flange. A round steel flange which mates with the bottom flange on the inner stub line was also welded to the top of the tubes. A rectangular steel flange which supports the inner drift tubes was then bolted to each welded tube assembly with an O-ring for vacuum sealing. A metal ring on the outer edge of the flange provides rf conductivity. All outside surfaces of the inner conductor are copper plated. Water cooling is provided to the inner conductor wall in the space between the two tubes.

For mechanical support the inner conductor is bolted to the bottom flange of the three inner stub lines with O-ring vacuum seal and metal ring seals for rf conductivity. The location of the inner conductor is off-center inside the

tank. The location of the stub lines from the front of the inner conductor is as follows:

Stub 1	44 cm
Stub 2	177 cm
Stub 3	357 cm

Each stub has a movable shorting plate which controls the gap voltage profile and resonant frequency of the structure. The approximate lengths of the stub inner conductors are 91 cm, 109 cm, and 118 cm for the three stubs, respectively. The shorting plate is fabricated from copper plate with copper cooling tubes soldered on the back side. Since the current at the inside edge of the shorting plate and the inner stub line is very high, about 35 amperes per linear cm, excellent rf contact at this location is mandatory. This was accomplished by using copper strips pushed hard against the walls by means of 6 mm jack screws.

B4.3 Drift Tubes

The Wideröe linac contains thirty-three drift tubes, plus two half drift tubes on the end walls.

The sixteen long outer drift tubes, which contain the focusing quadrupoles, are mounted on the bottom side of the tank wall, allowing relative ease in providing power, cooling, and alignment. Each outer drift tube is supported and adjusted from a single stem which contains both the coolant passages and magnet power leads.

The drift tubes are flooded with liquid Freon 113 which cools the magnet coils and the drift tube shells and stems. Since the drift tubes are supported from the bottom, the coolant passage was designed to prevent vapor buildup in the shell. The shell diameter is 20.3 cm and the length of the stem is about 40 cm. The shells and stems are fabricated of copper-plated steel. The drift tube stems are flange-bolted with O-ring and metal ring seals to the tank wall. A flexible copper diaphragm on the stem permits alignment of the drift tube.

The seventeen short inner drift tubes are flange-mounted and precisely aligned on the inner conductor which is suspended from the three inner stub lines. They do not contain quadrupoles. However, the shells and support stems

have water-cooling passages to dissipate the considerable rf power. Sealing of the stem flanges to the inner conductor is provided by O-rings and metal rings. The cooling lines for the drift tubes and inner conductor pass through the inside of the inner stub lines.

Alignment of the inner drift tubes on the inner conductor is provided by a support and alignment structure mounted on the top flange of the outer stub line. The shell diameter is 11.11 cm and the stem is about 40 cm long. The shells are fabricated of copper and stems are copper-plated steel.

The two copper half drift tubes, which also contain quadrupoles, are mounted on steel flanges which in turn are bolted to both tank end walls. The half drift tubes can be aligned and are Freon cooled. The diameter is 20.3 cm, the same as the diameter of the outer drift tubes.

The detailed drift tube schedule, shown in Tables B2 and B3, contains the physical and electrical parameters for the linac.

B4.4 Drift Tube Quadrupoles and Power Supplies

There are sixteen outer drift tubes in the Wideröe linac that contain focusing quadrupole magnets. These units are supported from the outer tank wall by a single vertical stem, and both power and cooling lines are contained in the stem. The stem is supported, adjusted, and aligned outside the tank, and movement is through a diaphragm seal.

The quadrupoles use tape-wound coils fabricated from copper strip conductor and machined to provide pole tip openings. The magnet yoke serves as the outer wall of the drift tube, and spun stainless-steel shells form the faces of the drift tubes. The drift tube is flooded with liquid Freon, which cools the magnet coil and the drift tube shells and stems. Drift tube lengths and apertures increase along the machine; the outer diameter remains constant at 20.3 cm. The magnets for these sixteen drift tubes are grouped into four different sets to minimize tooling and fixture costs, and to lessen the number of spare components required.

Design parameters for the four quadrupole groups (excluding the end-wall half drift tube elements) are listed below. A finished quadrupole magnet (before shells and copper plating) is shown in Fig. B-11.

An illustration of a finished drift tube during installation is shown in Fig. B-12.

TABLE B-2: PHYSICAL PARAMETERS FOR LINAC

CELL NO.	g/L	MODE	DT LTH (cm)	GAP (cm)	CTR GAP* (cm)	CTR DT* (cm)
1	.637	1	1.432	2.393	29.596	31.508
2	.626	3	9.797	2.542	33.495	39.665
3	.612	1	1.707	2.551	45.839	47.968
4	.599	3	10.901	2.682	50.163	56.954
5	.586	1	1.982	2.682	63.746	66.078
6	.574	3	11.944	2.791	68.464	75.832
7	.562	1	2.273	2.788	83.198	85.729
8	.549	3	13.057	2.889	88.310	96.283
9	.536	1	2.599	2.876	104.249	106.986
10	.523	3	14.215	2.987	109.769	118.360
11	.510	1	2.940	2.944	126.940	129.882
12	.497	3	15.335	3.014	132.859	142.034
13	.485	1	3.280	2.987	151.195	154.328
14	.474	3	16.411	3.051	157.494	167.224
15	.462	1	3.615	3.015	176.937	180.253
16	.451	3	17.390	3.058	183.591	193.815
17	.450	1	3.843	3.088	204.054	207.520
18	.450	3	18.247	3.201	211.042	221.766
19	.450	1	4.037	3.241	232.510	236.148
20	.450	3	19.159	3.361	239.848	251.108
21	.450	1	4.233	3.402	262.388	266.205
22	.450	3	20.085	3.524	270.084	281.889
23	.450	1	4.433	3.565	293.715	297.714
24	.450	3	21.002	3.686	301.774	314.118
25	.450	1	4.626	3.726	326.482	330.658
26	.450	3	21.864	3.840	334.891	347.743
27	.450	1	4.803	3.876	360.613	364.953
28	.450	3	22.649	3.980	369.344	382.658
29	.450	1	4.975	4.015	395.990	400.486
30	.450	3	23.487	4.126	405.036	418.843
31	.450	1	5.167	4.165	432.669	437.335
32	.450	3	24.419	4.289	442.063	456.417
33	.450	1	5.375	4.331	470.792	475.644
34	.450	3	12.600	4.453	480.559	495.385

* measured from inside entrance flange

TABLE B-3: ELECTRICAL PARAMETERS FOR LINAC

Cell No.	T (KeV/amu)	V gap (KV)	E gap (KV/cm)	TTF	Aperture (R cm)
0	15.76				.80
1	17.34	121.2	50.7	.718	.80
2	19.38	147.5	58.0	.761	.80
3	21.39	147.0	57.5	.750	.80
4	23.47	145.8	54.4	.784	.80
5	25.47	141.8	52.9	.778	.80
6	27.60	145.5	52.1	.801	.80
7	29.90	158.3	56.6	.803	.80
8	32.30	161.4	55.9	.817	.80
9	34.87	171.2	59.5	.825	.80
10	37.49	172.7	56.2	.833	0.80
11	40.10	177.7	60.4	.806	1.10
12	42.75	177.4	58.9	.823	1.10
13	45.41	176.7	59.2	.826	1.10
14	48.07	174.7	57.3	.838	1.10
15	50.67	169.3	56.2	.844	1.10
16	53.24	166.3	54.4	.850	1.10
17	55.87	169.1	54.8	.856	1.10
18	58.58	174.8	54.6	.854	1.10
19	61.62	193.2	59.6	.863	1.34
20	64.59	197.7	58.8	.826	1.34
21	67.77	211.0	62.0	.830	1.34
22	71.00	213.1	60.5	.830	1.34
23	74.32	218.1	61.2	.840	1.34
24	77.62	217.5	59.0	.834	1.34
25	80.92	213.6	57.3	.848	1.34
26	84.12	210.5	54.8	.838	1.34
27	87.24	200.7	51.8	.855	1.34
28	90.26	196.9	49.5	.840	1.34
29	93.62	215.2	53.6	.862	1.34
30	97.06	224.0	54.3	.842	1.34
31	100.99	249.0	59.8	.868	1.34
32	104.92	255.6	59.6	.844	1.34
33	109.21	269.9	62.3	.875	1.34
34	113.00	246.5	55.4	.846	1.34

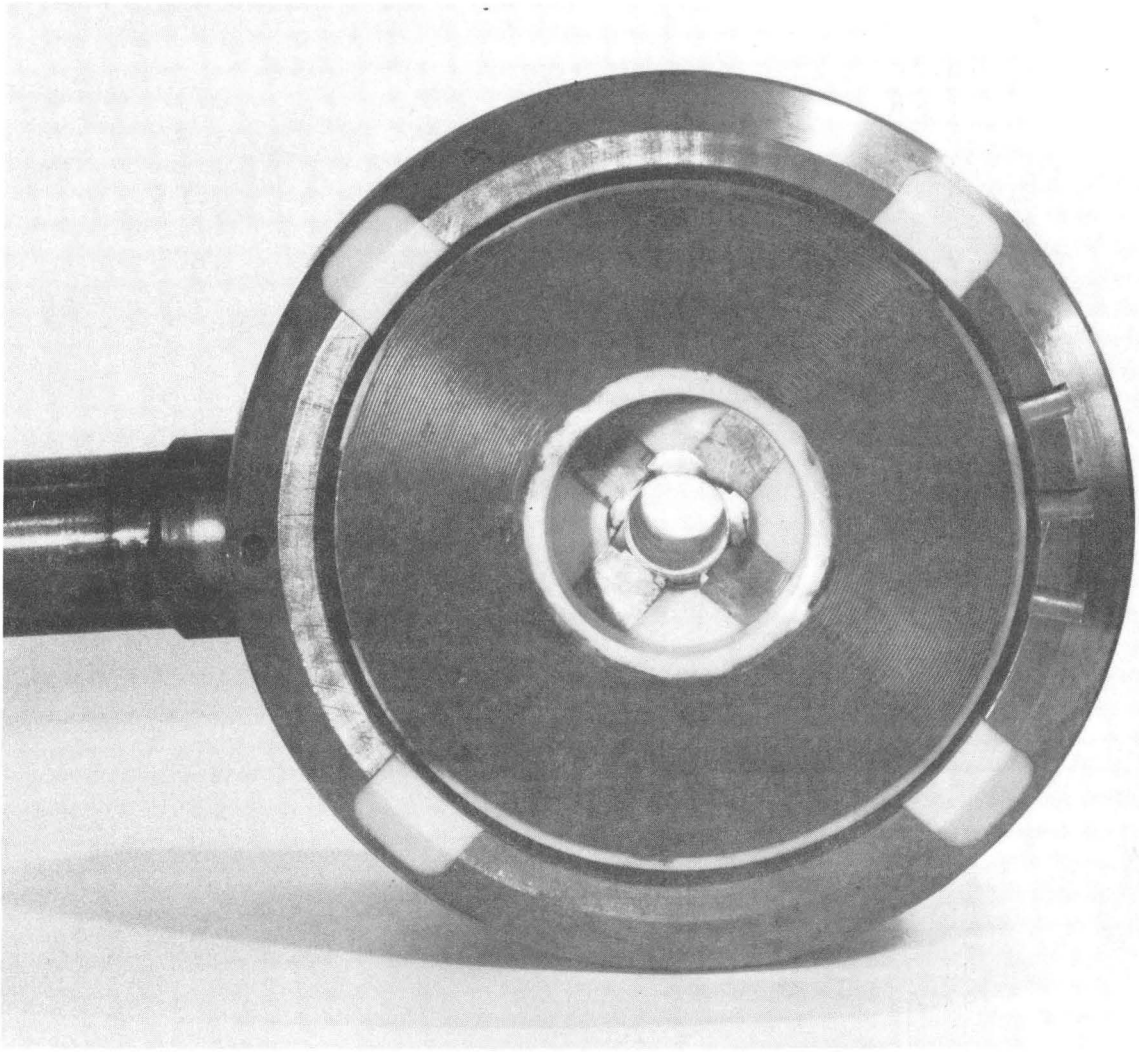

Figure B-11. Drift tube quadrupole magnet (CBB 800-14298).

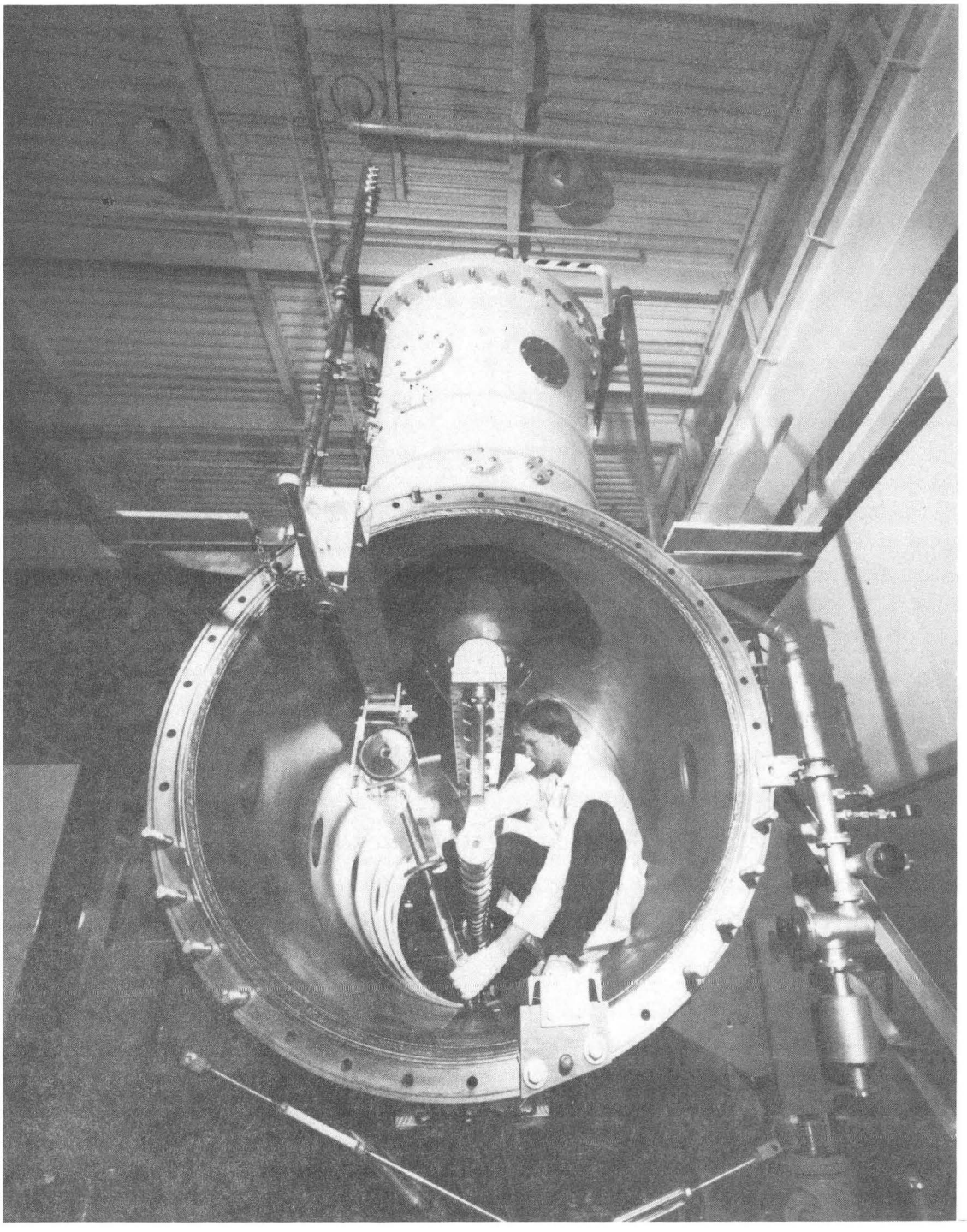

Figure B-12. Drift tube installation (CBB 811-892A).

Magnet Group Number	1	2	3	4
Drift Tube Numbers	2	4-8	10-18	20-32
Drift Tube OD, cm	20.3	20.3	20.3	20.3
Magnet Bore ID, cm	1.6	1.6	2.2	2.7
Pole Length, cm	7.2	7.7	10.9	15.8
Overall DT Length, min., cm	9.8	10.9	14.2	19.2
$B'L_{eff}$, kG	97.5	97.5	97.5	95.0
Current, A	185	160	185	185
Voltage, V	9	7	9	11
Power, kW	1.7	1.1	1.7	2.0
Cooling, gpm (Freon 113)	3	3	4	4

The drift-tube quadrupoles are powered from standard 250 A supplies, with several magnets in one group joined in series to run from one supply.

B4.5 Cooling System

Two separate cooling systems are required for the Wideröe linac. One is a Freon 113 closed-loop system, the other is a treated-water supply.

The power dissipation in the various elements of the Wideröe linac is based on a 50-percent duty factor, and includes 10-percent joint losses. Power losses in the drift tube shells have been estimated to be 20 percent of the stem losses. Losses in the half drift tubes are considered negligible. Actual loss measurements for the various components have not been made.

Drift tube quadrupoles	37.1 kW
Outer drift tubes - (16 shells and stems)	1.1
Inner drift tubes (17 shells and stems)	1.6
Tank wall	0.9
Inner stub lines (3)	16.0
Stub line shorting plates (3)	2.7

Outer stub lines (3)	7.0
Total power dissipation	66.4 kW

Freon 113 is used to cool the magnet coils and shells and stems of the sixteen outer drift tubes and the two end wall half drift tubes.

The closed-loop cooling system consists essentially of two circulating pumps (one standby), one heat exchanger, a surge tank with a sight glass, a filter and a drier, supply and return manifolds, and various valves, pipes, tubes, and fittings. The system also contains temperature and pressure gauges, a flow indicator and alarm, and interlock switches. Each drift tube has a flow switch and a balancing valve in the return line. Flow rates of 80 to 100 gpm and a pressure differential of 40 to 50 psi have been adequate for all outer drift tube cooling needs.

The complete Freon 113 cooling system actually supplies both the terminal house needs and the Wideröe linac with a total flow rate of 120 to 140 gpm and a common pressure differential of 40 to 50 psi.

Treated water is used to cool the tank wall, the inner drift tubes with the coaxial conductor, and the three stub lines with their shorting plates. Additional water cooling was required by the rf drive loop and the three tuning loops. Approximately 20 to 30 gpm of treated water is required and this is supplied by the central system at the SuperHILAC.

B4.6 Vacuum System

The vacuum requirements for the Wideröe linac are in the 10^{-7} Torr range. The total copper surface exposed to the vacuum from the tank, stubs, inner conductor, and drift tubes is about 54 m^2.

Two high-vacuum pumping stations are connected to the tank. Each station contains a cryogenic pump (1500 liters/s), and the necessary valves, traps, piping, and instruments. A separate roughing station is provided using standard mechanical pumps.

Another mechanical pump (500 liters/min) is used to evacuate the space inside the three inner stubs and the inner conductor. This secondary vacuum serves to protect the high vacuum in the tank in case of small water leaks in the cooling tube joints.

B4.7 RF System

An overview of the rf system is shown in Fig. B-13.

An EIMAC 4CW100K/8959 Running Class AB_2 tube is used in the final amplifier stage. This tube can deliver well over 200 kW in this mode, giving us ample reserve to supply cavity losses and an expected 20 to 40 kW beam loading. Running at 30-percent duty factor, we have ample plate dissipation even when supplying reactive power to the beam load. In normal operation we run at reduced filament voltage to extend tube life. It has been our experience that, with filament voltage reduced to about 90-percent rated value, we can expect over 50,000 hours (5 to 7 years) life on this type of tube. A block diagram of the rf final amplifier appears in Fig. B-14. The installed final amplifier is shown in Fig. B-15.

The power supply for the final stage is a stand-alone twelve-phase oil-filled unit with taps to select 10-, 15-, 18-, or 20-kV operation. The primary power is taken directly from the Bank 71 480-V buss. The output is connected to a small capacitor bank of about 100 μf for despiking. Using a separate power supply for the Wideröe gives us maximum flexibility in operation and has proven to be very cost effective.

The driver stage is a 4CW2000 Class AB tube used in a semi-linear mode. The low-level stage is an Amplifier Research Corporation 10-W solid-state unit.

Phase and amplitude modulation is accomplished at the 0 dbm level. This gives us maximum flexibility for future dual beam operation and provides at least a decade of additional frequency response over high-level modulation. This additional bandpass is required to overcome beam-induced rf instabilities due to the reactive nature of the beam loading, especially when running "noisy" beams (PIG sources having typical 10- to 100-kHz modulation components).

The rf frequency control (see Fig. B-16) used existing SuperHILAC designs and components, with only very minor modifications required to adapt to the lower (1/3) frequency. The existing SuperHILAC frequency system had provisions for additional expansion to contain the extra channel. The detector and servo system is a double-wide NIM module complete with a 200-W motor-drive amplifier. The tuner itself penetrates the vacuum with a single O-ring seal and is liquid-cooled. It is driven with a low-inertia printed-armature servo motor and a zero-backlash gear reducer of the same design that has proven very reliable on the SuperHILAC.

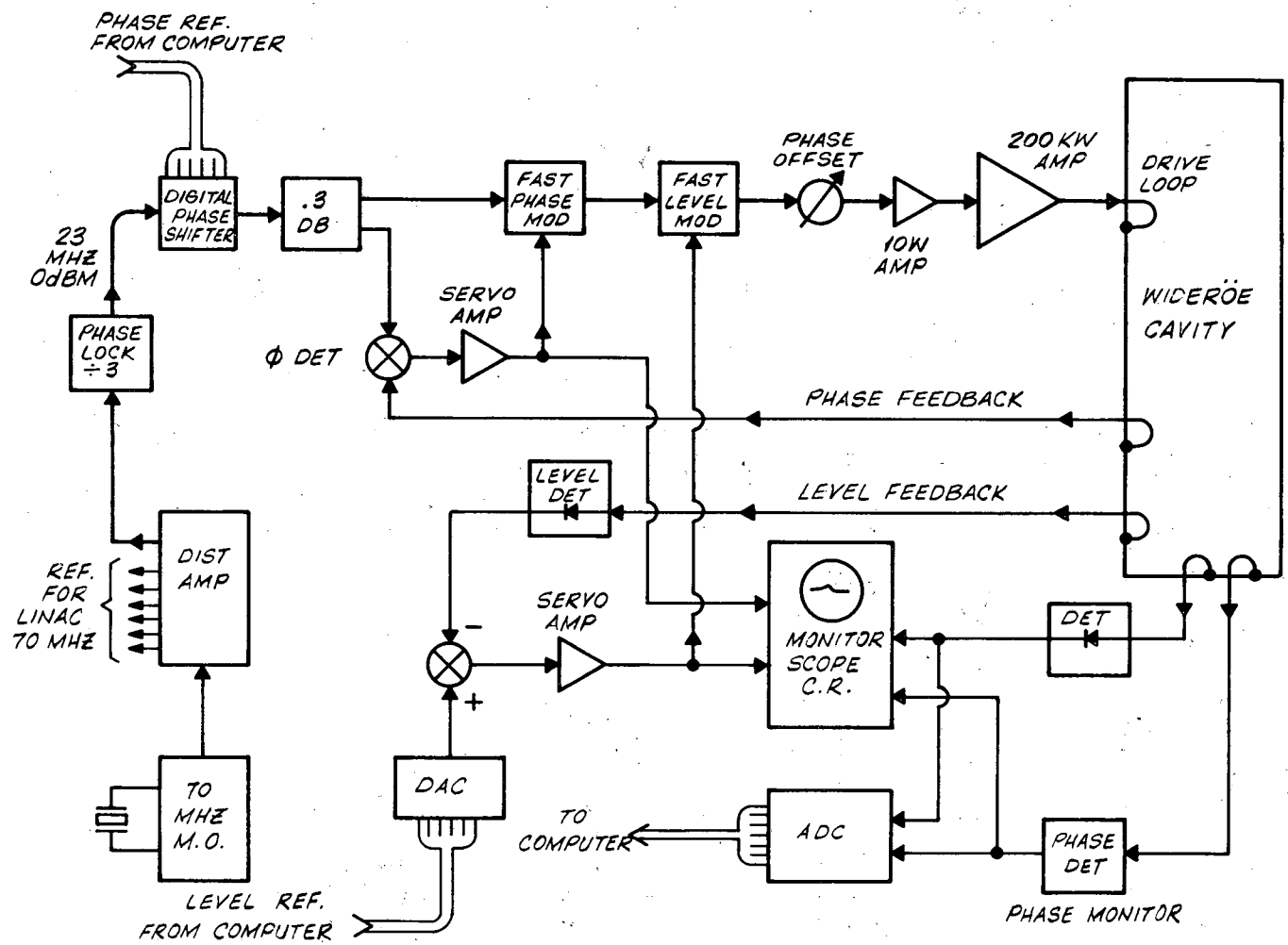

Figure B-13. rf system with instrumentation (XBL 827-10721).

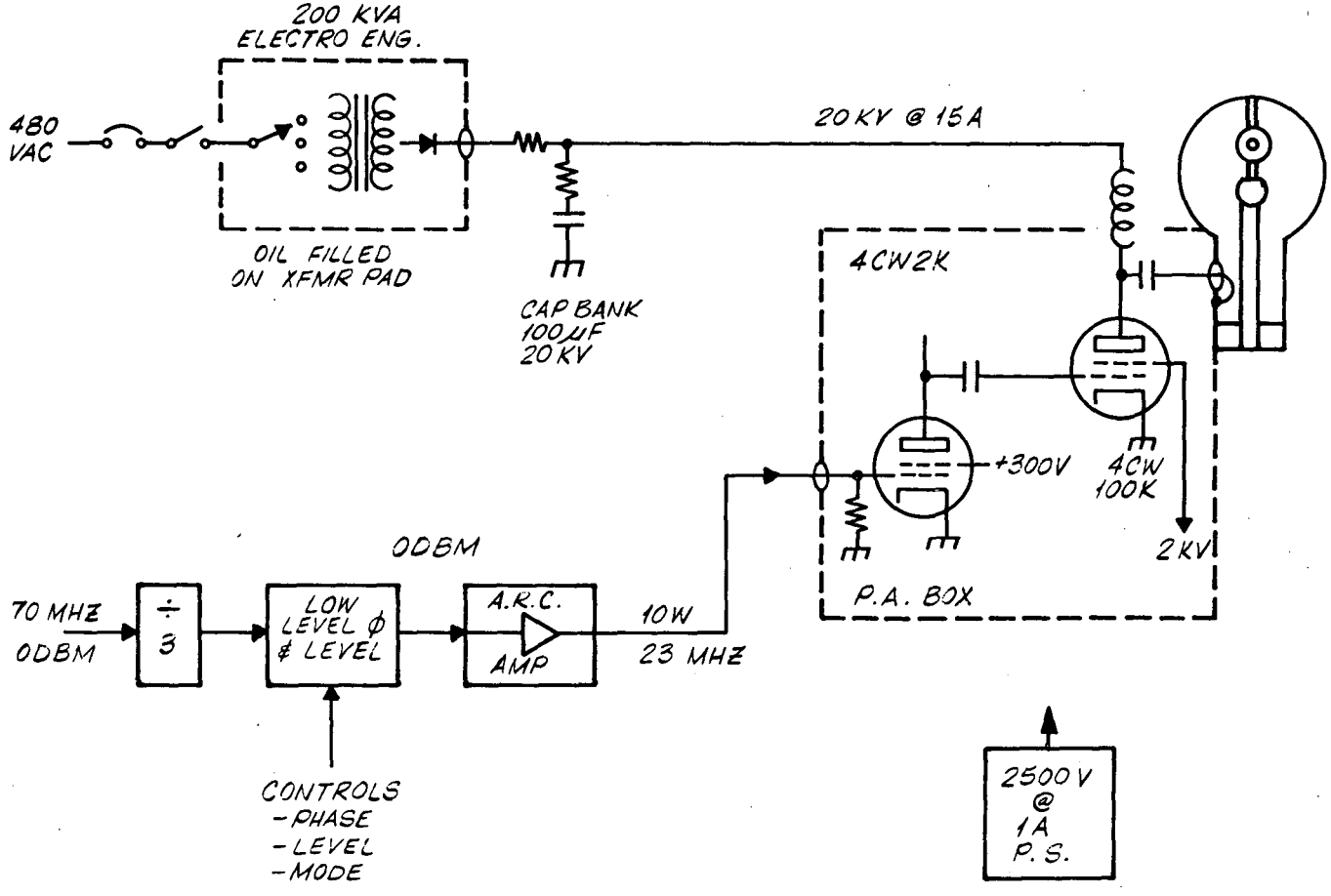

Figure B-14. Main rf amplifier block diagram (XBL 827-10719).

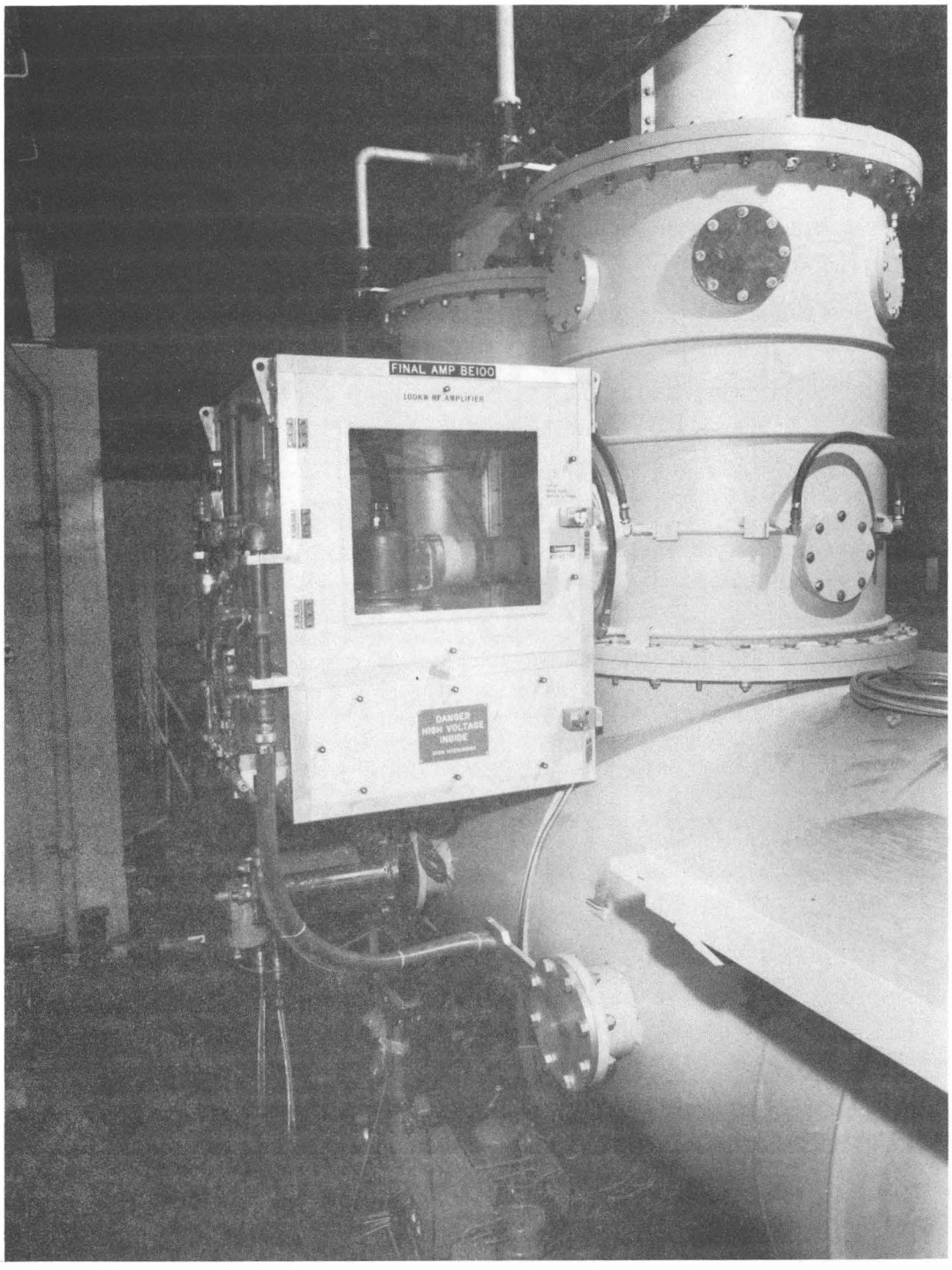

Figure B-15. Wideröe accelerator and final rf amplifier (CBB 812-1743).

each knob has a 12-character addressable LED for labeling the controlled device (see Fig. B-20). Alternatively, the device parameter value can be displayed in this space. Buttons located on the panel below the knobs are used to move a cursor on the CRT parameter list display, to scroll the list, to assign knobs to parameters, to change knob sensitivity, etc.

Four vector graphics display units are mounted at each console above the touch panels. These units, in addition to displaying graphs with alphanumerics, allow mixing of real-time analog signals with the digital plots. This can be thought of as an oscilloscope with labels under program control. These signals are added to the output of the graphics translator using a chopper technique (see Fig. B-21). The adder also provides for limited changing of the gain and time base. In Fig. B-22, the display is an example of the use of this analog capability to present three wave forms from the ion source: extractor voltage, sputter current, and arc current.

B5.1.3 Portable Console

The portable console (Fig. B-23) can be connected to any IOMM for local operation of any of its controlled devices. A 5-inch CRT permits display of parameters and monitored values. There is no touch panel, but a row of buttons located immediately below the CRT can be labeled through software. Two control knobs are also provided. It is possible, using the portable console, to modify the ROM data base dynamically. This is done by duplicating the IOMM data base in RAM, and using this for control and possible modification. This is most valuable during checkout of an IOMM, when many of the data base parameters (limits, allowable tolerances, etc.) have only been tentatively assigned, and need to be refined while operating the actual device. The revised data base information is then impressed onto a new ROM chip, which then replaces the old ROM chip in the IOMM. The entire process of changing ROM values is fast--a few minutes--while the IOMM is "down" for only the few seconds required to change chips.

Another important use for the portable console is to run accelerator equipment tied to the IOMM for checkout during maintenance periods, when the computer control system is also usually down for maintenance or for the installation of new programs, etc. Without such a local control capability, a full set of parallel controls would need to be installed for such critical equipment as ion sources and rf, which require operation as an integral part of maintenance.

It is possible to operate and monitor all functions on the accelerator, both high level and low level, independently of the computer in local control from the equipment racks in "E" area.

B5 SUPERHILAC AND CONTROL CENTER MODIFICATIONS

The computer control system of the third injector allows operator control of the Cockcroft-Walton and its associated source parameters, the beam line into the Wideröe, the Wideröe itself, and the beam line into the pre-stripper of the SuperHILAC.

B5.1 Computer/Operator Control

A modern microprocessor-based system of the "star" type is provided (see Fig. B-17) with the following distinguishing features.

- Use of a large number (~25) of microprocessor boards, each executing a simple task, or a series of simple tasks.
- In each chassis there are several processors operating in parallel.
- Use of a distributed data base in ROM (read only memory), so that local, stand-alone control of accelerator components can be readily accomplished.
- Use of fiber optics, permitting high bandwidth and noise-free data transmission.
- Modular construction, which permits easy expansion of both control points and of effective memory.
- Update and repair are easily accomplished.
- Use of a de facto industry standard card cage and bus--the Multibus--which has a large number of suppliers of compatible components.
- A loosely structured network concept, having the result that, since there is not a single central computer through which all data must flow, the system cannot develop a processing bottleneck which limits performance.
- All programming is done with higher level languages.

Figure B-17 shows schematically the major components of the system. Each of the blocks represents a card cage with 8 or 12 slots served by an internal Multibus. The IOMM modules interface to the accelerator equipment, collect and

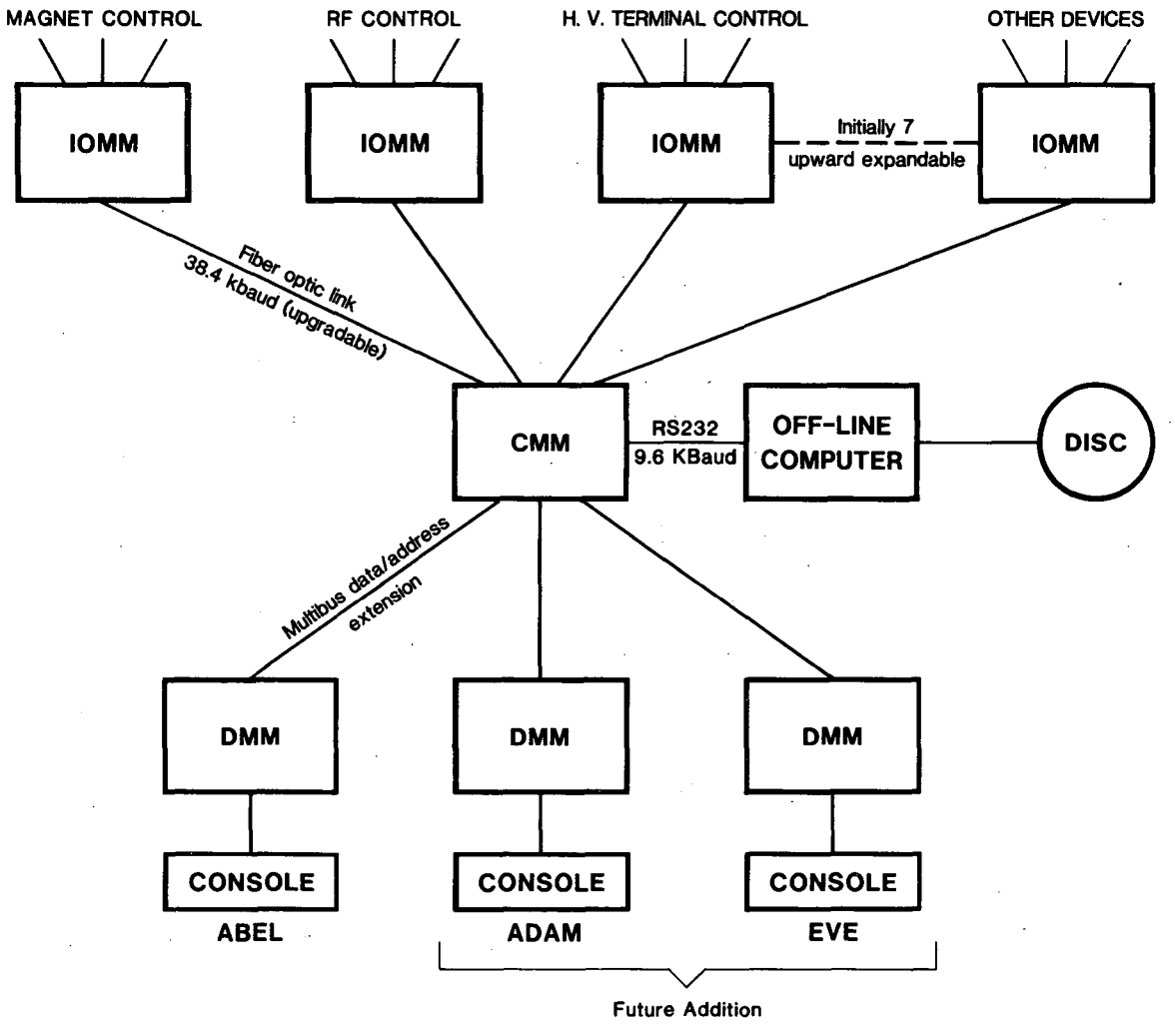

Figure B-17. Schematic of system architecture (XBL 8010-12480).

digitize data, and transmit control instructions to the hardware. These units contain the local data base in ROM. The CMM module serves as a collector for all data sent to and from the IOMM's. It contains a copy of each IOMM data base. There is one processor in this unit for every 8 IOMM's; as more IOMM's are added, additional boards are added to the CMM as necessary to handle the increased traffic. DMM modules are used to service the operator consoles. Their access to the CMM database is by means of a Multibus extension. This is a pair of boards designed in-house which extend the address and data lines from the CMM to the DMM. Several DMM's can be connected in parallel to the CMM. The three shown in Fig. B-17 correspond to three control stations at the Super-HILAC, one for each injector. At present, injectors 1 and 2 remain under analog control.

B5.1.1 DMM

Figure B-18 shows schematically the computer boards used in the DMM at present--more can be added as needed. The alphanumeric display boards are used to write to the two CRT's. Output of the console touch screens is through the console computer board. A graphics computer board is used to support four vector graphics displays. The operating computer is used to execute standard operating tasks, as well as to provide a link to a separate computer system used for a number of development activities. All of these computer boards have direct access to the data base in the CMM via the Multibus extension.

B5.1.2 Operator Console

The portion of the console which is served by the microprocessor control system is shown in Fig. B-19. There are two control panels, each containing a CRT for displaying alphanumerics. These are overlaid with touch screens having a spatial resolution corresponding to the size of one character. Two 16-button pads to the right of each CRT allow entry of numbers and special commands. These are input in parallel to the touch screens and give a little more flexibility to the system. All commands could be given through the touch screens, but this would result in a great deal of wasteful paging back and forth in some cases.

SuperHILAC beams require frequent retuning, on the order of several times per week, because of experimental requirements. Consequently, knobs for operator use are important. Each CRT at the control station has 8 knobs, and

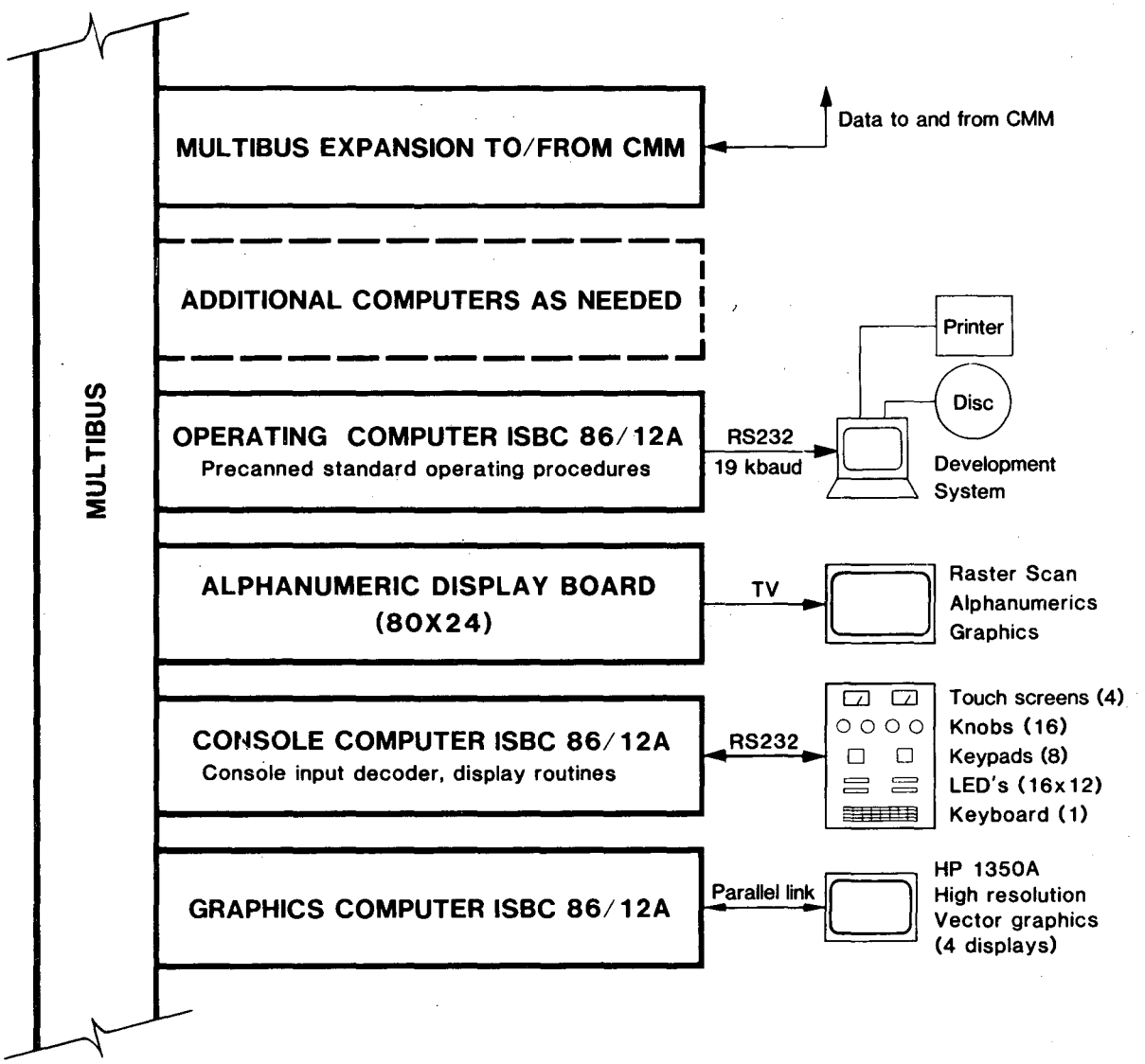

Figure B-18. Schematic of DMM configuration (XBL 8010-12479).

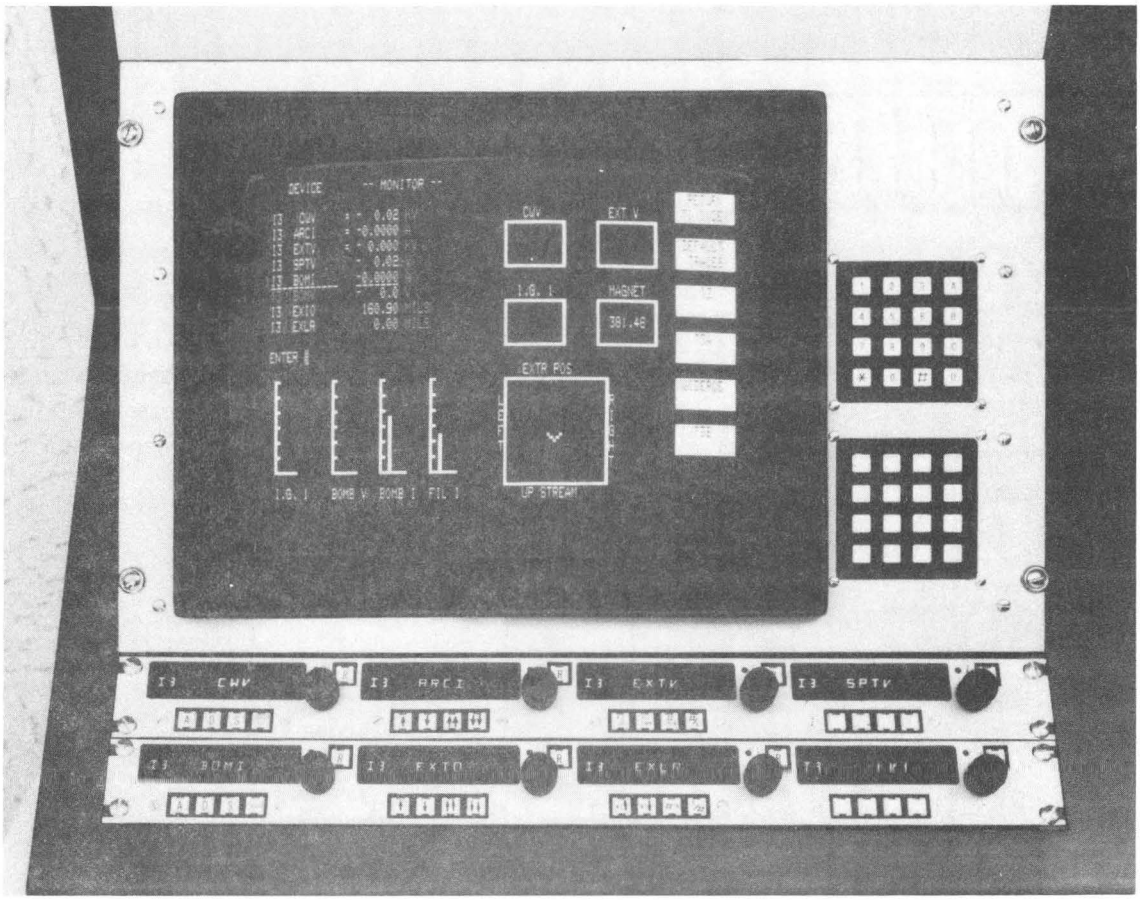

Figure B-20. Closeup of touch panel CRT with associated controls (CBB 812-1901).

each knob has a 12-character addressable LED for labeling the controlled device (see Fig. B-20). Alternatively, the device parameter value can be displayed in this space. Buttons located on the panel below the knobs are used to move a cursor on the CRT parameter list display, to scroll the list, to assign knobs to parameters, to change knob sensitivity, etc.

Four vector graphics display units are mounted at each console above the touch panels. These units, in addition to displaying graphs with alphanumerics, allow mixing of real-time analog signals with the digital plots. This can be thought of as an oscilloscope with labels under program control. These signals are added to the output of the graphics translator using a chopper technique (see Fig. B-21). The adder also provides for limited changing of the gain and time base. In Fig. B-22, the display is an example of the use of this analog capability to present three wave forms from the ion source: extractor voltage, sputter current, and arc current.

B5.1.3 Portable Console

The portable console (Fig. B-23) can be connected to any IOMM for local operation of any of its controlled devices. A 5-inch CRT permits display of parameters and monitored values. There is no touch panel, but a row of buttons located immediately below the CRT can be labeled through software. Two control knobs are also provided. It is possible, using the portable console, to modify the ROM data base dynamically. This is done by duplicating the IOMM data base in RAM, and using this for control and possible modification. This is most valuable during checkout of an IOMM, when many of the data base parameters (limits, allowable tolerances, etc.) have only been tentatively assigned, and need to be refined while operating the actual device. The revised data base information is then impressed onto a new ROM chip, which then replaces the old ROM chip in the IOMM. The entire process of changing ROM values is fast--a few minutes--while the IOMM is "down" for only the few seconds required to change chips.

Another important use for the portable console is to run accelerator equipment tied to the IOMM for checkout during maintenance periods, when the computer control system is also usually down for maintenance or for the installation of new programs, etc. Without such a local control capability, a full set of parallel controls would need to be installed for such critical equipment as ion sources and rf, which require operation as an integral part of maintenance.

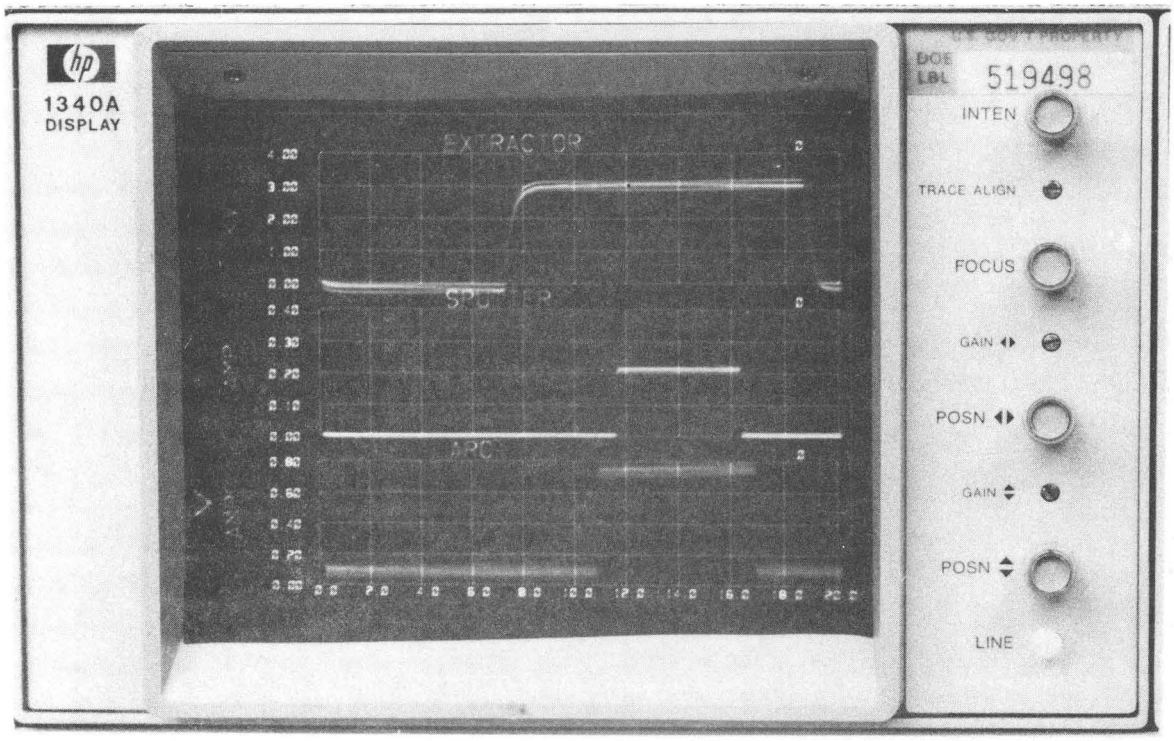

Figure B-22. Closeup view of graphics display with added analog signals (CBB 812-1897).

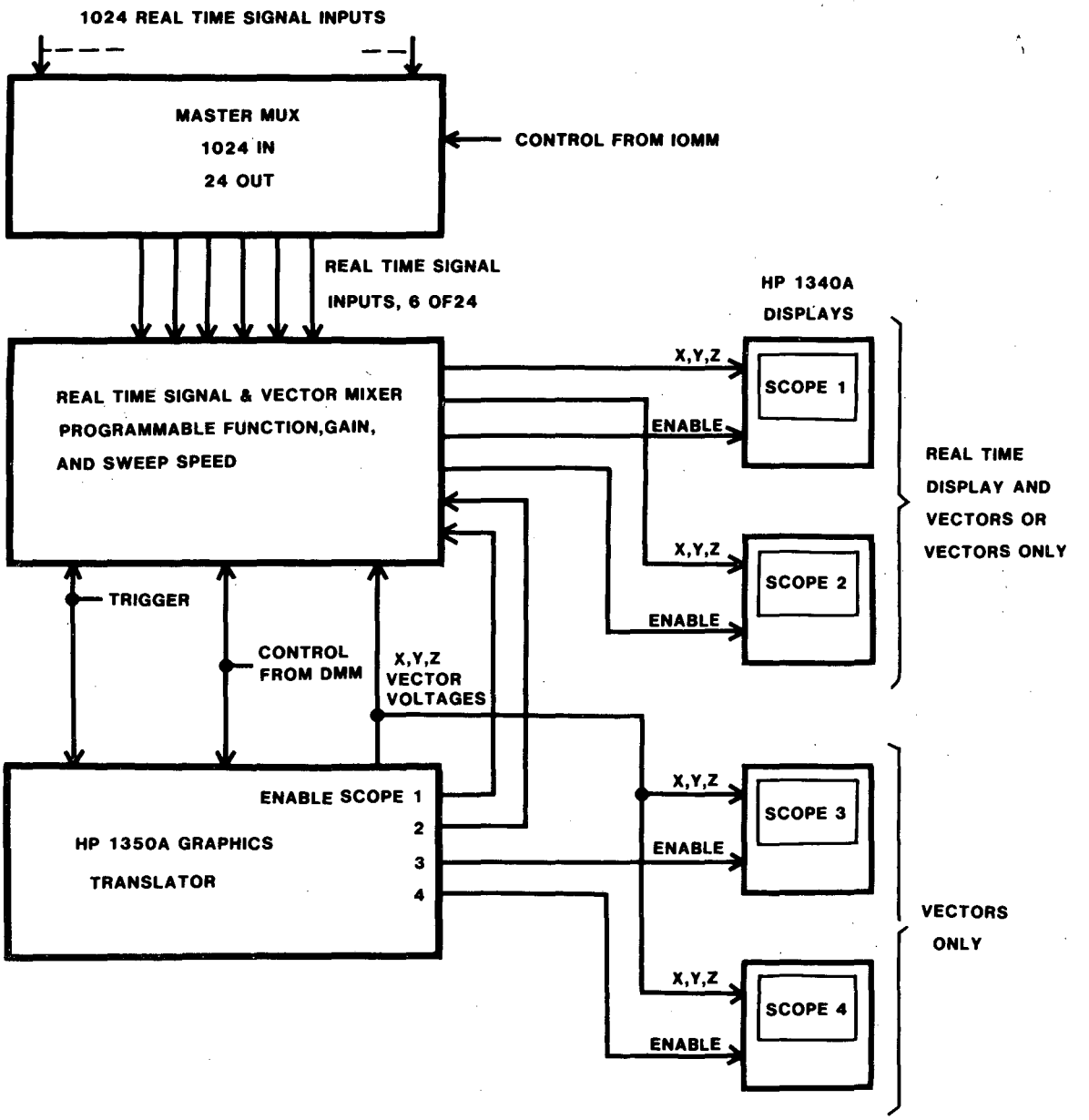

Figure B-21. Schematic of video mixing of analog signals with vector graphics output (XBL 813-8402).

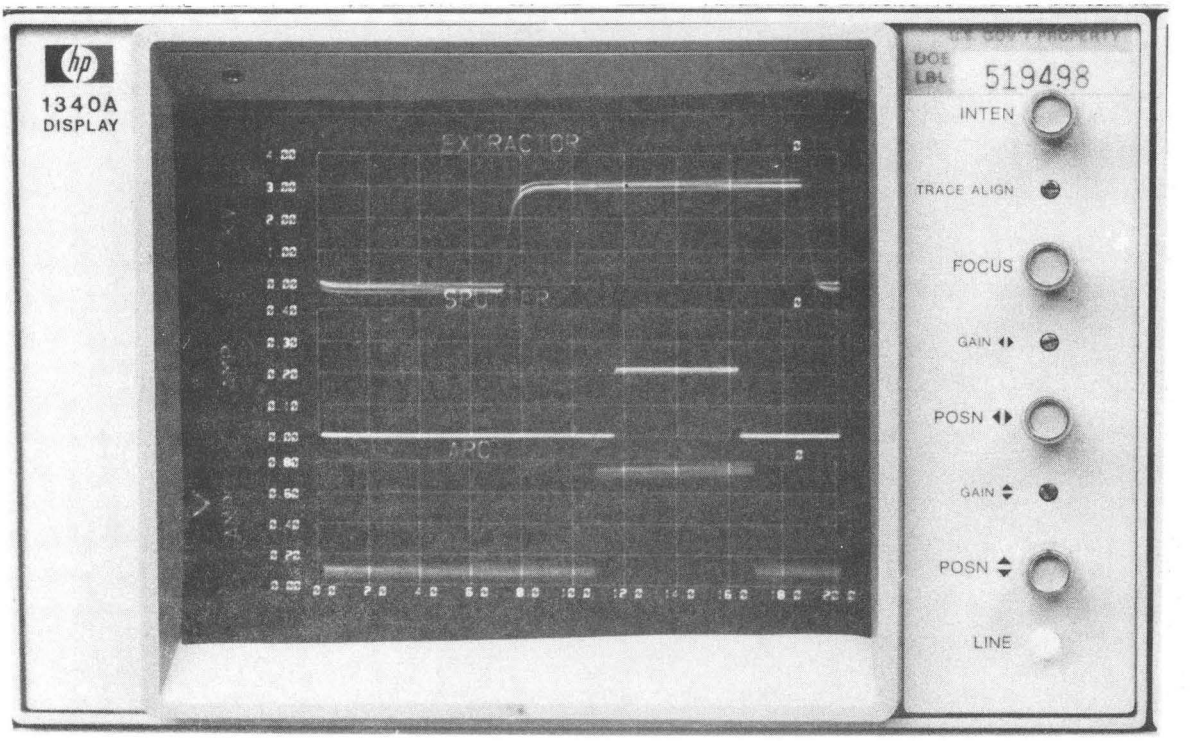

Figure B-22. Closeup view of graphics display with added analog signals (CBB 812-1897).

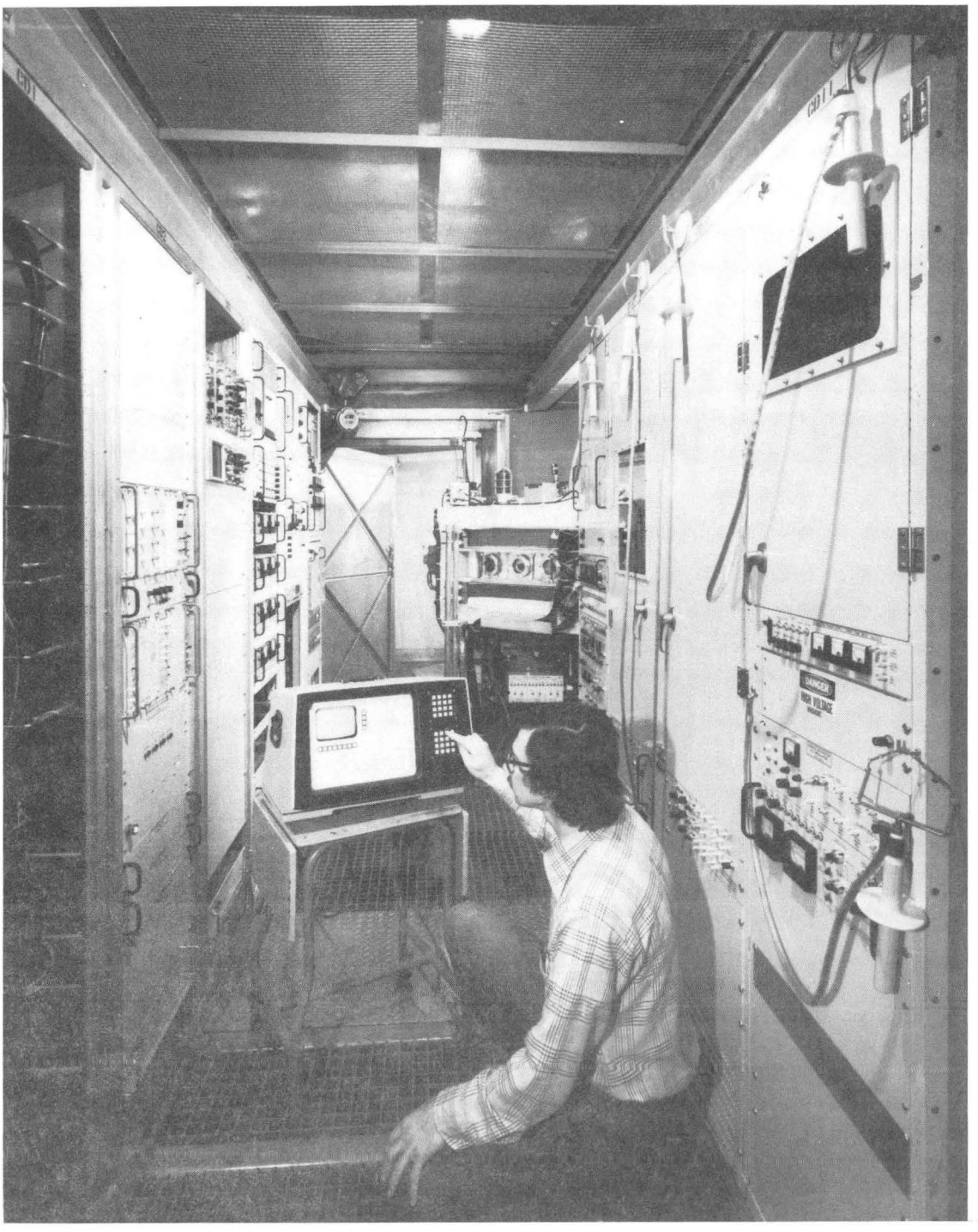

Figure B-23. Portable console being used in Cockcroft-Walton terminal (CBB 812-1891).

Finally, the portable console could be provided with special programs and output plugs used to check out and isolate problems associated with control system components, such as multiplexers, timing modules, and graphics equipment, independent of the IOMM.

B5.1.4 System Status

This control system meets or exceeds all of its design specifications. However, a very important test for any control system is its ability to adapt to new requirements. We will want to add many new controlled elements and many more beam monitoring devices to the present system. With a 36-Hz machine, requirements for data collection and analysis can grow to almost any limit. We would like the system to be able to handle as much as possible. Fortunately, the microprocessor technology that we have chosen to follow is moving in this direction. It will be possible to meet all of these goals inexpensively with standard hardware and with modest software additions.

B5.2 Instrumentation, Controls and Interlocks

Frequent changes of ion species and output energies during normal SuperHILAC operations made it mandatory to include adequate facilities for rapid diagnosis of tuning problems. Faraday cups, collimating slits and apertures, and wire profile grids are used to monitor the beam. They are mounted upstream and downstream from the bends in the transport line, preceding and following the linac, and at other critical locations. Attenuators were also provided downstream of the Wideröe linac.

The signals and controls for this diagnostic instrumentation are fed to the operator console in the SuperHILAC control room.

Controls were provided in the SuperHILAC control room to operate all equipment necessary for third injector operations. In addition, local controls are available at each piece of equipment for testing and trouble-shooting.

Hardware interlocks were provided to protect against overstressing of equipment. Personnel-safety hardware interlocks protect against hazardous conditions. Alarms, when appropriate, reside in the SuperHILAC control room to give equipment status information. Software interlocks are used only for components that do not affect personnel safety.

C. SUPERHILAC BUILDING ADDITIONS

C1 INTRODUCTION

The building enclosures for the High Intensity Uranium Beams project consisted of additions to the west end of the existing SuperHILAC (Building 71) totaling 1715 gross square feet divided among three areas of differing size and shape as follows:

Cockcroft-Walton Injector Enclosure. An 80-square-meter (~10 by 8 m) concrete and steel structure conforming in appearance to the existing building and located near the present injector area of the SuperHILAC. It is air conditioned to produce the necessary controlling of temperature and humidity for the special equipment.

Beam Transport Deck. A 40-square-meter open metal structure supported on steel columns and piers.

Power Supply Enclosure. A 70-square-meter concrete and steel structure to house the power supplies for the new Wideroe linear accelerator.

The new linear accelerator space was provided within the existing building, and required that the building be structurally modified in one area to support the accelerator equipment. The existing roadway was modified slightly in the vicinity of the west end of the existing building to accommodate the new building additions.

C2 SCOPE

C2.1 Architectural

The Cockcroft-Walton injector enclosure consists of a reinforced-concrete foundation with steel-framed walls and roof, and a floor-to-roof height of 11 m. The enclosure is thermally insulated in accordance with ERDAM 6301 requirements.

The beam transport deck is a steel-framed structure with metal decking. The floor is elevated 4.3 m above the existing grade.

The power supply enclosure is an on-grade slab with steel frame and metal siding. Floor-to-roof height is 4.3 m.

Uniform Building Code Criteria for the proposed additions are these:

Site designation	Fire Zone 3
Estimated number of occupants	16
Occupancy classification	F-2
Type of construction	Type 3

C2.2 Structural

The Cockcroft-Walton injector enclosure is composed of a heavy reinforced-concrete slab on grade, concrete grade beams, caissons, and a steel frame with metal siding and roof deck.

The beam transport deck consists of an elevated steel-plate floor which supports the transport line between the third injector and the linear accelerator. The deck is supported with steel columns and caissons.

The power supply enclosure consists of a concrete slab on grade, concrete grade beams, caissons, and a steel frame with metal siding and roof deck.

The Wideröe linear accelerator structural support system is located above an existing injector. This required modifications to an existing deck, and an additional framing system was built above the existing injector using the existing concrete walls for support.

Structural designs for building elements of this project were based on LBL Lateral Force Criteria which are more stringent than the latest Uniform Building Code. The foundation design was based on soils reports prepared for previous additions to the existing SuperHILAC Building.

C2.3 Required Mechanical Utilities

All required mechanical utilities were extended from existing systems in Building 71. Cooling water requirements include cooling tower water, treated water (TRW) and low-conductivity water. Capacity of the existing building utilities was adequate to extend all of these cooling systems to the injector area.

C2.4 Heating and Cooling

No conventional air conditioning systems were installed. The Cockcroft-Walton enclosure has a build-up air cooling and dehumidifying system consisting

of an air handling unit, air filter unit, heating coil, cooling and dehumidifying coils, temperature and humidity control system, and water/glycol chiller. The power supply enclosure has roof-mounted air exhaust fans for summer heat removal.

C2.5 Fire Sprinklers

Dry pipe sprinklers were installed in each enclosure. They are supplied from an existing dry pipe system which includes all of the west end of the existing building except the high bay. The existing fire department connection for the west end of the building has been relocated next to the roadway.

C2.6 Electrical

The estimated electrical power demand for the proposed building additions in the SuperHILAC area was as follows:

Lighting.		6.0 kVA
Interior	4.5 kVA	
Exterior	1.5 kVA	
Convenience Receptacles		2.0 kVA
Building Heating, Ventilating, and Air Conditioning.		40.0 kVA
Research Power.		225.0 kVA
Total		273.0 kVA

The above power was available at 480 volt, 3 phase, 3 wire in the main switchgear area at the SuperHILAC (Building 71).

D. BEVALAC TRANSFER LINE

D1 Magnets

To make full use of the SuperHILAC capabilities, the Bevalac transfer line must accommodate the heaviest full-energy particles stripped to their equilibrium charge state ($q/A = 0.29$). To accomplish this, the magnetic rigidity limit in the transfer line was increased from the original 10.3 kG-m to 14.6 kG-m. The transfer line elements include 8 magnetic dipoles, 26 quadrupoles, 22 steering magnets, and an electrostatic inflector. The inflector, steering magnets, quadrupoles, and most dipole magnets were adequate for the higher rigidity, and only one dipole magnet had to be completely replaced.

The last magnet in the line is the thin septum inflector magnet, BL18MH. This magnet was installed inside the tangent tank chamber and had to be modified to make it compatible with the new ultra-high vacuum environment. To overcome the cooling limitation on the thin septum coil resulting from driving the magnet to the necessary higher fields and higher power densities, it was decided to pulse the magnet to the high field only during the actual injection beam pulse. This minimized the provisions of additional cooling and cabling, and has proven to be very satisfactory. The modifications to BL18MH required for vacuum compatibility are described in section E3.5.1.

Two other magnets in the line, BL15MH and BL16MH, are also now pulsed to the higher field levels only during injection times, and no longer operate DC at these higher power levels. The BL17MH dipole, however, not only had a cooling limitation at these new operating levels, but also had a magnetic saturation limit and would not reach adequate field levels even under a pulsing mode. This magnet bends the beam 35° directly into the inflector channel, and it is positioned very close to the existing Bevatron main magnet.

A new magnet was designed to basically reproduce the optical properties of the old unit, and no additional changes were required in the transfer line to maintain the original beam transport characteristics. To minimize the magnetic flux that had to be carried by the new magnet, and thereby minimize the volume of steel required in this very congested area, a "window-frame" style magnet was designed. The new magnet was made slightly longer than before (effective

length is 91 cm vs 77 cm before) to more effectively utilize the beam line space. New coils and steel yokes were designed and fabricated, and an adapter base plate was installed to make use of the existing magnet support and alignment system.

Figure D-1 is a schematic diagram of the transfer line; the element that was replaced has been accented.

D2 Power Supplies and Instrumentation

To drive the transfer line magnets to the higher field values, increased power supply capacity was required. However, by rearranging the existing supplies, almost all of the magnet power supply requirements were met, and only two power supplies needed to be upgraded. One was required for the BL02MV-BL04MV magnet combination and one for the BL07MH-BL09MH magnet combination.

Higher current operation required the installation of higher capacity electrical cabling in many magnets. Water cooling lines were also added, since a number of quadrupoles in the line were previously run so far below rated capacity that no water cooling had been provided for them.

Special new supplies were provided for the pulsing magnets BL15MH, 16MH, and 18MH. The supplies, not only provided higher power levels, but also were enhanced to provide the ultra-high regulation, stability, and reproducibility required for these critical injection dipoles.

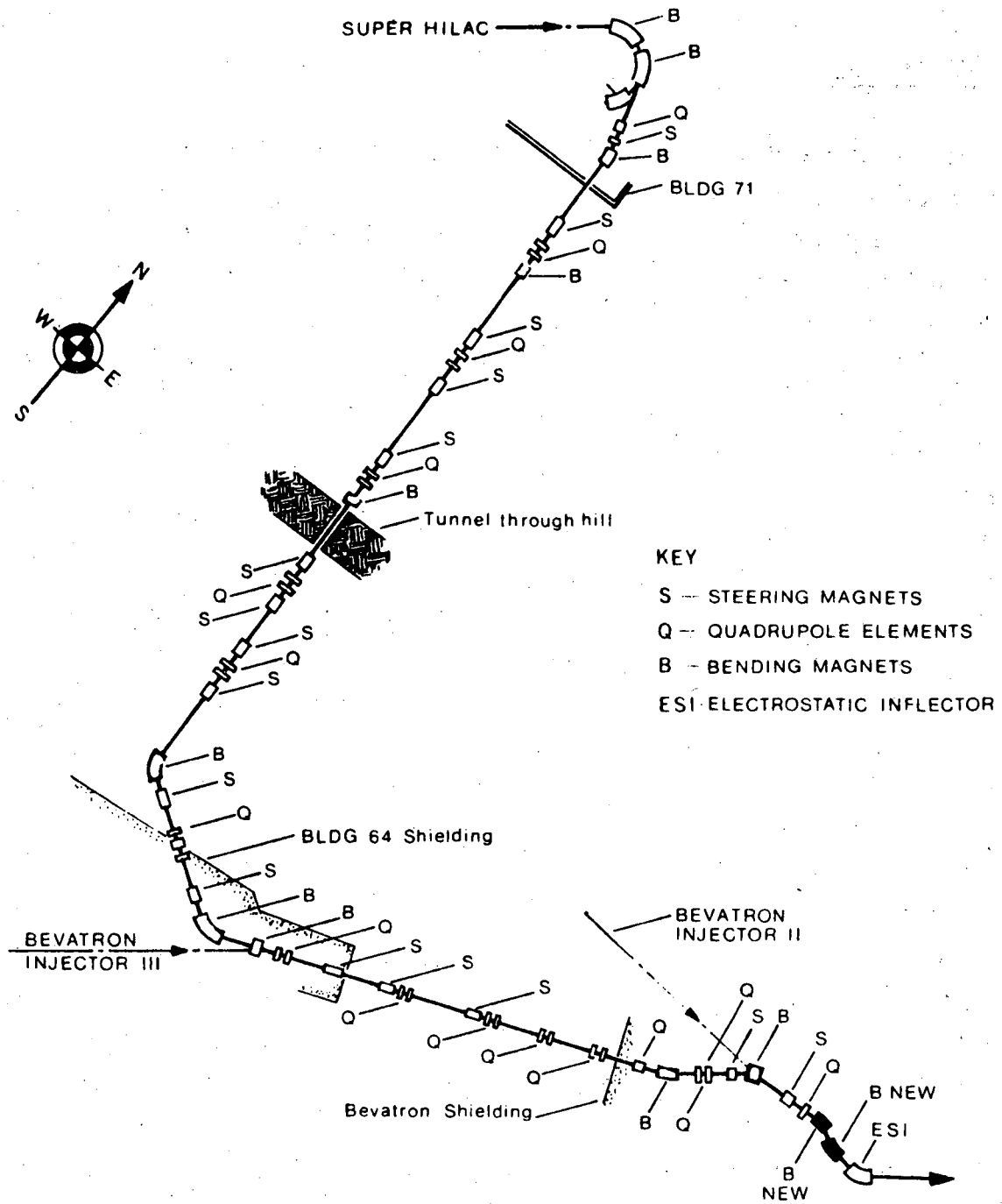

Figure D-1. Schematic of Bevalac transfer line (XBL 766-8100A).

E. BEVATRON VACUUM IMPROVEMENT

E1 VACUUM GOAL

The vacuum necessary to accelerate partially-stripped ions in the Bevatron is directly dependent on how easily these ions undergo charge-exchange interactions with residual gas atoms. Any change in charge state will cause the ion to spiral into the vacuum chamber walls and result in the loss of that ion from the beam. An evaluation of expected beam survival in the Bevatron is shown in Fig. E-1. This graph is based on experimental measurements, conducted at the SuperHILAC, of electron pickup and loss cross sections in nitrogen gas for Ar, Kr, Xe, and Pb ions at energy values up to 8.5 MeV/amu. It is seen that a molecular density corresponding to 10^{-10} Torr of N_2 at room temperature will provide a very comfortable safety margin for the survival of all ion species stripped at the SuperHILAC exit.

Residual hydrogen gas in the vacuum chamber was measured to have a much lower probability of causing charge exchange, so the molecular density of H_2 in the Bevatron can correspond to $\sim 10^{-8}$ Torr of H_2 (room temperature) without significant loss of beam.

Pressure within a vacuum system, strictly speaking, is a force per unit area due to kinetic motion of the gas molecules. However, vacuum ionization gauges that are used to measure "pressures" below 10^{-3} Torr really measure molecular density instead. As a result, the term "pressure" has become virtually synonymous with "molecular density." Charge-exchange interactions with residual gas (about which the project is primarily concerned) are proportional to molecular density (for any given gas). Pressure and molecular density are proportional at a constant temperature. However, pressure varies inversely as absolute temperature for constant molecular density. Since various portions of the new Bevatron vacuum system operate at widely different temperatures, and since molecular densities are the primary concern, pressures throughout this report (unless stated otherwise) are the room temperature (293°K) pressures corresponding to the molecular density within the region being considered. In other words, it is the pressure that would exist at room temperature for the

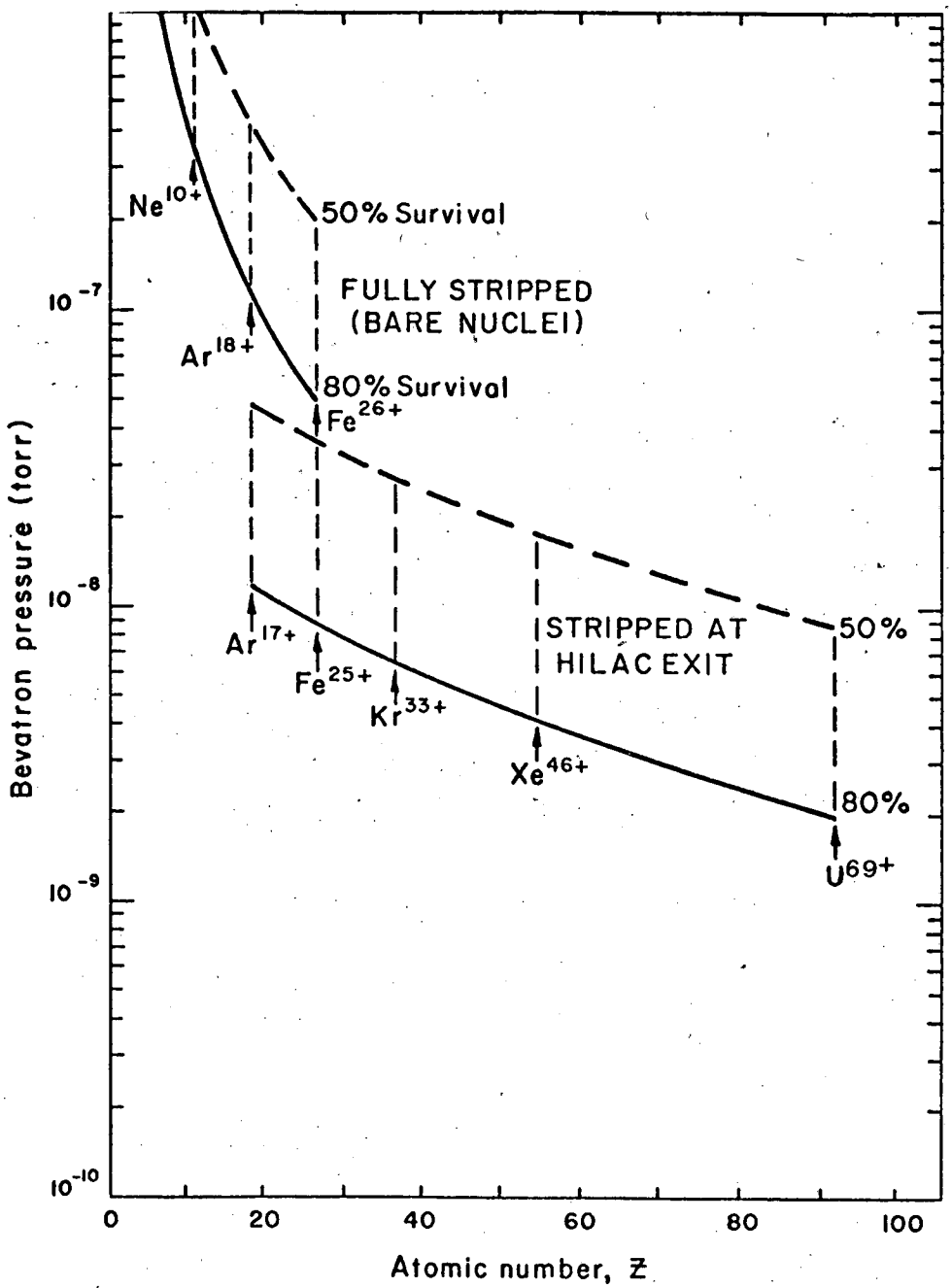

Figure E-1. Survival of heavy ions through the full Bevatron acceleration cycle as a function of molecular density, expressed as room temperature equivalent pressure (XBL 827-10670).

same molecular density. Pressure is expressed in Torr (mm Hg, 0°C) where 760 Torr equals one atmosphere of pressure.

E2 DESIGN APPROACH

In the past, pressures in the Bevatron ranged from the mid-10^{-6}-Torr range down to the mid-10^{-7}-Torr range. To achieve the greatly lowered pressure (10^{-10} Torr) required for acceleration of the heavier ions, the new design approach had to make very significant improvements with respect to both reducing gas load and increasing pumping speed.

The basic approach was to install a new cryogenically-cooled liner (cold bore) inside of the existing Bevatron vacuum chamber, as shown in Fig. E-2 and succeeding figures. The Bevatron particle beams now are circulating within this new cold-bore liner. The interior surfaces of the liner are maintained at a temperature of ~12°K throughout the quadrants and the west tangent region (91 percent of the Bevatron circumference) and generally at ~80°K in the other tangent regions. At these temperatures, the outgassing of the cryogenically-cooled surfaces is virtually zero. Two magnets in the tangent regions are impractical to cool to cryogenic temperatures so they operate at near room temperature, but are encapsulated in a stainless-steel shell. Thus, the gas load within the beam circulation region of the Bevatron has been greatly reduced.

The 80°K surfaces effectively "pump" CO_2, water, and organic vapors, while the 12°K surfaces pump N_2, O_2, CO, and some other gases. H_2, and to some extent He, are pumped by activated charcoal surfaces maintained at ~12°K. This resulted in an enormous increase in pumping speed over the old system.

The "beam stay-clear" region for the new cold-bore liner is 15.2 cm vertically (±7.6 cm about midplane) and 110 cm radially (from 1468 cm R to 1578 cm R). All components were designed so as not to interfere with this region, even with anticipated installation position errors. The stay-clear region for beam being extracted from the Bevatron is discussed in Section E3.3.3.

A detailed description of the new cold-bore approach is presented in Section E3, the calculated performance of the system is described in Section E4, and some initial performance results for the new systems are described in Section E5.

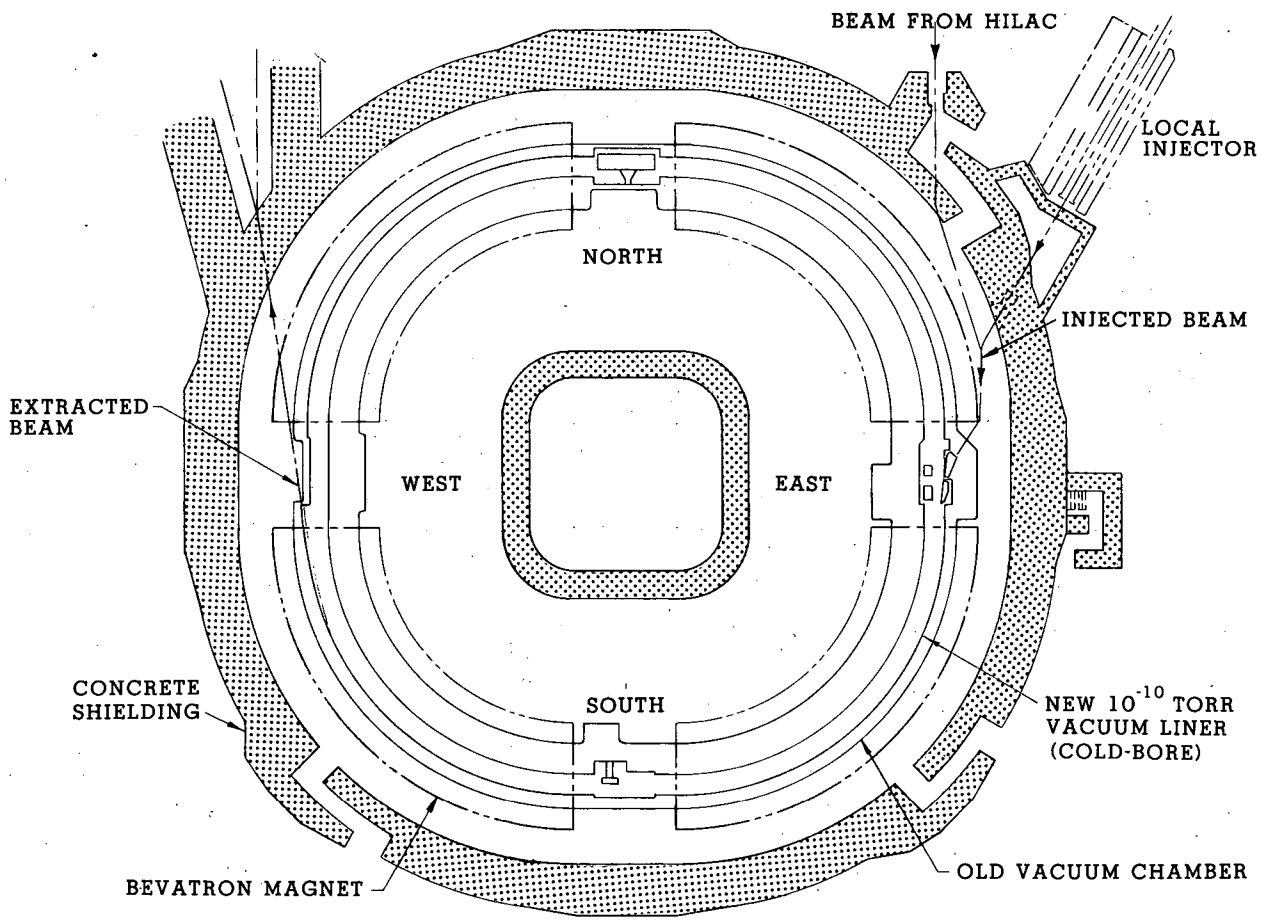

Figure E-2. New Bevatron cold-bore vacuum chamber (in red) within existing old chamber (BBC 827-6055).

E3 SYSTEM DESCRIPTION

E3.1 Quadrant Modifications

In the Bevatron quadrant (curved) regions, the principal modification was the fabrication and installation of new, cryogenically cooled liners.

E3.1.1 Quadrant Liners

As shown in Figs. E-3 through E-6, the quadrant liners are basically multi-wall curved rectangular tubes. They consist of three concentric boxes with multi-layer superinsulation between them to minimize heat transfer. The outer box rests between the magnet poles of the Bevatron at near ambient temperature (~300°K). It is surrounded by a vacuum of ~10^{-6} Torr (frequently referred to herein as the "guard vacuum"). The intermediate box is cooled to a temperature of ~80°K while the inner box is cooled to ~12°K.

The floor, ceiling, and walls of the inner box (12°K) were fabricated of printed-circuit-board material consisting of 3-mm-thick fiberglass-reinforced plastic (FR-4) clad with 2-ounce (0.7-mm) copper on both sides. Both sides of the floors and ceilings of the liner boxes have a striped pattern etched into the copper (0.25-mm etching between 1-mm copper strips) as shown in Fig. E-7. The striped pattern minimizes eddy currents due to the time-varying Bevatron magnetic field, yet provides sufficient thermal conduction to keep the boards cool because of copper's enhanced conductivity at cryogenic temperatures. A central stripe provides an electrically-continuous path through each quadrant to carry image currents induced by the circulating ion beam. The image stripe is capacitively-coupled with resistive damping at the tangent regions to prevent the formation of a closed loop that could pick up large induced currents from the time-varying Bevatron magnetic field. The floor and ceiling circuit board panels for the inner (12°K) and the intermediate (80°K) boxes were made almost 1.2 m wide by 3.33° arc (0.9 m) in the beam direction, which economically utilizes standard 0.9-m x 0.9-m printed-circuit panels. The outer and inner edges of these panels were cut to a radius to match the curvature of the Bevatron quadrants. The sidewalls of the boxes are also stripe-etched with the same pattern as the floor and the ceiling.

The floor, ceiling, and sidewalls of the outer box (300°K) were constructed of unclad, fiberglass-reinforced plastic (polyester) panels. Otherwise, their construction is similar to that for the inner and intermediate boxes.

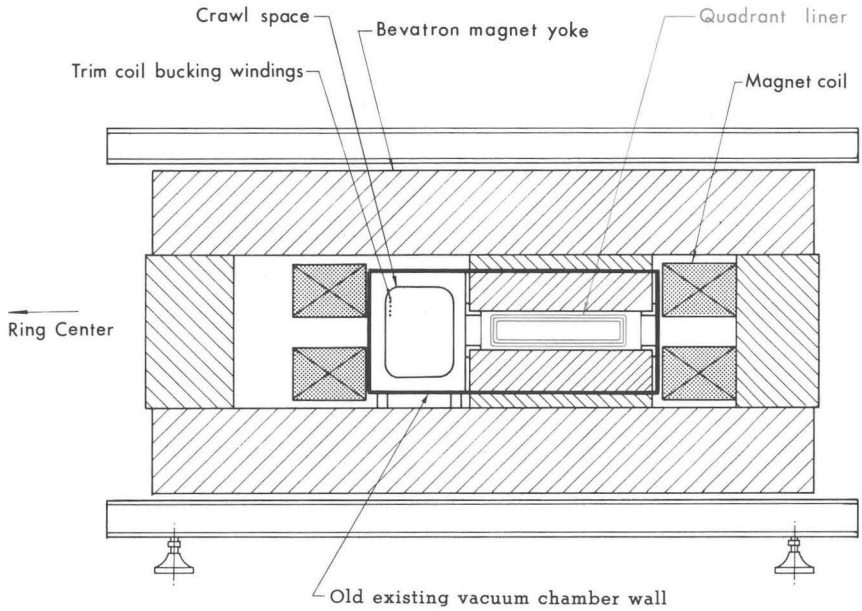

Figure E-3. Typical quadrant cross section (new construction shown in red) (BBC 827-6051).

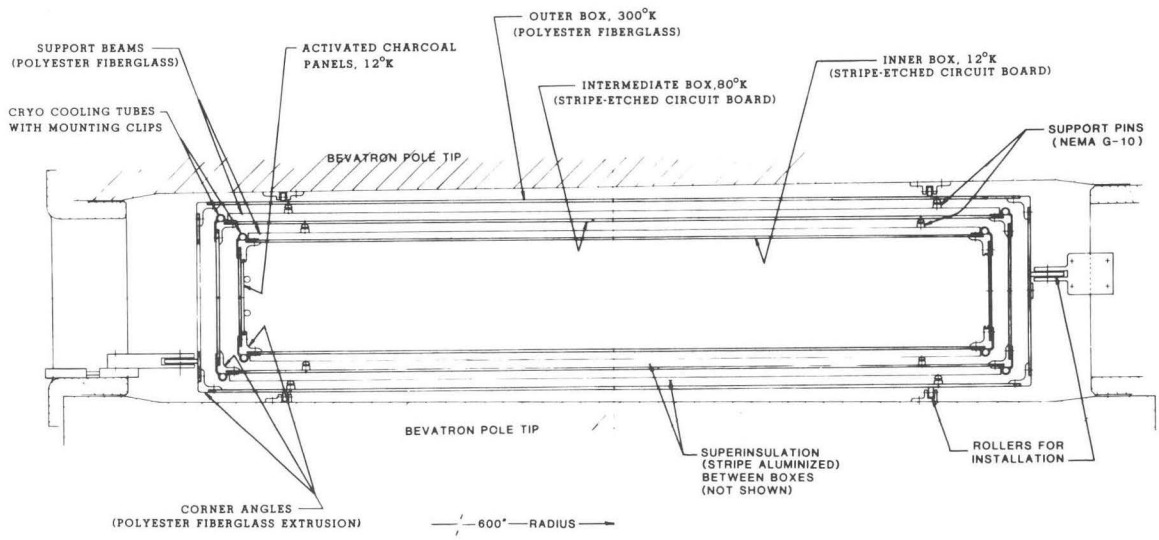

Figure E-4. Enlarged cross section of new quadrant liner installed between Bevatron pole tips (XBL 828-10996).

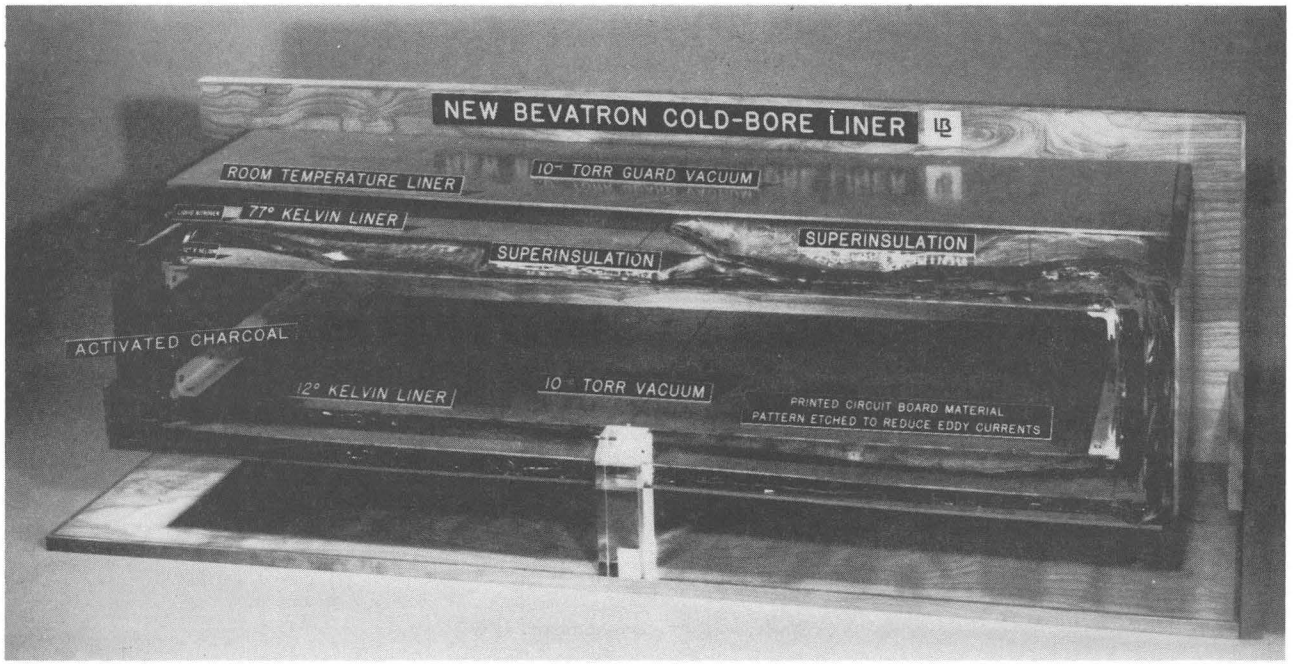

Figure E-5. New quadrant liner model (CBB 817-6460).

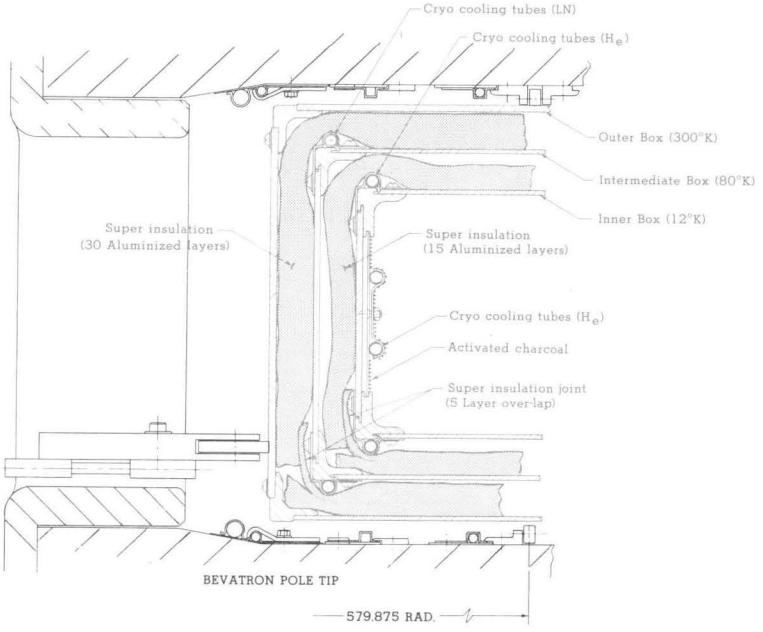

Figure E-6. New quadrant liner details, transverse section (new construction shown in red) (BBC 827-6049).

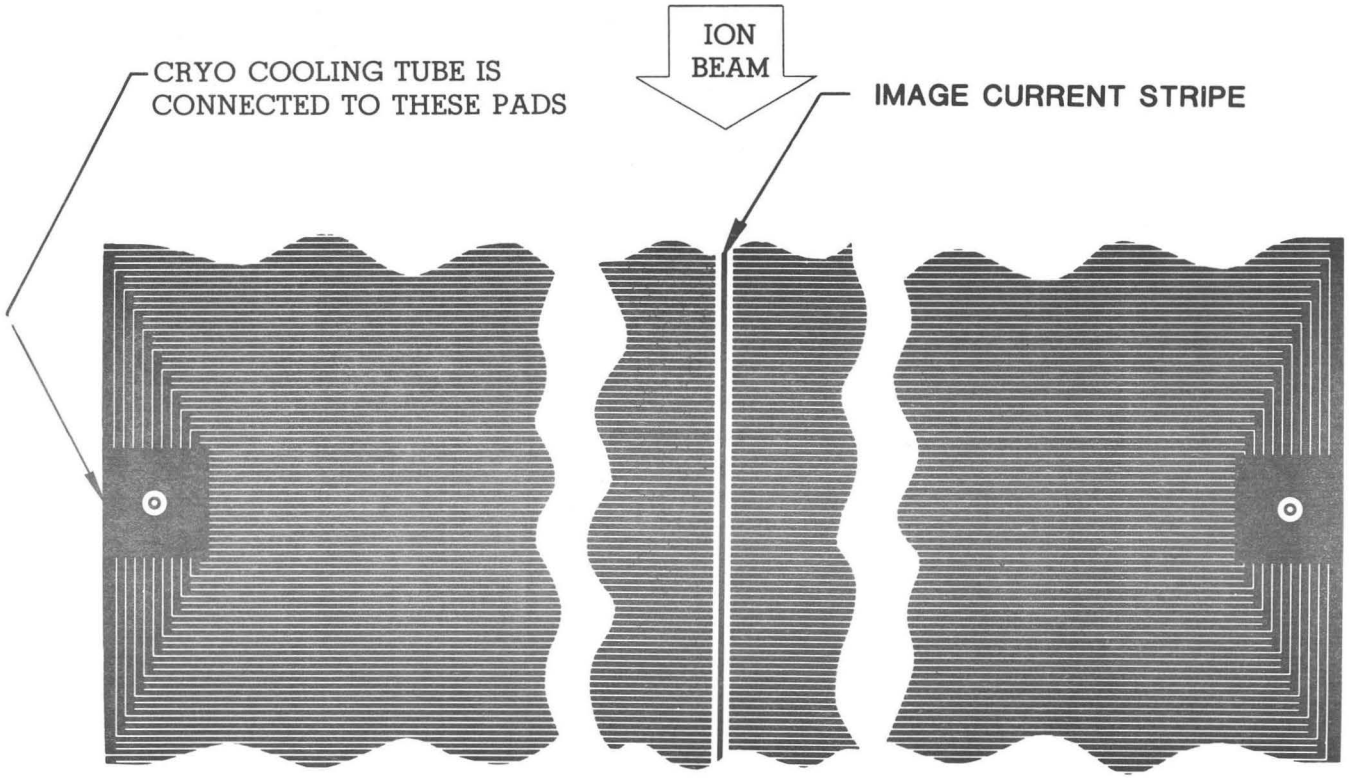

Figure E-7. Etched pattern on printed-circuit boards of quadrant liner. Dark portions are copper while light portions are etched away (shown approximately full size) (XBL 827-10683).

The corners of the boxes are fiberglass-reinforced-plastic "pulltruded" angles with a custom configuration for each type of box. Threaded inserts were placed into the corner angles so that screws could be used to assemble the boxes. The three boxes (inner, intermediate, and outer) are spaced away from each other by fiberglass-reinforced-plastic standoffs that were designed to minimize heat transfer while still fulfilling their positioning function.

The inner (12°K), intermediate (80°K), and outer boxes were each pre-assembled into modules corresponding to 10° arc (~9' arc length). Each box module had full-length corner angles, and the floor, ceiling, and wall were each made up of panels ~3.3° in arc. The 10°-arc length was selected as the longest module that was realistically consistent with the installation method used (see next subsection). Radial beams of fiberglass-reinforced plastic support the joint between adjacent 3.3° floor and ceiling panels. The radial beams at the ends of each 10° module incorporate a tongue-in-groove expansion joint to accommodate the 1 cm thermal contraction during cooldown. These end beams also were designed to accommodate hairpin expansion loops in the refrigerant tubing. The joints in the boxes effectively are labyrinth seals so that almost all gases (except hydrogen and helium, which will be discussed later) are pumped before they can get through the joints. Figure E-8 is a photo of several quadrant modules (without tubing) temporarily joined together to check fit and alignment. Figure E-9 is a diagram giving specification numbers for each cold-bore module.

Curved cold-bore Modules 19 through 21 (near the exit of Quadrant II) had to be specifically modified on the outer-radius sidewall to stay clear of the path for the extracted ion beam. Module 19 has a slight bulge in the outer wall. The bulge becomes bigger through Modules 20 and 21. Module 21 incorporates a vertical septum wall (12°K) that separates the extracted beam from the circulating beam. Figure E-10 shows a photo of Module 21.

At both ends of all four quadrants, there are short, straight, 12°K cold-bore sections that pass through the transition regions from the curved sections to the four tangent tanks. Modules 1, 12, 25, and 36 (at the upstream end of each quadrant) are the same height and are of similar construction to the curved cold-bore sections. Modules 11, 22, 35, and 46 are taller so as to accommodate beam probes and clippers (see Section E3.2). Figure E-11 is a cross section through one of the transition liners which shows the rolled

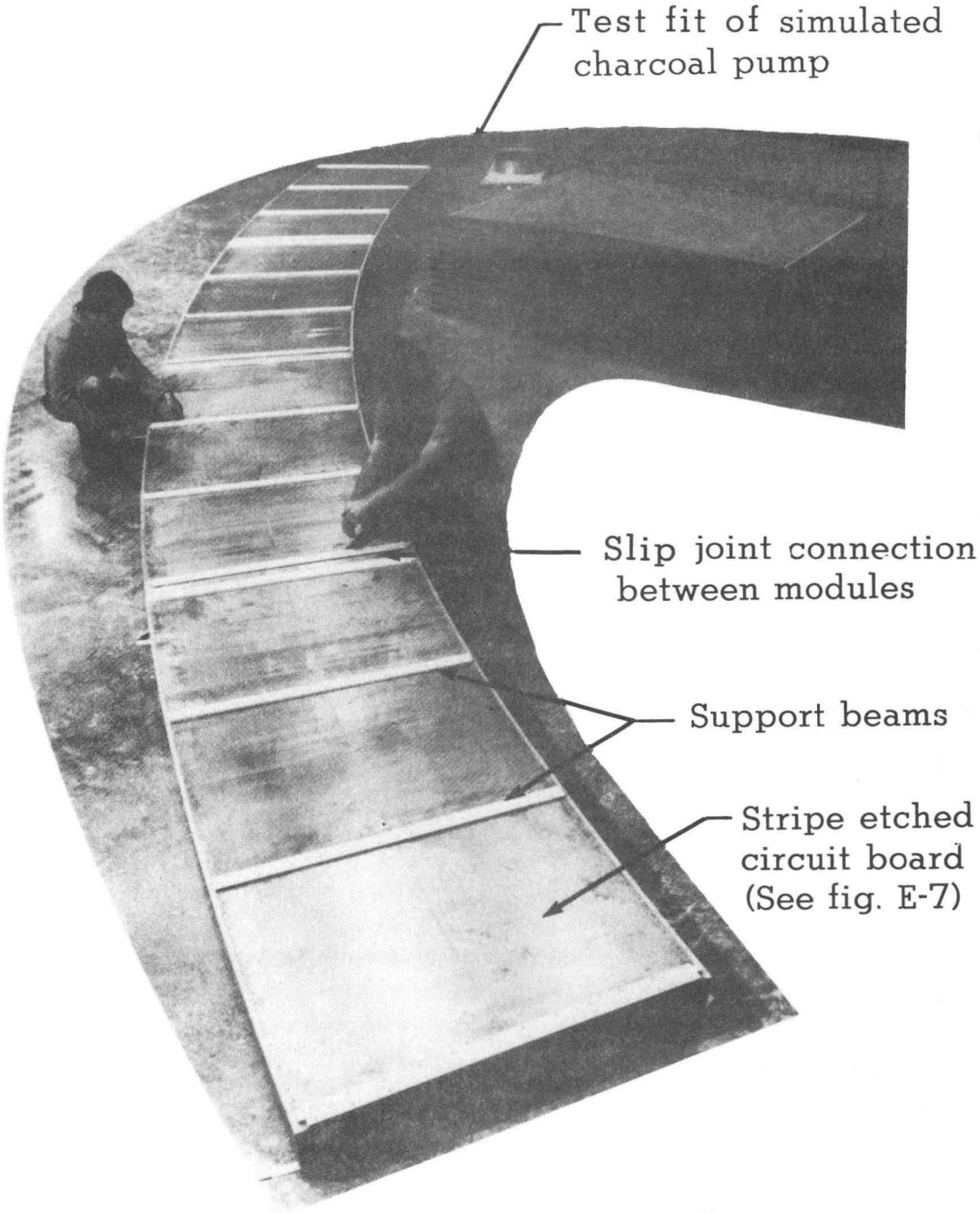

Figure E-8. Pre-assembly check of four inner-box (12°K) modules. Shown without tubing (XBB 815-4082A).

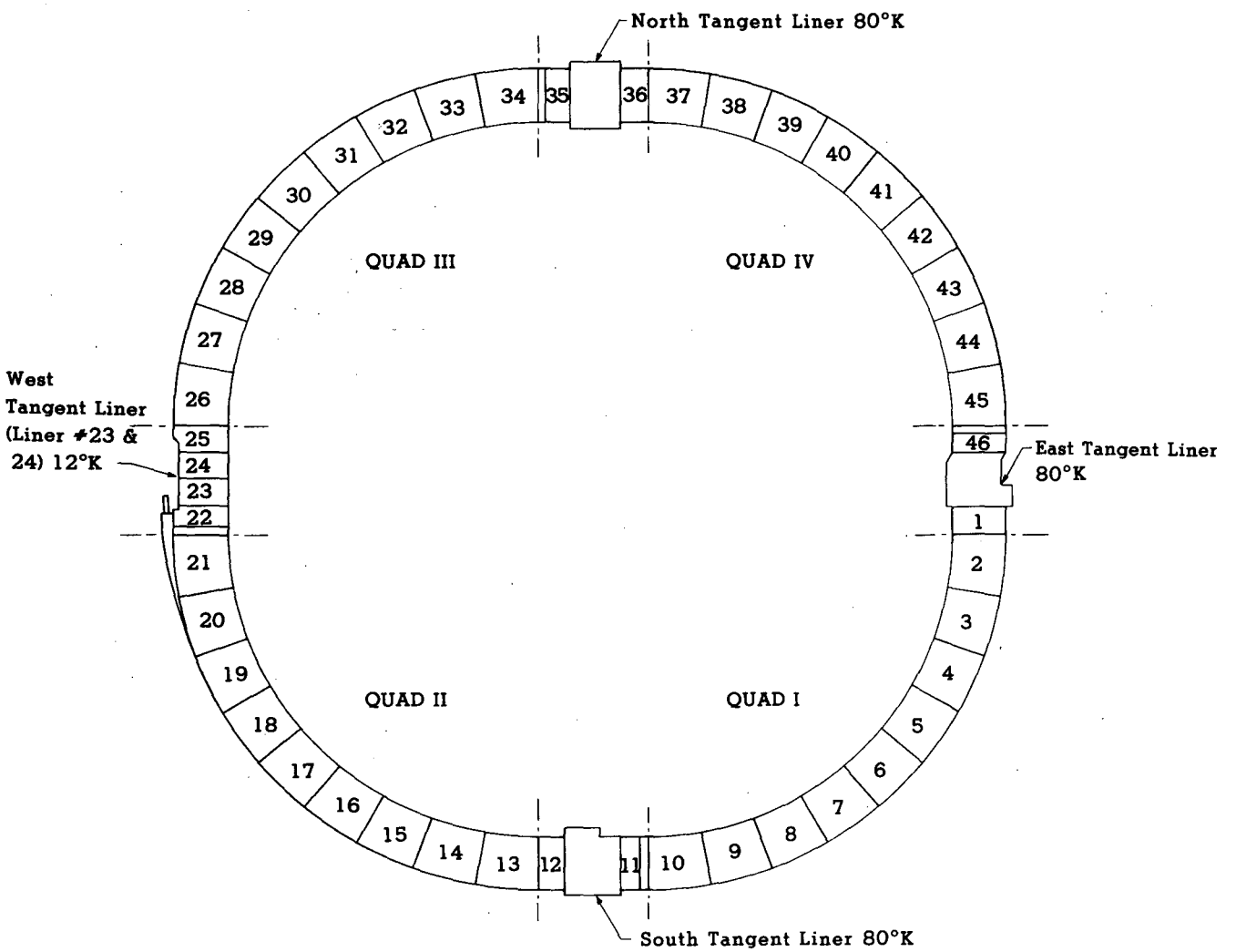

Standard curved cold-bore liners: #2-10, 13-21, 26-34
Special curved cold-bore liners: #19, 20, 21
Tall transition cold-bore liners: #11, 22, 35, 46
Regular transition cold-bore liners: #1, 12, 25, 36
} ~12°K

North, East & South tangent liners operate at 80°K

West tangent liner operates at 12°K

Figure E-9. Quadrant module identification numbers (XBL 827-10673).

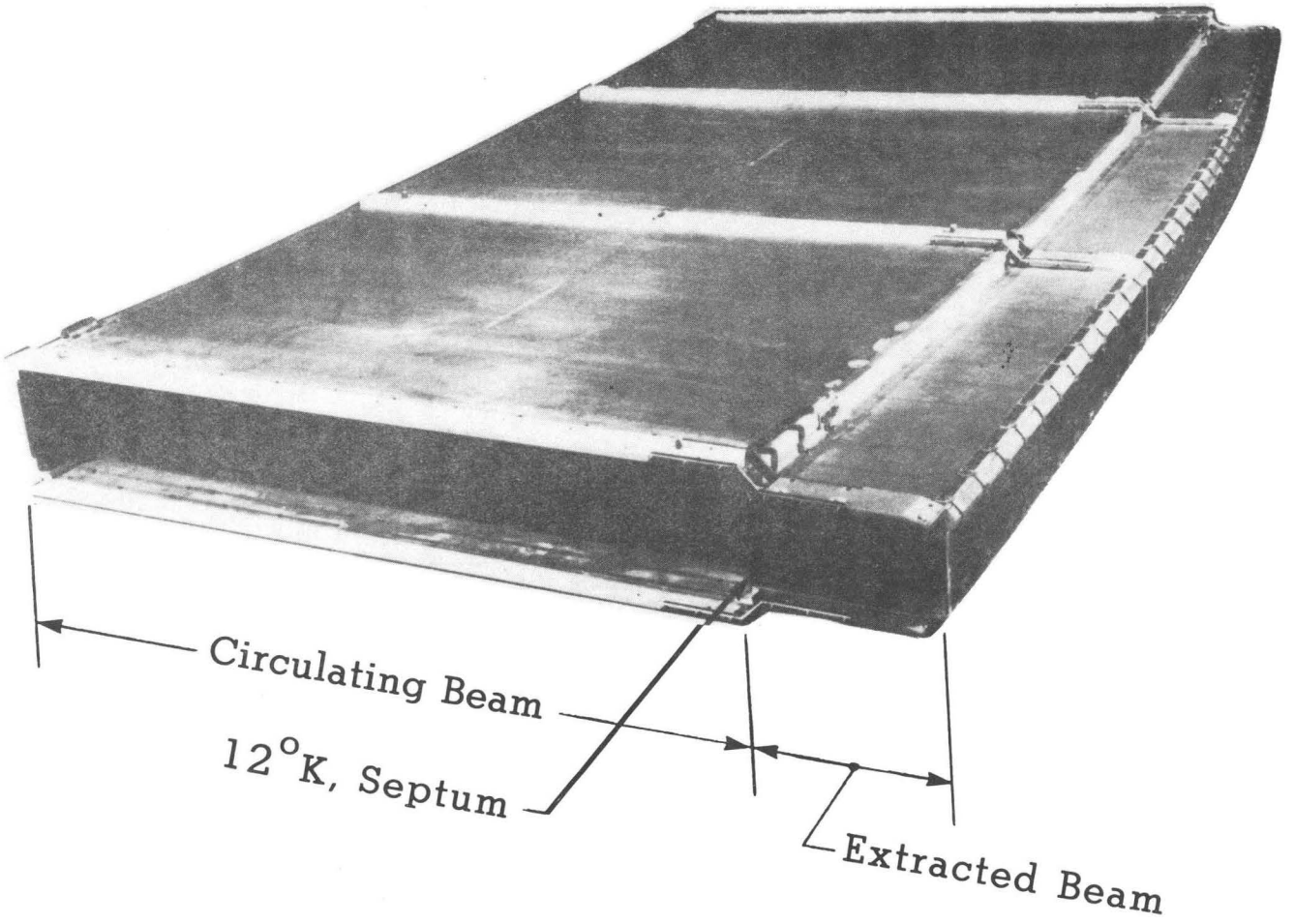

Figure E-10. Quadrant liner Module 21, inner-box (12°K) subassembly without tubing (XBB 818-7570).

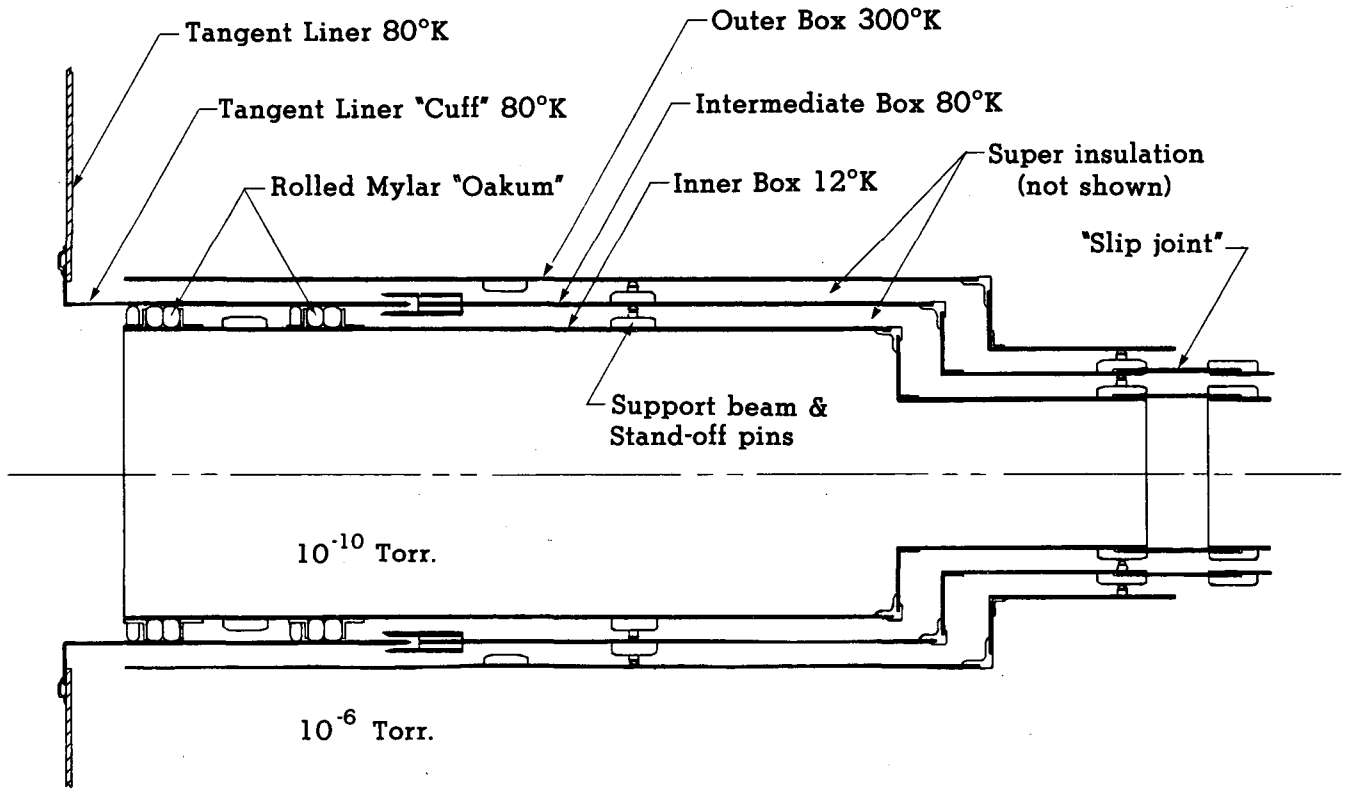

Figure E-11. Longitudinal section through transition cold-bore Module 35 (XBL 827-10682).

mylar "oakum" that was stuffed into the joint where the transition liner joins the 80°K tangent liner section to minimize leakage of hydrogen (or helium) into the cold bore.

The corner angles of the inner box (12°K) have grooves to receive vertical sheet metal panels. The panels adjacent to the inner-radius walls (nearest the center of the Bevatron) have activated-charcoal pellets epoxied to the surface. At 12°K, these pellets will pump hydrogen and, to some extent, helium. A refrigerant (12°K) tubing loop is soldered directly to these panels so that the pellets can be separately warmed (~100°K) for regeneration of their pumping capability. These panels correspond to 90° arc and can be withdrawn through the tangent tank if major servicing should be required. Plain bronze panels were installed in the grooves adjacent to the outer-radius walls in Quadrants I and II (except in the extra-width "extraction" Modules 21, 20, and 19) so that any beam loss onto these walls would strike metal rather than plastic.

Multi-layers of aluminized mylar, called "superinsulation", are commonly used for cryogenic thermal insulation. Conventional superinsulation could not be used because the time-varying magnetic field of the Bevatron would have induced excessive eddy currents in the thin aluminum coating on the mylar. Instead, stripe-aluminized mylar was used in which both sides of the 0.006-mm thick mylar sheet were stripe-aluminized with 1.2-cm-wide stripes separated by a 0.25-cm-wide unaluminized band inbetween. The stripes on top of the superinsulation sheets were shifted one-half pitch relative to the stripes on the bottom so that the nonaluminized regions did not line up and permit thermal radiation to pass through. Crinkled, clear 0.01-mm thick mylar sheets were interposed between the stripe-aluminized sheets to prevent the top of one stripe-aluminized sheet from electrically shorting out stripes on the bottom of the next stripe-aluminized sheet. Successive sheets were stacked into blankets such that the inner blankets (between inner and intermediate boxes) consisted of 16 crinkled mylar sheets interposed with 15 striped sheets, while the outer blankets (between intermediate and outer boxes) consisted of 31 crinkled mylar sheets interposed with 30 striped sheets. Where blankets joined, the sheet edges of the adjacent blankets were "shuffled" to minimize heat leakage. Extra strips of clear mylar sheets were interposed at these joints to prevent a stripe-aluminized sheet of one blanket from electrically shorting stripes on the adjacent blanket.

The inner box is cooled by stainless-steel tubing outside of the four corners of the box. This tubing carries helium gas at ~12°K. Special copper clips were soldered to the tubing during installation such that holes in the clips aligned exactly with the eye of the pad of the printed-circuit pattern (see Fig. E-7). Mating surfaces of the clips and the circuit board were "pre-tinned" with a gallium alloy to get good thermal conduction when the joint was screwed together at installation. The number of weld joints in the tubing (possible sources of leakage into the ultra-vacuum) was reduced to a minimum by utilizing the longest commercially-available lengths of tubing, corresponding to ~80° of arc. Those welded joints that were necessary were located so as to be as accessible for inspection as possible but, unavoidably, some are not readily accessible. The intermediate box is similarly configured except that the refrigerant tubes carry liquid nitrogen (~80°K) at slightly above atmospheric pressure.

Louvered openings in the intermediate (80°K) box, together with coincident full openings in the outer 300°K box and in the superinsulation, provide cryopumping of the 10^{-6}-Torr guard vacuum regions. In this arrangement, H_2O, CO_2, and organics will be pumped on the 80°K louvers, while CO, N_2, and O_2 will pass through the louvers and will be pumped on the 12°K wall. The louver area was selected to provide essentially the same amount of cryopumping speed as existed for the cryopanels that previously had been in the Bevatron.

E3.1.2 Quadrant Installation

The Bevatron was turned off on July 6, 1981 to commence installation related to this project. Quadrant cold-bore liner modules were installed from the tangent regions to avoid dismantling the quadrants of the Bevatron. The modules for each quadrant were installed from the tangent region immediately downstream, i.e., Quadrant I (southeast) from the south tangent region, Quadrant II from the west, etc. (see Fig. E-9). Small rollers were installed on the top, bottom, and sides of the Bevatron magnet gap. The full-length refrigerant tubes were pre-installed in the downstream quadrant. Then, a special installation fixture was placed at each tangent region.

Module 1 was assembled onto the installation fixture in the following sequence:

a) assemble inner box,

b) attach 12°K refrigerant tubes,

c) place and shuffle inner superinsulation blankets,

d) assemble intermediate box around the inner box,

e) attach 80°K refrigerant tubes,

f) place and shuffle outer superinsulation blankets,

g) assemble outer box around assembly.

Module 1 and the refrigerant tubes then were moved into the quadrant just far enough to permit assembling Module 2 in the same sequence as above. This "assemble, move-forward" sequence was repeated for each module through Module 11, after which the completed quadrant liner was pushed forward to its final position. The installation for the other three quadrants was done similarly.

The west cold-bore liner Modules 23 and 24 were installed immediately after all quadrant cold-bore liners had been installed. Then, in September 1981, the Bevatron was evacuated and the cryogenics systems were turned on; it was verified that the heat load of the cold-bore modules was well within the refrigeration capability of the cryogenic refrigerators.

E3.2 Beam Instrumentation

The Bevatron employs instrumentation and monitoring for control and tuning of the ion beams. New beam diagnostic equipment, as diagrammed in Fig. E-8, had to be built for compatibility with the spatial, vacuum outgassing, and cryogenic temperature requirements of the new liner. Future instrumentation can be added as shown in Fig. E-12.

E3.2.1 Beam Induction Electrodes

The beam induction electrode system (located in the south tangent region) provides information on beam intensity, radial position, and beam-bunch phase. The active electrodes consist of a continuous "sum" electrode and a split "difference" electrode. A ground plane is located adjacent to the ends of both active electrodes and is electrically isolated from the active electrodes and from the 80°K liner box. Radial information can be obtained from the individual halves of the difference electrode, while total beam-current and beam-phase information can be obtained from the sum electrode. A re-entrant section was made in the outer tangent tank cover to allow close proximity of the preamplifiers to the electrodes.

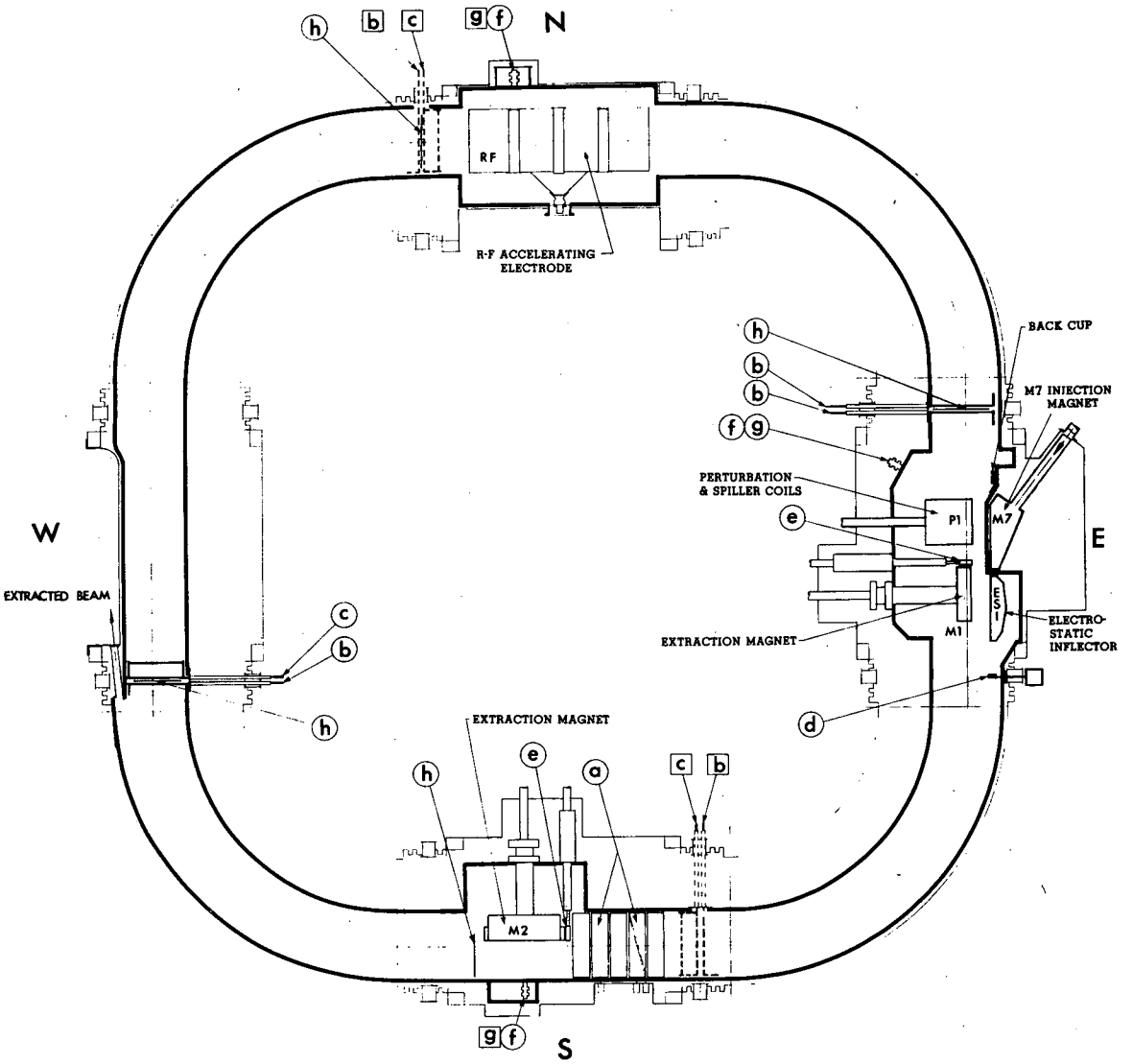

Figure E-12. Bevatron beam instrumentation (XBL 827-10672).

a.	Beam induction electrode	e.	Multi-wire chambers
b.	Finger probes	f.	Ion gauges
c.	Vertical clippers	g.	Residual gas analyzer
d.	Inflector (E.O.S.) cup	h.	Fixed beam scraper

= Newly installed (this project) = Possible future instrumentation

E3.2.2 Finger Probes

A radially-positionable pair of finger probes in the east tangent region and a single finger probe in the west tangent region provide beam diagnostics as well as radial beam position and width information necessary for tuning the resonant extraction system. Each finger probe consists of a shaft on the end of which is mounted a 1.25-cm square metal finger ~18 cm long which can be flipped up into the beam aperture in 300 nsec (measured as 210 msec going up and 320 msec coming down). The finger is electrically isolated from the shaft and an electrical coaxial lead is used to carry the signal through the shaft to the outside. The finger end of the probe is located in the tall transition cold-bore liner (Modules 22 and 46) so the finger will operate at temperatures approaching the 12°K temperature of the liner.

The shaft passes through the wall of the cold-bore liner and then through the main vacuum chamber wall to the outside. The penetration through the cold-bore wall incorporates a cryogenic seal, as shown in Fig. E-13, in which almost all of the gas which tries to get through the seal is pumped on a surface cooled to ~12°K. An 80°K shroud (garage) radiantly cools ~1.5 m of shaft length outside of the cold-bore wall so that there will not be excessive heat radiation to the 12°K cold bore when the probe is inserted. The drives provide a radial motion of 91 cm maximum, and are initially set with the outermost position of the outer face of the finger at R = 15.70 m (618") and R = 15.79 m (621.5") for the two probes in the east, and at R = 15.80 m (622.1") for the single probe in the west.

A support frame, which supports and positions the finger probe shaft, engages pre-installed alignment sockets in the floor of the tall transition cold-bore liner. The finger probes, together with their associated support frame and cryogenic seals, can be removed for servicing (if the Bevatron is not under vacuum). The finger probes are actuated by driving mechanisms that are outside of the vacuum.

Space is available to add a pair of finger probes in the north region and a single finger probe in the south region should it prove desirable to do so in the future.

E3.2.3 Vertical Clippers

A single horizontal bar target provides vertical beam diagnostic information. The bar, 1 cm in diameter, covers the full radial aperture of the Bevatron beam, and can be moved vertically through the beam in 200 msec

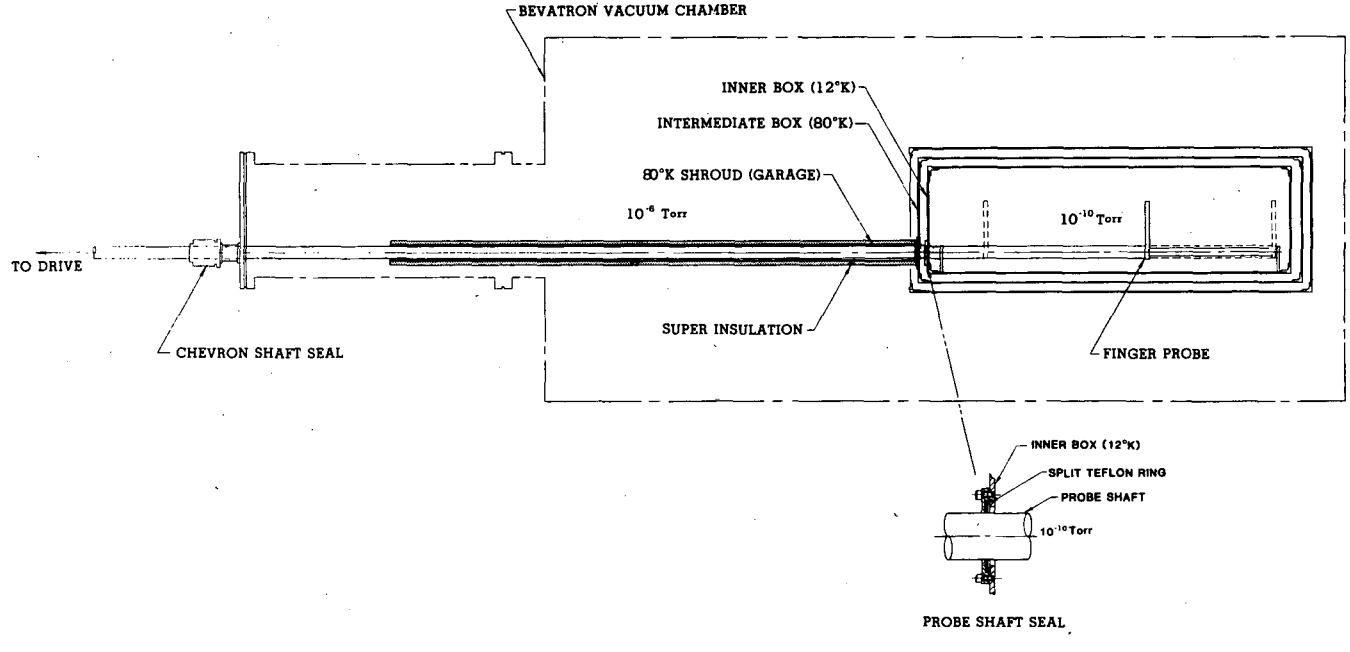

Figure E-13. Finger probe assembly, transverse section (XBL 827-10680).

(measured as 200 msec going up and 250 msec coming down). Presently, there is one vertical clipper in the west tangent region, but others can be added in the north and south, and possibly in the east tangent region, in the future. The clippers are mounted similarly to the radial finger probes with the locking mechanisms located outside of the vacuum. The penetration through the cold-bore liner has a cryogenic seal similar to that for the radial finger probes.

E3.2.4 Inflector Cup

A fast-plunging Faraday cup at the exit of the electrostatic inflector (East Outside South) can be inserted into the injected beam to provide information for tuning the injection line and preventing unwanted beam from being injected into the Bevatron. The probe is withdrawn whenever beam is to be injected into the Bevatron. The cup contains vertical 0.25-mm diameter gold-plated tungsten wires on 1.6-mm centers, and similar horizontal wires on 0.5-mm centers to give beam-profile information. The beam which does not strike the wires is collected in a carbon cup to indicate total beam current. The cup assembly is cooled by liquid nitrogen in order to reduce heat load radiated to the 12°K cold-bore liner and to minimize outgassing from the cup. The cup is supported by a shaft that goes outside of the vacuum and which has a cryogenic seal (somewhat similar to those for the finger probes) where the shaft penetrates the cold-bore liner. The cup is actuated from outside the vacuum. The cup travels through a stroke of 7 cm in 200 msec (measured as 200 msec going in and 200 msec coming out).

E3.2.5 Back Cup

Ions injected into the Bevatron oscillate about the equilibrium orbit and, after every three revolutions, the ions return to the outer radius where they come close to, or hit, the electrostatic inflector or the outboard wall of the east liner tank adjacent to the BL18MH (IHM7) injection magnet. To facilitate tuning of the injected beam, an electrode was installed on the outboard wall of the east liner tank to intercept beam that otherwise would have hit the liner tank or the electrostatic inflector. Historically, this electrode has been called the "back cup." The electrical signal from this electrode is carried by a cable that passes through the tangent cyropump in the ceiling of the liner tank (and is therefore cryo-sealed) and then to the outside world.

E3.2.6 Multi-wire Chambers

Two new movable multi-wire chambers, somewhat similar to previous ones, are used with the plunged beam extraction system. One chamber is located just upstream of the M1 extraction magnet in the east tangent tank, while the other is placed just upstream of the M2 extraction magnet in the south tangent tank. Each chamber contains 0.05-mm (0.002") wires on 3-mm (0.12") centers, both vertically and horizontally, and is filled with a mixture of 80-percent argon/ 20-percent carbon dioxide at approximately one atmosphere pressure absolute. Filling is accomplished through a tube from the outside so that the chamber can be evacuated to determine if it is a possible source of leakage into the ultra-vacuum. The upstream face of the chamber is stainless-steel foil 0.25-mm thick to facilitate measurement of low-energy heavy ions. A resistive heater is built into the wire chamber assembly to keep the temperature from dropping below -75°C and thus to avoid condensation of the internal gas mixture.

Each chamber is mounted on the end of a shaft which passes through the tangent cold-bore liner (80°K) and through the tangent-tank wall to the outside. A 12°K proximity seal was installed where the shaft penetrates through the tangent cold-bore liner so that there is high probability that any gas molecules (e.g., N_2, O_2) trying to get through the seal will be pumped on the 12°K surface. The chamber and its support shaft are actuated from outside of the vacuum system. In normal operation, the chamber is parked in its retracted position where it does not intercept beam. When the chamber is to be used, the plunged extraction magnet (M1 or M2) is stopped in its retracted position. Then, a pneumatic cylinder is activated to push the cylinder inward until it engages an alignment socket on the magnet which positions the chamber relative to the aperture of the magnet. Pneumatic pressure continues to push the chamber into its socket such that, when the magnet is plunged and then retracted, the chamber remains engaged into the socket of the magnet. The chamber is withdrawn to its retracted position when it is no longer needed. Interlocking has been provided to automatically retract the chamber should the chamber fail to remain fully seated in the socket.

E3.2.7 Fixed Scrapers

The plastic rollers used for quadrant cold-bore installation (see Section E3.1.2) were installed in the fall of 1980, and were in place while the Bevatron was operated from January through June, 1981. After opening the

Bevatron, it was noted that some of the rollers had suffered radiation damage due to being struck by beam, probably during the first few turns. This raised the concern that beam striking onto the printed-circuit boards of the new cold-bore liner might result in sufficient radiation damage to cause copper stripes to peel off and obstruct the beam.

To alleviate these concerns, it was decided that fixed beam scrapers would be installed so that most, if not all, beam striking the walls would hit metal surfaces. In the south region, a pair of scrapers (one above and one below the beam aperture) were installed on the downstream face of the new tangent liner tank. This azimuthal location is favorable because it is near maximum vertical amplitude for injected ions leaving the electrostatic inflector with an upward or downward component of velocity. In the north, east, and west regions, a pair of scrapers (one above and one below the beam aperture) were attached to the support frame for the radial finger probes (Section E3.2.2). The scrapers have a clear vertical aperture of 14 cm and are at least 1.25-cm-thick plate (some aluminum and some stainless steel), which is sufficient to fully stop ions at injection energy. Each plate is electrically isolated and a signal wire is brought outside so that beam striking the scrapers can be sensed.

Adjustable vertical scrapers have been installed in the injection line upstream of the BL17MH (IHM6) magnet. It is planned that these scrapers will be adjusted to the point where beam is no longer sensed on the fixed-beam scrapers inside of the Bevatron, and then these injection-line scrapers will remain fixed at that position.

E3.2.8 Beam Electronics and Control

Implementation of the aforementioned items required modifications to the electronics and control system. A new set of preamplifiers and superheterodyne systems for monitoring the circulating heavy-ion beams was built to interface with the new beam induction electrode system. The new finger probes required revised control and interlocking as well as new preamplifiers and associated electronics for the electrically-isolated probe fingers. Minor changes to the controls and interlocking for the new vertical scrapers and the inflection cup were required. The multi-wire chambers required new electrical leads and also required special motion interlocking with the extraction magnets, as previously mentioned.

E3.3 Tangent Tank Modifications

The old existing tangent tanks are made of hot-rolled mild steel, and are connected to corrugated stainless-steel transition sections which are then connected to the old existing quadrant (curved) tanks. The tangent tanks previously housed equipment for injection, acceleration, extraction, and diagnosis of the ion beam. Six 81-cm (32") diffusion pumps were mounted underneath each tangent tank.

New tangent cold-bore liner tanks were built and installed within the existing tangent tanks in the north, east, and south regions. The arrangements are different for each of the three tangent regions, as described in the following subsections. The west tangent region utilized cold-bore techniques similar to those for the quadrants, and is described in a following subsection.

E3.3.1 East Tangent Modifications

The main element is a new tangent liner tank, as shown in Fig. E-14, that is cooled to 80°K by liquid nitrogen flowing through tubes welded to the tank. It was impractical to cool this liner tank to 12°K (as for the quadrants) because the M1 extraction magnet operates at nearly room temperature, and the thermal radiation heat loss to 12°K would have been excessive. The liner tank was constructed primarily of 6-mm stainless-steel plate with welded joints. Cover strips were welded over each weld joint so that all weld joints could be vacuum-leak checked prior to installation. The irregular shape of the liner tank was dictated by the components that had to be accommodated. The liner tank wall adjacent to the BL18MH (IHM7) inflection magnet was machined thinner and the whole liner tank was pulled against the magnet in order to minimize the "septum" thickness between the incoming ion beam and the circulating beam.

Penetrations were provided through the liner tank wall for the support shafts of the M1 extraction magnet, the (M1) multi-wire chamber, and the perturb/spill magnet, each of which is described below. There is a 0.5-mm-diameter personnel-access port with a stainless-steel door that is sealed with Gore-tex (a Teflon-like ribbon) and heavily bolted. There are rectangular openings in each end wall for the circulating beam to pass through; these are joined to the transition cold-bore liners (Modules 1 and 46) previously described. (For this connection, see Fig. E-11.) There also is a cryo-sealed opening to accommodate the rectangular beam tube of the BL18MH (IHM7) inflec-

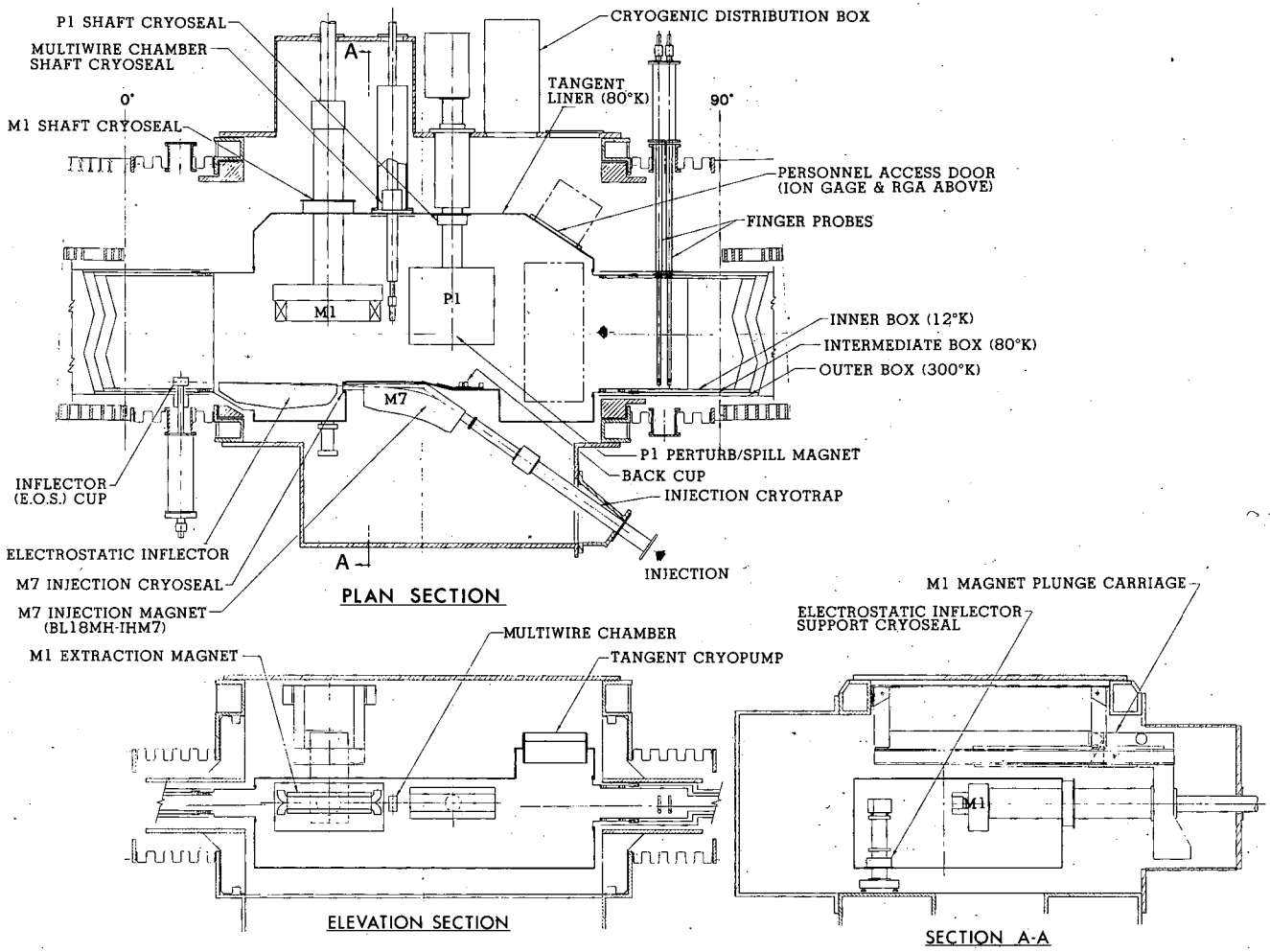

Figure E-14. East tangent region (new construction shown in red) (BBC 827-6059).

tion magnet through which the incoming ion beam enters. Small tubular housings with optically-dense baffles are welded to the inner wall to accommodate two vacuum ionization gauges and a residual gas analyzer head. In the top there is a rectangular opening to accommodate the tangent cryopump (see Section E3.4). There is another larger rectangular hatch opening, through which internal components (e.g., M1 magnet, perturb/spiller magnet) were installed, which is closed over with a stainless-steel sheet cover that is cryo-sealed around the edges as shown in Fig. E-15. In the bottom, there is a hole, also cryo-sealed, to accommodate the support post for the electrostatic inflector.

The exterior of the liner tank is covered with two blankets of multi-layer superinsulation, each consisting of 15 layers of 0.006-mm crinkled mylar aluminized on one side only, for a total of 30 layers. Since the magnetic field strength in the tangent regions is not significant, the aluminized mylar sheets were solid-coated on one side; i.e., they were not stripe-coated.

The tangent liner tank is supported by rods hung from the upper frame of the main tangent tank that are connected to the liner tank at the beam median plane. A fiberglass-reinforced-plastic (G-10) insert reduces thermal conduction to the liner tank. A flexible copper strap is connected to the bottom of the hanger rods in order to keep them near room temperature so that the rods do not contract significantly during cooldown and thereby raise the position of the liner tank. The hanger rods provide no horizontal restraint so this is taken care of by pulling the liner tank hard against the BL18MH (IHM7) magnet (as mentioned previously), and is taken care of longitudinally and yaw-rotationally by seismic restraints attached to the bottom of the liner tank. The restraints are designed so that, during cooldown, the liner shrinks longitudinally relative to the M1 plunge center line, laterally relative to the IHM7 inflection magnet, and vertically about the midplane.

The old, large inner-radius coverplate of the east tangent tank could not accommodate the new retracted position of the M1 extraction magnet, so a new coverplate with a larger doghouse was fabricated. The old cover-plate was reused in the west region.

E3.3.2 South Tangent Modifications

The main element is a new liner tank, as shown in Fig. E-16, that is cooled by liquid nitrogen flowing through tubes welded to the tank. The liner

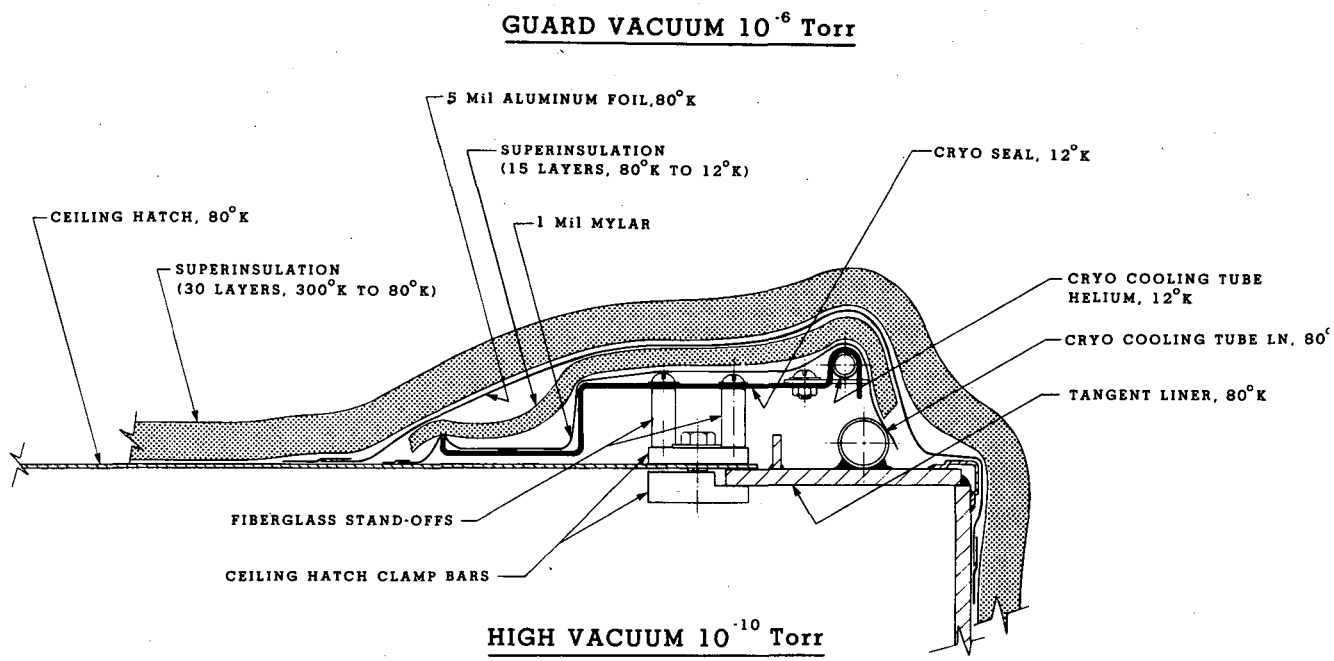

Figure E-15. Cross section of cyrogenic seal for ceiling hatch, east and south tangent liners (XBL 827-10681).

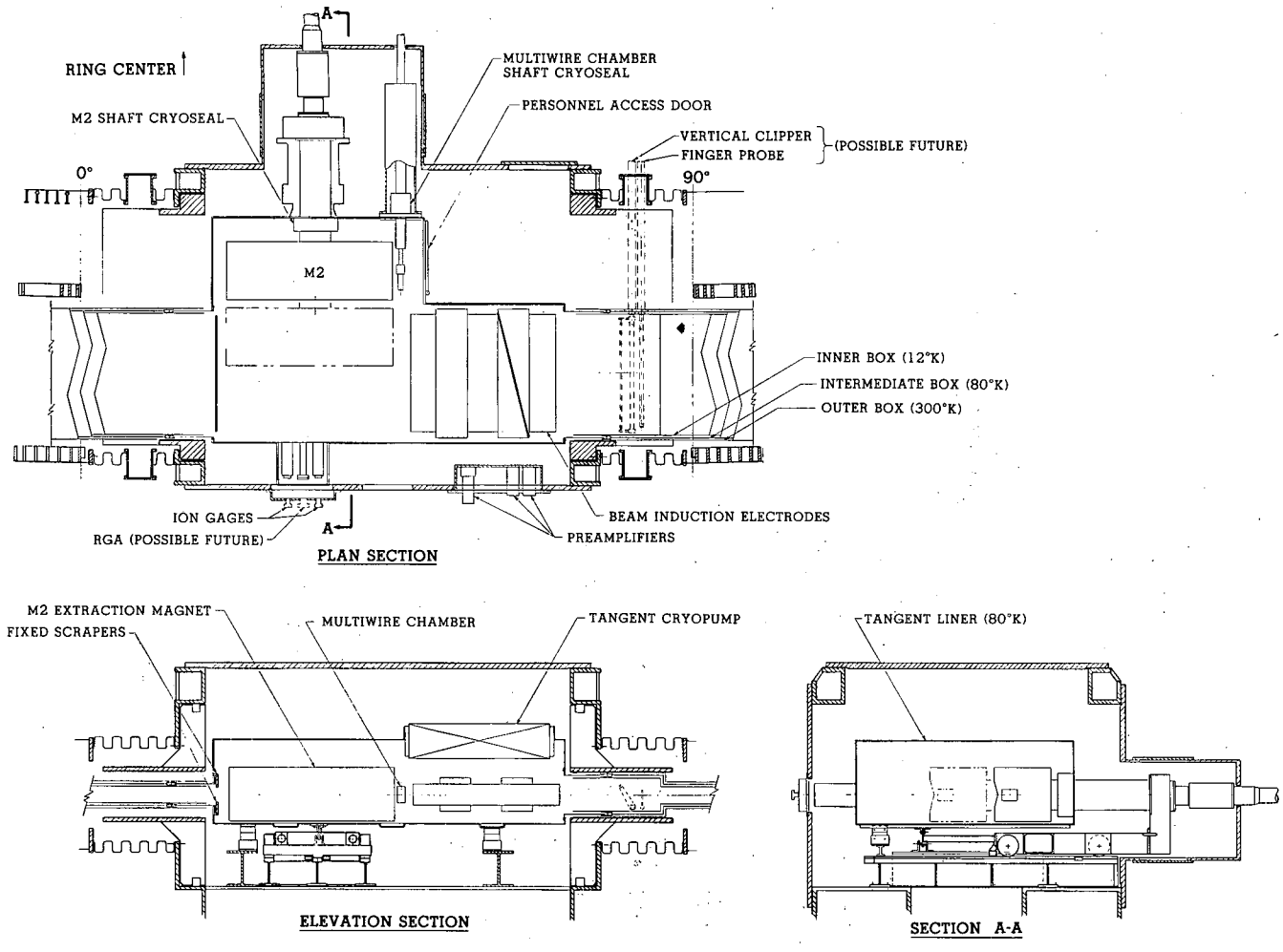

Figure E-16. South tangent region (new construction shown in red) (BBC 827-6061).

tank construction and superinsulation are similar to that for the east liner tank described above.

Penetrations for the personnel-access door, the wire chamber, the M2 extraction magnet (versus M1 in the east), the tangent cryopump, the ionization gauge/RGA tubular housings, the circulating-beam openings, and the top access hatch are all similar to their counterparts in the east liner tank. Support clips for the beam induction electrode are attached to the inside of the liner tank. Separate feedthrough ports are built into the sidewall for the sum and for the two difference electrodes.

The tangent liner tank is supported by hanger rods from the tangent tank frame, as for the east liner tank. However, in this case all lateral and longitudinal bracing is provided by seismic restraints attached to the bottom of the liner tank. The restraints are designed so that, during cooldown, the liner shrinks longitudinally relative to the M2 plunge center line, laterally relative to the beam center line, and vertically relative to the mid-plane.

As in the east target area, the large inner-radius coverplate of the tangent tank could not accommodate the new retracted position of the M2 extraction magnet. Here too, a new, larger doghouse was fabricated to accept the magnet. The large outer-radius coverplate was modified to receive an inward projecting doghouse so that the preamplifiers for the beam induction electrodes could be placed as close to the electrodes as possible.

E3.3.3 West Tangent Modification

Because there are only a few components to be accommodated, none of which are at room temperature, the cold-bore liner through the west region can be operated at 12°K. The liner sections here are very similar to the quadrant sections except that they are straight and the circuit boards are not stripe-etched. The two cold-bore modules in the west are numbered 23 and 24. The west region is shown in Fig. E-17 together with the adjacent portion of Quadrant II (southwest).

Special modifications were required to accommodate the exiting ion beam as it approaches the west region. The Bevatron beam-extraction system functions by perturbing the beam so as to slowly spill the beam into the M1 septum magnet at the inboard side of the east tank where it is inflected inward to the inboard south region where it passes through the M2 extraction magnet and is strongly deflected outward so as to be as far outboard as possible upon arrival

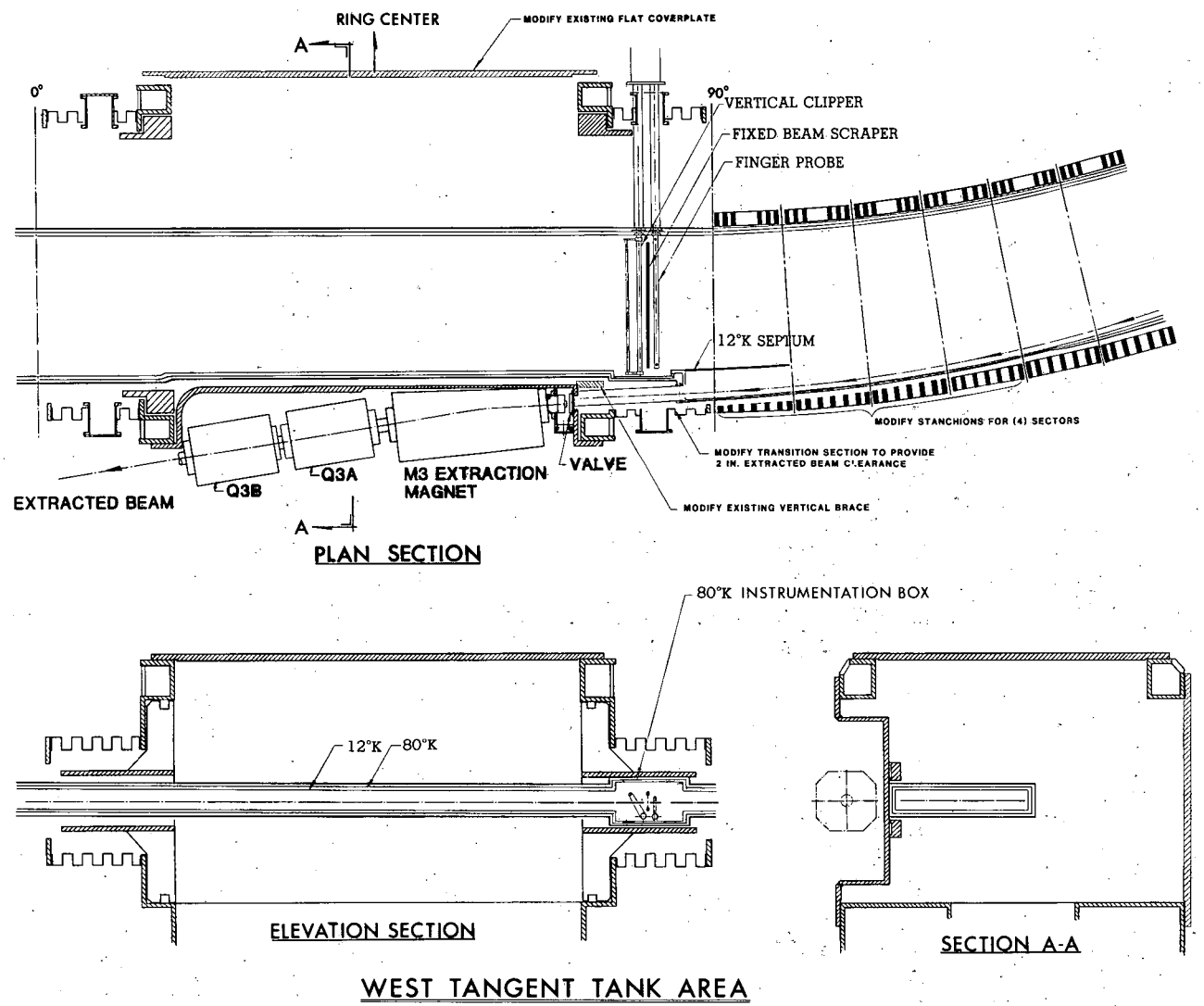

Figure E-17. West tangent region (new construction shown in red) (BBC 827-6053).

at the west where the beam enters the M3 extraction magnet. Ions of lower magnetic rigidity take slightly different paths than those of higher rigidity. The criterion was established that all beam obstructions should be at least two inches away, vertically and horizontally, from the center line of these extraction paths. This necessitated that quadrant liner Modules 19, 20, and 21 be specially constructed as described earlier and shown in Fig. E-10. In the transition region from Module 21 to where the exiting beam leaves the tangent tank (near the valve adjacent to the M3 extraction magnet), the beam passes through an exit tube that is cooled to 80°K by liquid nitrogen, except for the last fraction of an inch which is open to the guard vacuum.

The Bevatron had to be modified to accommodate widened Modules 19, 20, and 21, and the exit tube, together with their superinsulation. Some of the outboard stanchions (that hold the magnet poles apart) were slimmed down. A portion of the "picture frame" vacuum flange (joining quadrant vacuum envelope to transition bellows) was machined away. The sidewall of the transition bellows was reworked so that the corrugation amplitude was significantly reduced. The vertical leg of the tangential brace (which tangentially restrains the end of the quadrant magnet) was machined away to provide clearance.

The vacuum consequences of the exit port were studied extensively. Instead of a foil or a beam line cyrotrap, or an ultra-clean exit beam line (all of which had problems), a favorable arrangement evolved in which the cold-bore sections themselves provide adequate cryopumping so that relatively few gas molecules from the exit beam line get into the beam stay-clear region for the circulating beam. A septum (conduction-cooled to 12°K), as shown in Figs. E-10 and E-17, was installed in Module 21 between the exiting beam and the circulating beam. As mentioned previously, the gap at the end of the exit tube is open to the Bevatron guard vacuum ($\sim 10^{-6}$ Torr) so that many of the gas molecules coming up the beam line are pumped by the guard vacuum. It also serves to establish the pressure at the downstream end of the cryo exit tube at approximately that of the Bevatron guard vacuum ($\sim 10^{-6}$ Torr). Of the gas molecules at the gap that move upstream into the exit tube, most are pumped on the walls of the exit tube, the septum, and the 12°K cold bore. Only a relatively few graze the exterior of the beam circulation region, and these few are just passing through (a streaming flow) on their way to hitting a cold wall where they will be pumped. The effect of these few molecules is minimal as only

those circulating ions that have quite large horizontal betatron oscillations traverse this region; the ions are near full outboard amplitude only a fraction of the time, and this region represents only a small fraction of the Bevatron circumference. Thus, gas molecules "leaking in" through the exit port produce only a negligible effect on the effective vacuum in the cold bore.

There is a finite chance that a rupture in the exit beam line may occur that would result in it suddenly going towards atmospheric pressure. Can the new cold bore survive such an accident? The mass flow into the Bevatron is limited by the sonic velocity of air at the rupture and by the ~4"-diameter aperture of the exit beam line. It is true that there are shock-wave fronts associated with the entering gas, but these are quite rarified, so the pressure they can exert on any object is not great. Also, the shock waves, for the most part, are striking surfaces at a glancing angle, thereby further reducing any forces. Thus, substantial damage appears very unlikely.

E3.3.4 North Tangent Modifications

The main element is a new, large tangent liner tank, as shown in Fig. E-18, that is cooled by liquid nitrogen (~80°K) flowing through tubes welded to the tank. The liner tank construction, superinsulation, personnel-access door, and ion gauge/RGA tubular housings are similar to those for the east and south liner tanks previously described. The equipment-access hatch through the ceiling (for installation of internal components) has a stainless-steel sheet cover that is welded closed (with welded cover strips for leak checking) because it is not likely that any of the internal components will need removal for servicing.

The new tangent liner tank was made as large as could fit into the existing tank so as to minimize the change in capacitance of the system. Nevertheless, the new liner tank is unavoidably smaller than the old rf tank. This increase in capacitance was offset by reworking the rf electrode to reduce its overall height, thereby lowering the capacitance to near its original value. Removable wheels were installed on the bottom of the new liner tank so it could be rolled in through the outer-radius opening of the tangent tank, as the new liner tank would not fit through the top opening. An rf pickup electrode similar to the old one was installed at the top of the new liner tank.

The rf electrode is supported by the same, but shortened, insulating tubes as formerly used. The old ceramic feedthrough insulator is used but the

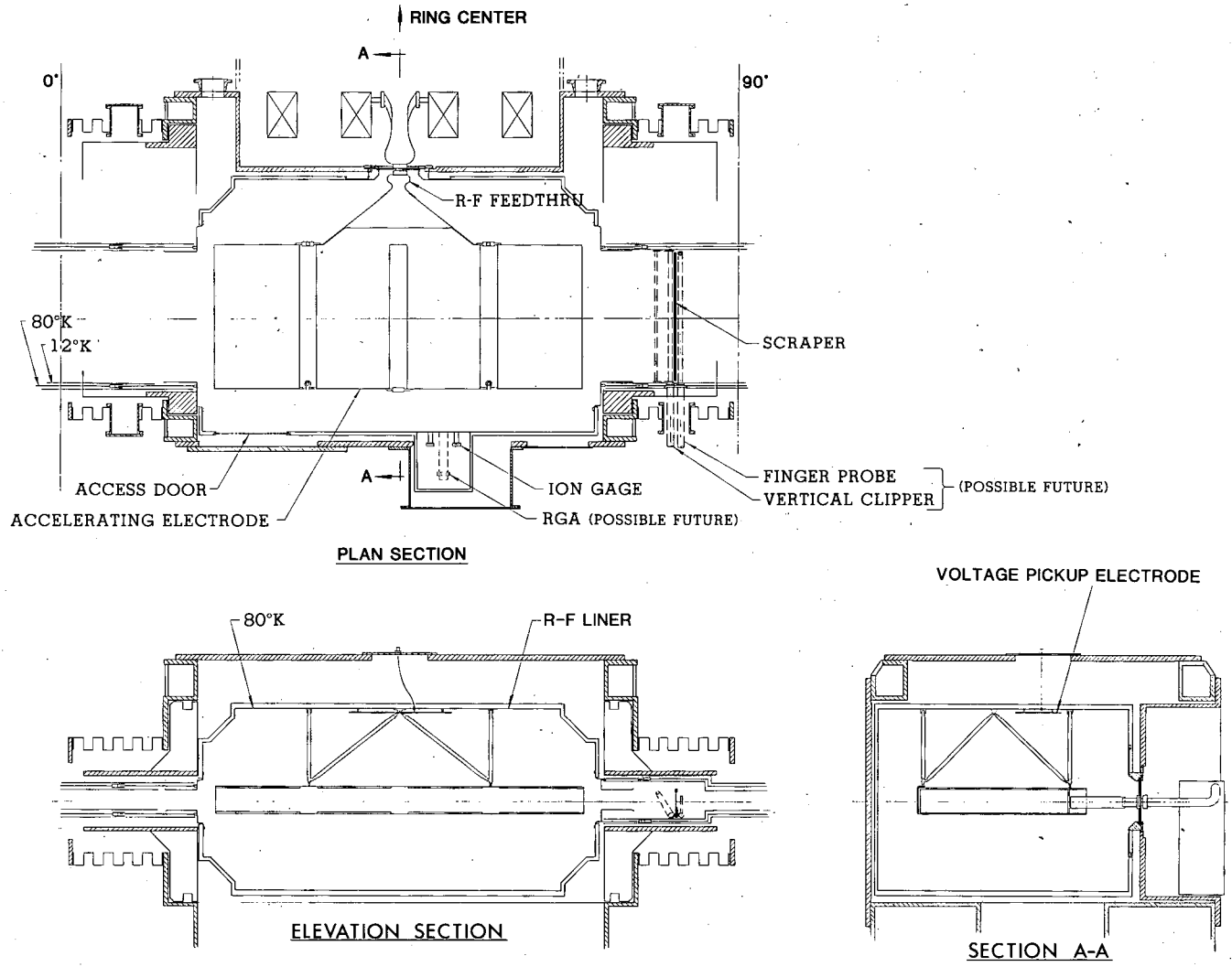

Figure E-18. North tangent region (new construction shown in red) (BBC 827-6057).

gasketing arrangement was changed so that the gaskets next to the 10^{-10}-Torr vacuum are aluminum wire to minimize outgassing. The inner radius wall of the new liner tank was thinned down to a diaphragm in order to provide a thermal gradient from the rest of the liner tank at 80°K and the feedthrough insulator at near room temperature. The inside diameter of this diaphragm is joined to the old main tangent tank at the outside diameter of the feedthrough insulator. Thus the diaphragm supports the new liner tank vertically and longitudinally, but has some compliance for lateral motion. To minimize dead-weight loading on the diaphragm, two spring-loaded support rods were tensioned to carry the dead weight. Two "solid" hanger rods were provided on the outer radius side. Seismic restraints similar to those in the east and south were attached to the bottom of the liner tank. The support system was designed so that the thermal contraction during cooldown would shrink toward beam center line at mid-length of the rf electrode.

E3.3.5 Tangent Installation

After all of the cold-bore modules for the quadrants and for the west region (23 and 24) had been installed and tested, the Bevatron was re-opened for tangent installation.

Following is the installation sequence for the major tangent components: The extraction magnets (M1, P1, and M2) and the inflection components, together with their associated support and plunge systems, were pre-installed, aligned, doweled, and most were then removed. Next the tangent liner tanks were installed, and the "cuffs" that connect the liner tanks to the cold-bore modules were inserted. Then the extraction magnets and the electrostatic inflector were installed, the beam instrumentation was put in place, cryogenic seals were installed, and hatch covers were sealed. Finally, all cryogenic lines and all electrical wires were connected, the interior was cleaned and the personnel access doors were closed.

E3.4 Vacuum Pumping and Cryogenics

This section describes the vacuum pumping components and the cryogenic systems. The quadrant liners were described in Section E3.1, and will not be described further here even though they are the main pumping elements for the new system.

The helium (~12°K) and the liquid nitrogen (~80°K) cryogenic circuits are shown in elementary schematic form in Fig. E-19. The remote supply tanks and the local supply tank of the liquid nitrogen system, together with their pumped transfer line, already existed at the Bevatron. All of the other items were new construction. The helium and liquid nitrogen circuits within the Bevatron vacuum envelope are shown schematically in more detail in Figs. E-20 and E-21.

E3.4.1 Tangent Cryopump

A tangent cryopump was installed in the top of the east tangent liner tank, and another was installed in the top of the south tangent liner tank. Each consists of four layers of copper chevrons as shown diagrammatically in Fig. E-22. The uppermost layer that faces the guard vacuum is cooled by tubes carrying liquid nitrogen at ~80°K. It acts as a heat shield for the second layer, and as a pump for water and organic vapors in the guard vacuum region. The second and fourth layers are cooled by tubes carrying helium at ~12°K, and act as a pump for N_2, O_2, etc., in the guard vacuum and in the 10^{-10}-Torr region respectively. The third layer has its chevrons coated with activated charcoal pellets which, at 12°K, act as a pump for hydrogen and, to some extent, helium. Since the adjacent second and fourth layers provide pumping for almost all gases except hydrogen and helium, this leaves the pumping sites of the activated charcoal available for pumping these two gases. The third layer is on a separate 12°K helium circuit so that the activated charcoal can be regenerated, if needed.

Each tangent cryopump has nominal dimensions of 59 cm x 140 cm for a nominal area of 0.83 m^2. For the guard vacuum region, this provides a pumping speed of about 122,000 liters/second for H_2O and, because of the ~25 percent baffle transmission efficiency, 24,000 liters/second for N_2, O_2, and CO. Because of the lower molecular velocity ($[80/293]^{1/2} = 0.52$) inside of the 80°K tangent liner tank, the effective pumping speed for N_2, O_2, and CO inside of the tangent liner tank is ~50,000 liters/second, and that for H_2 (considering a 0.25 baffle factor and a 3.8 velocity factor) is ~48,000 liters/second.

The louvers of the tangent cryopump serve an additional valuable function in limiting differential pressures imposed on the cold-bore walls to negligible values. At pressures in the laminar flow regime (greater than ~0.1 Torr), the louvers have high conductance between the cold-bore and guard-vacuum regions to limit the differential pressures to less than 0.1 psi, not only during routine

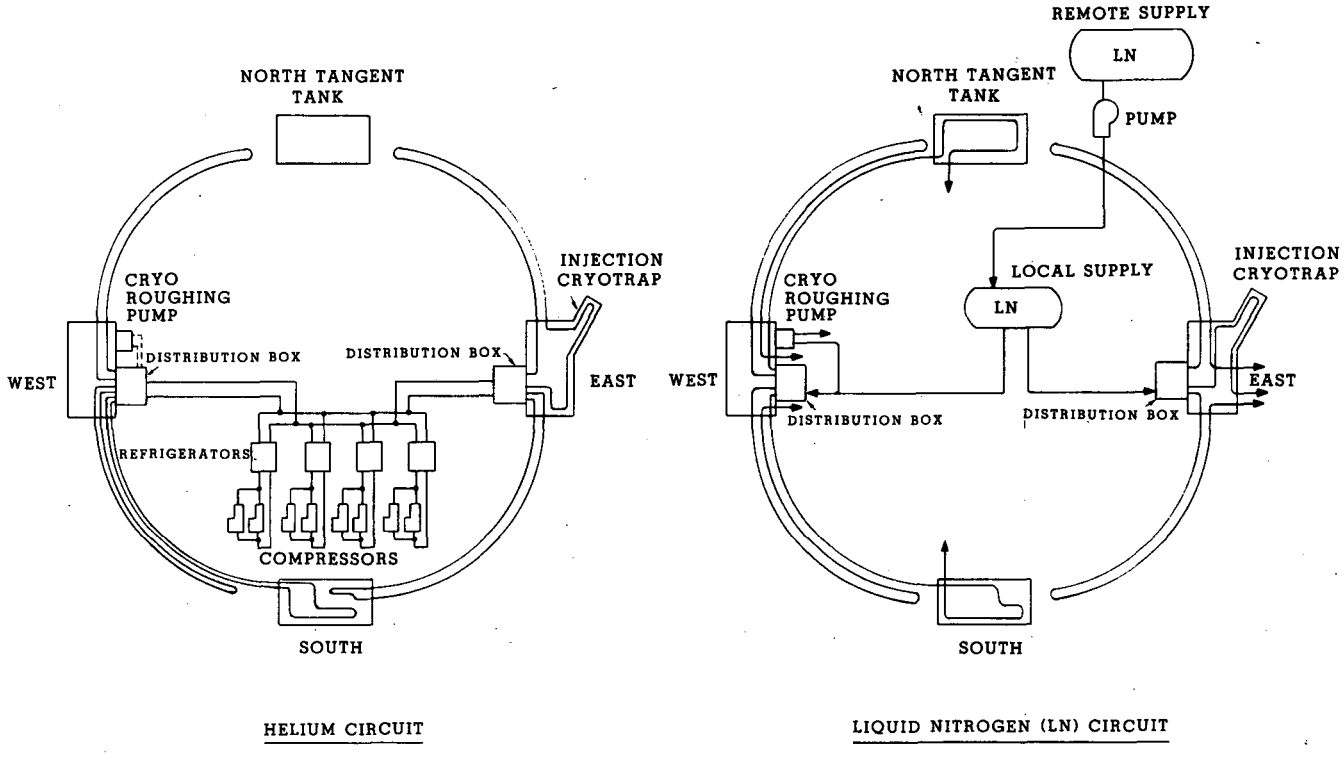

Figure E-19. Elementary schematic of the cryogenic-cooling system (XBL 827-10679).

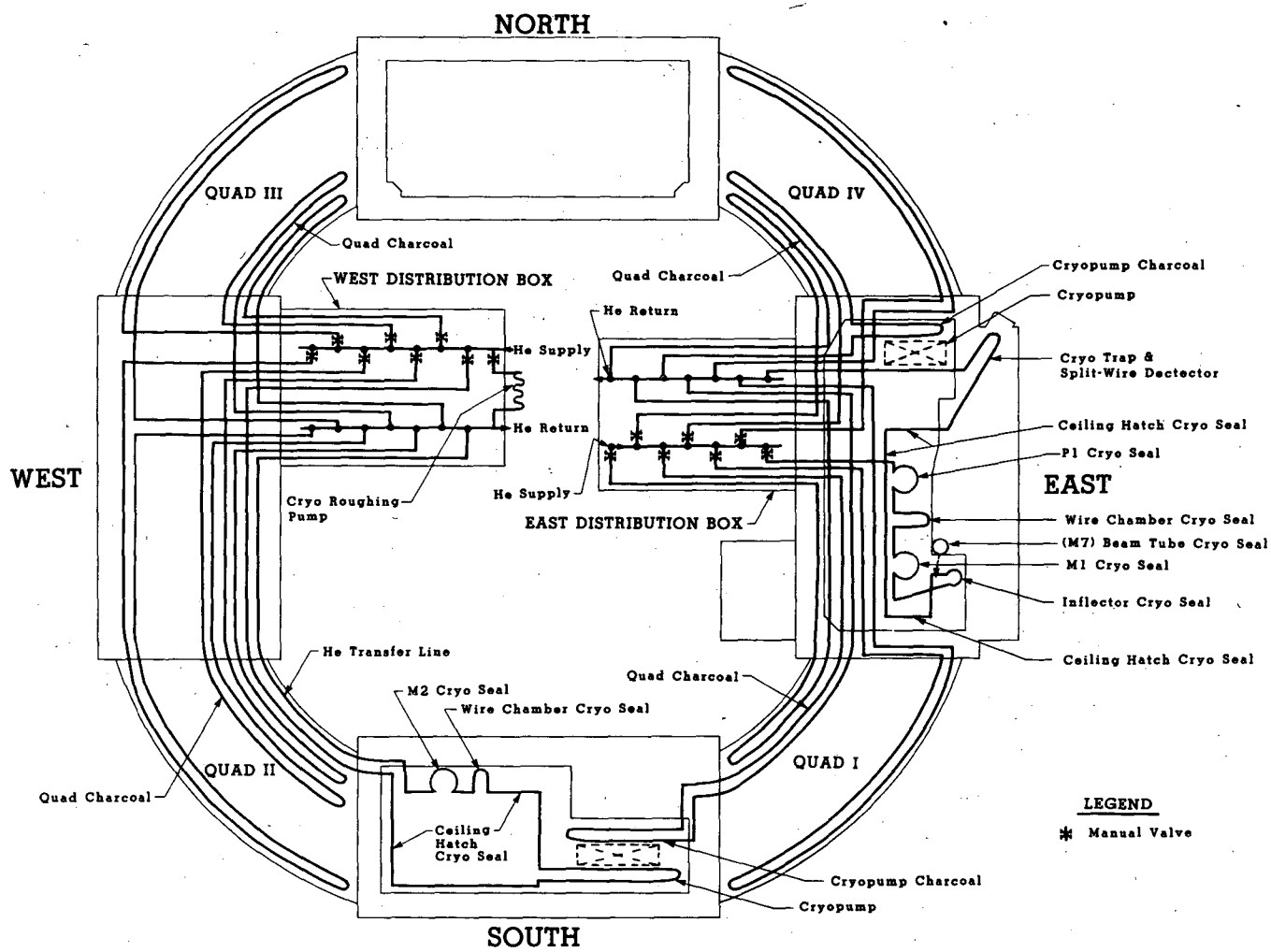

Figure E-20. Helium cryogenic-cooling system schematic (XBL 827-10678).

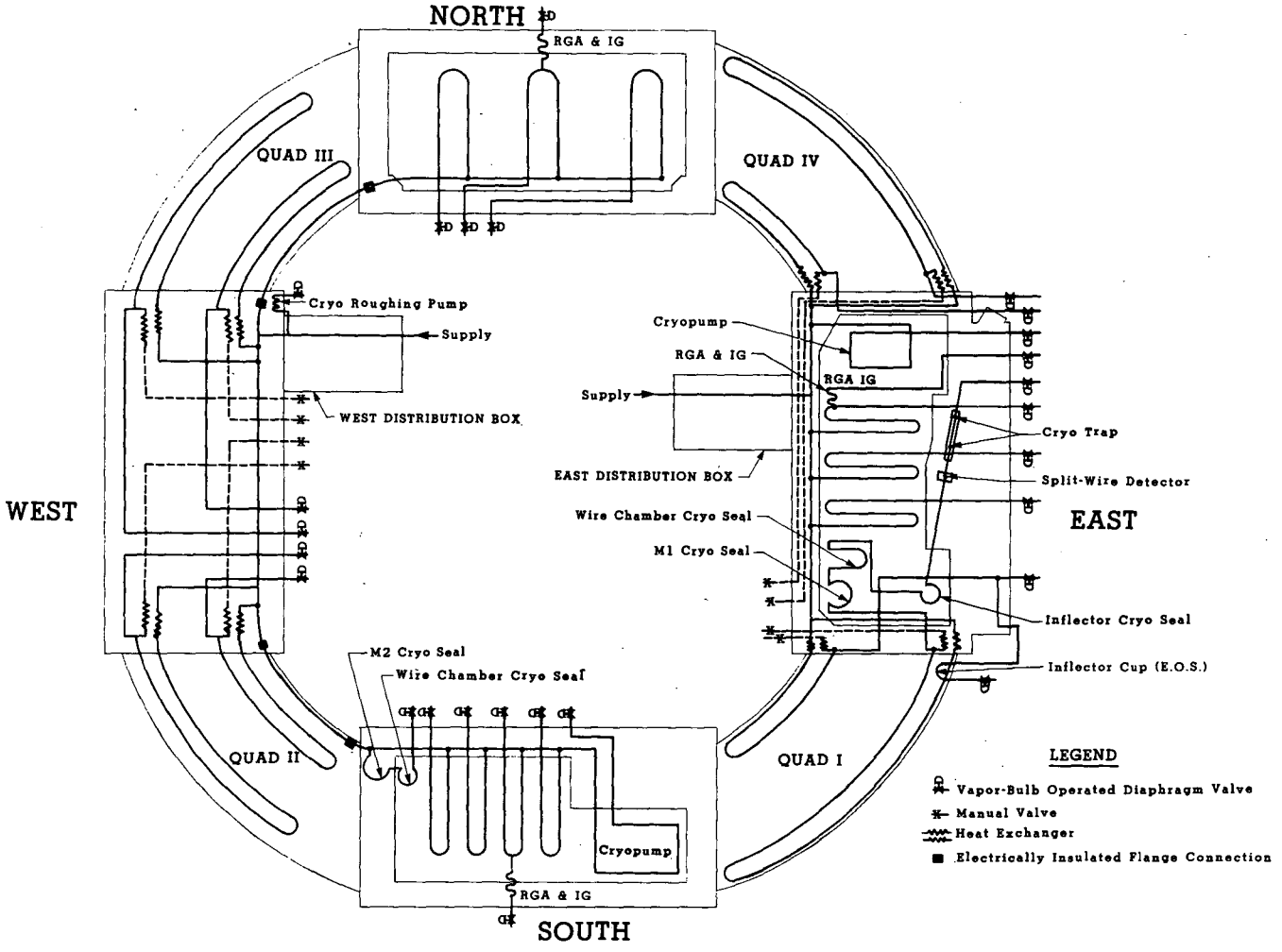

Figure E-21. Liquid-nitrogen cyrogenic-cooling system schematic (XBL 827-10676).

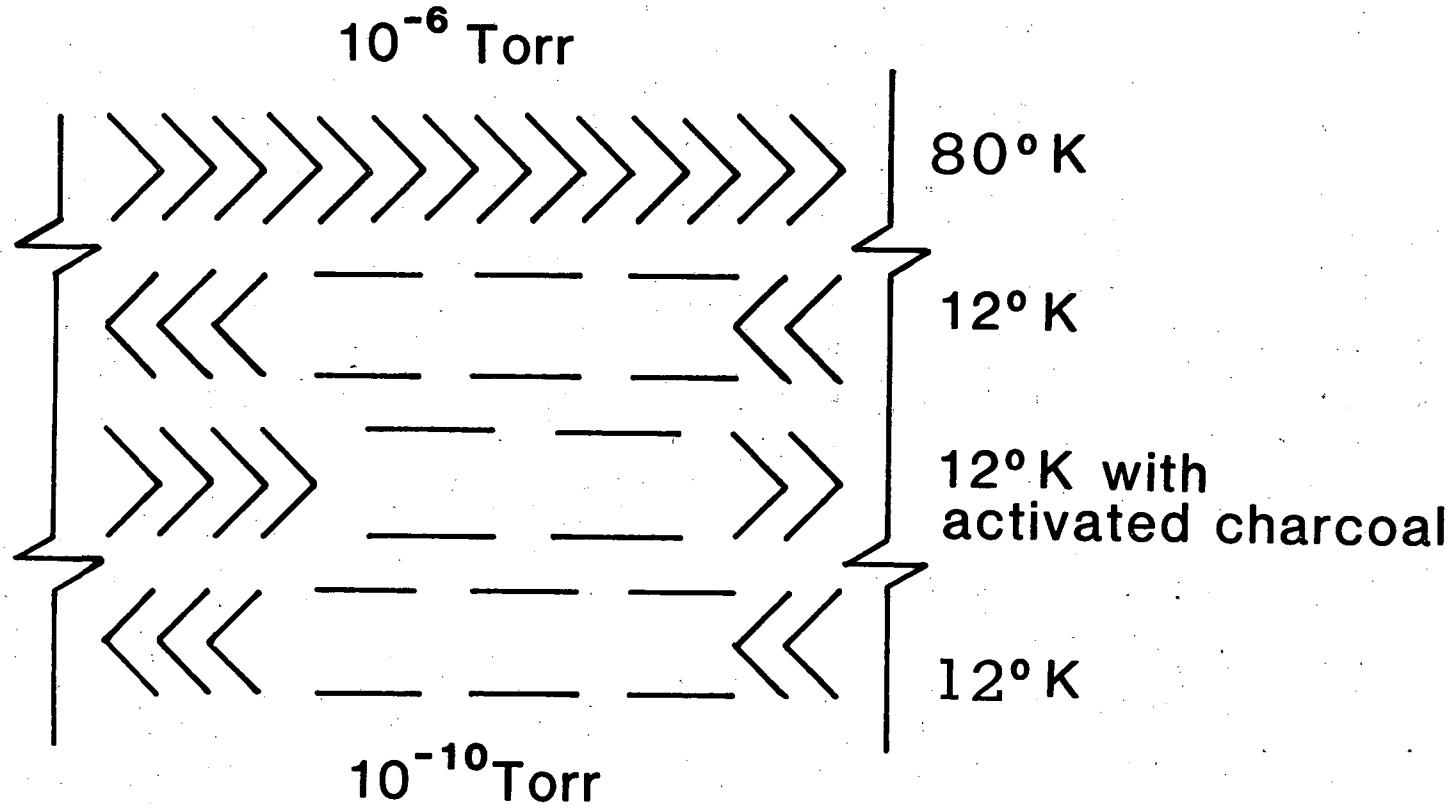

Figure E-22. Diagrammatic arrangement of copper chevrons in the tangent cryopumps (XBL 827-10674).

evacuation and venting of the Bevatron vacuum envelope, but also in the unlikely case that a rupture should occur in the injection or extraction beam lines and the associated beam line valves should fail to close. In contrast, once the Bevatron vacuum system is in the molecular flow regime (below $\sim 10^{-3}$ Torr) and the cryopump surfaces are cold, they provide very effective isolation between the guard vacuum and the cold-bore regions. Thus, the tangent cryopanels function as a fail-safe "relief valve."

E3.4.2 Injection Cryotrap

First, consider the case if there were not any injection cryotrap. The molecular conductance of the beam tube through the BL18MH (IHM7) inflection magnet is on the order of 30 liters/second. If the partial pressures of N_2, O_2, and CO at the entrance of this magnet were 10^{-6} Torr, then the throughput into the liner tank would be $[(30)(10^{-6})] = 3 \times 10^{-5}$ Torr-liter/second and, noting that the tangent cyropump in the east liner tank provides about 50,000 liters/second pumping speed, the corresponding pressure increment within the east liner tank would be equal to 6×10^{-10} Torr. This would constitute the dominant gas source into the east liner tank, and it was considered very desirable that it be reduced (particularly so if the guard-vacuum partial pressure should be greater than 10^{-6} Torr). Flow of H_2O or organic vapors into the liner tank are not of significant concern because the 80°K walls of the liner tank are a huge pump for such vapors.

Therefore, an injection cryotrap was installed upstream of the inflection magnet. The principal element is a tube cooled to 12°K that is 10-cm diameter by 95-cm long. A liquid-nitrogen tubular shield extends beyond the end of the 12°K tube at both ends to reduce the room-temperature radiative heat load to the 12°K surfaces. It is estimated that only approximately one gas molecule in a thousand gets through the injection cryotrap so that the corresponding pressure increment, mid-10^{-13} Torr, is negligible.

E3.4.3 Auxiliary Pumping

This subsection describes the vacuum system components that provide for initial roughing of the Bevatron vacuum envelope and for pumping during regeneration of the cryopumps, if such should ever be required. The total volume of the Bevatron vacuum chamber is ~300 cubic meters, of which slightly less than 25 percent is inside of the new cold-bore liner.

Initial roughing to slightly below 1 Torr is accomplished by the existing Bevatron mechanical pumps. It turns out that 90,000 square meters of surface area, mostly multi-layer superinsulation, have been added within the Bevatron vacuum envelope, all of which tends to absorb water vapor. Consequently, when roughing below ~5 Torr, it has been found that water tends to collect in the oil of the mechanical pumps, thus reducing pumping capability. This can be alleviated by periodically isolating individual mechanical pumps and bleeding air through them to remove water that has accumulated in the pump oil.

When a Bevatron vacuum of ~0.5 Torr is reached, further roughing is accomplished with a "cryoroughing" pump in the west tangent region, and the mechanical pumps are valved off. This cryoroughing pump consists of an array of chevrons (somewhat similar to the tangent cryopump) that are located in an existing valve box above one of the old 81-cm (32") diffusion pumps (which has been removed). The first layer of chevrons is cooled to ~80°K by liquid nitrogen, the second layer is cooled by tubes carrying helium at ~12°K, and a third flat layer is coated with activated charcoal that is cooled to ~12°K by a conduction strap from the 12°K chevron layer. This strap is sized so that the 12°K chevrons cool down a few hours sooner than the activated charcoal, allowing N_2 and O_2 to be pumped by the chevrons rather than by activated charcoal. The activated charcoal layer has an electrical heater so that it can be regenerated if needed.

Liquid nitrogen and helium for the cryoroughing pump are supplied from the west distribution box. Provision was also included for the 12°K surfaces to be cooled from a liquid-helium 4°K supply, but there are no immediate plans to use this feature. The chevron layers have a nominal size of 1 m wide by 0.9 m high (with a 10-cm-square hole to accommodate the valve actuation shaft) for a nominal area of 0.88 m^2. This provides nominal pumping speeds of about 135,000 liters/second for water and 25,000 liters/second for N_2, O_2, and CO. The old rectangular plate valve (previously used with the removed diffusion pump) is used for opening the cryoroughing pump to the Bevatron vacuum. If the valve were suddenly opened at a pressure in the vicinity of 1 Torr, the temperature of the 12°K surfaces might increase (due to condensation of N_2 and O_2) above 24°K, where they would no longer cryopump. Instead, the valve is opened manually (slowly) while making certain that the vapor bulb thermometer on the return helium line does not indicate above 20°K. Typically, this requires

only a few minutes until the valve can be fully opened. The pressure in the Bevatron falls to ~10^{-8} Torr in less than five minutes.

Three options are available for the balance of the pumpdown cycle. One option is to let the west refrigeration system continue to cool down the cryoroughing pump while the east refrigeration cools the eastern half of the Bevatron cold bore, and, when it starts cryopumping, the cryoroughing pump can be turned off and the western half of the Bevatron cold bore can then be cooled down using the west refrigeration system. A second option is to use liquid helium from a dewar to cool the cryoroughing pump so that the east and west halves of the Bevatron cold-bore can be cooled concurrently. A third option is to turn on one diffusion pump in each of the four tangent regions but with the gate valve opened no more than one inch to minimize backstreaming. Next, the cryoroughing pump is shut down, and the east and west refrigeration systems are used to cool the Bevatron cold bore concurrently. The last option has been preferred operationally because it is easy to do, it provides concurrent cooldown, and the diffusion pumps permit use of conventional helium-leak detection during cooldown (and afterwards).

The cryogenic pumping systems do not remove gas but instead freeze it on cold surfaces. During the course of one year, approximately five pounds of gas will be pumped by the Bevatron. Ultimately the frozen gas may interfere with pumping either by thermal shorts or by development of thermal gradients across thick gas deposits. If uniformly distributed on the cryogenic pumping surfaces of the guard vacuum, the five pounds of gas would form a layer only several thousandths of an inch thick. However, since such uniform distribution cannot be relied on, regeneration every few months may be required. Regeneration can be accomplished by letting the cryo surfaces warm up. Electrical heating of the activated charcoal helium supply will provide preferential regeneration of the charcoal so as to maximize its pumping capacity for hydrogen and helium. During regeneration, the gas evolved can be pumped by the cryoroughing pump and/or slightly opened diffusion pumps.

E3.4.4 Distribution Boxes

As indicated in Figs. E-19, E-20, and E-21, two new distribution boxes (one each in the east and west) were constructed to provide distribution, valving, and temperature monitoring for the helium and liquid-nitrogen cryogenic circuits. The liquid nitrogen supply goes through the distribution box

but the various liquid nitrogen circuits exit through convenient locations in all four tangent regions. Each LN circuit is vented to atmosphere through a thermostatically controlled valve which is intended to vent boil-off gas without venting liquid. Each distribution box, plus its connecting transfer lines, is evacuated by a separate small diffusion pump system. The internal components of the distribution boxes are fully shielded by liquid-nitrogen-cooled surfaces to minimize heat load.

E3.4.5 Helium Refrigeration

Helium refrigeration is provided by eight helium compressors feeding four CTI 1400 helium refrigerators (often called "cold boxes" or "expanders") that are equipped with liquid nitrogen precool. Half of these components were reused from the previous Bevatron cryogenic cooling system. Four compressors and two refrigerators are allocated to the east distribution box and an equal number are allocated to the west. Valves permit cross-connects to the east and west systems if desired. The refrigerators are located on top of the Bevatron concrete shielding where they can be serviced during operation and yet be fairly close to their respective distribution boxes. The compressors are located in the mechanical pump room (where their noise is isolated) so that they can be conveniently serviced. Make-up helium comes from a bottle rack located outside of the concrete shielding.

E3.4.6 Cryogenic Transfer Lines

Three transfer lines connect from the area on top of the Bevatron concrete shielding to the east distribution box and an equal number connect to the west. These lines are for helium supply, liquid-nitrogen supply, and helium return. The cryogenic lines are surrounded with multi-layer superinsulation and a vacuum jacket to minimize heat load.

E3.4.7 Vacuum/Cryo Electronics and Controls

It is impractical to provide vacuum monitoring inside of the 12°K cold-bore sections, primarily because of heat from hot filaments. Therefore, vacuum monitoring is accomplished at the north, east, and south tangent regions only. Two dual-filament "nude" ion gauges are located at each tangent region with each gauge tube being mounted inside of the baffled tubular housings previously described in Section E3.3. These gauge tubes are monitored by ion-gauge power supplies intended to read pressures to below 10^{-10} Torr.

Provision was made in the north, east, and south tangent liner tanks for mounting of a residual gas analyzer (RGA) head. Initially, this has been implemented in the east region only.

Electrical power, monitoring, and control circuits were revised significantly.

Gas-filled bulbs and thermocouples are used to monitor temperatures at appropriate points on the 80°K and 12°K cold surfaces.

E3.4.8 Vacuum/Cryo Installation

Most of the components of the vacuum/cryo systems were installed concurrently with the installation of the quadrant cold-bore sections. The vacuum/cryo systems were turned on and tested during with September 1981 cryogenic heat-load tests of the quadrant cold-bore sections described previously in Section E3.2.1.

E3.5 Injection

The magnetic and electrostatic components for the inflection system were modified to be compatible with the new cold-bore design. The two injection elements in the east tangent tank are the BL18MH (IHM7) inflection magnet which bends the beam by 32.7°, and a thin-septum electrostatic inflector to deflect the beam the final 2.3° required for injection.

E3.5.1 BL18MH (IHM7) Inflection Magnet

This magnet was designed to bend particles (50 MeV protons) with magnetic rigidity of $B\rho$ = 10.3 kilogauss-meters, and to operate continuously. For the heavier ions now contemplated (through uranium), and with stripping at the SuperHILAC exit, a magnetic rigidity of 15.4 kilogauss-meters is required.

Study indicated that the existing magnet could operate magnetically at the higher excitation level but that the coil temperature rise would be large if operated continuously. Therefore, it was decided that the magnet should be operated on a pulsed basis to reduce average heating and save on power costs. The new parameters for the BL18MH (IHM7) magnet are:

Magnetic rigidity	15.7 kG-m (= 618 kG-inch)
Flux density, nominal	9.17 kG
NI	45.3 kAT
N	32 turns

Current, maximum	1450 A
Voltage, maximum	80 V
Power, instantaneous, maximum	116 kW
Average power, maximum	48 kW
Duty factor (at 1450 A), maximum	41 percent
LCW Δp, mininum	40 psi
LCW flow	5.7 gpm
LCW ΔT	32°C

A portion of the magnet yoke was machined away so that the magnet could nestle closer to the east tangent liner tank, thereby minimizing the effective system thickness. A magnetic shielding array was placed between the magnet and the tangent liner tank in order to reduce the magnitude of the stray field in the Bevatron circulating beam region. The shielding array consists of a 0.05-mm-thick sheet of copper and then two 0.1-mm-thick sheets of M3 grain-oriented silicon steel with this arrangement repeated for a total thickness of 28 mm.

A very rigid support system was constructed for the BL18MH (IHM7) magnet because the east tangent liner tank is pulled hard laterally against it. Therefore the support provides the lateral restraint of the tank and must withstand any seismic forces in that direction.

The beam tube of the BL18MH (IHM7) magnet continues on and passes through the wall of the east tangent liner tank. The beam tube is not welded to the liner tank (as originally planned), but instead has a 12°K cryoseal to pump gases that otherwise would leak through from the guard vacuum into the ultra-high vacuum.

E3.5.2 Electrostatic Inflector

The existing electrostatic inflector (ESI) was reused since its length permits handling of beams as heavy as uranium with less than 50 kV on the electrode. The ESI is cooled by its surroundings, and after several days approaches a temperature of 80°K. The mounting of the carbon septum was modified to provide for thermal contraction during cooling.

The ESI is located within the new tangent liner tank so new supports were required. It is mounted on a post which in turn is supported from the BL18MH

magnet support so that close alignment can be held between these two components. Most of the post operates at 80°K, but the bottommost portion has a thermal gradient from 80°K to room temperature. Copper rings at both ends of the thermal gradient minimize any azimuthal variation of temperature which would tend to bend the post and thereby cause misalignment. A 12°K cryoseal is used where the post penetrates through the liner tank in order to pump gases which otherwise would leak through from the guard vacuum into the ultra-vacuum.

E3.6 Extraction

The extraction magnets were funded as an Accelerator Improvement Project (AIP) but are described here in the interest of completeness.

In the east tank, the Q1 quadrupole magnet was eliminated and the existing, large, plunging M1 extraction septum dipole magnet was replaced with two units: a laminated steel perturbation/spiller dipole magnet (sometimes designated P1) containing perturbation and spiller coils, and a new, laminated, plunging thin-septum extraction magnet (designated M1).

In the south tank, the Q2 quadrupole magnet also was eliminated. The plunging M2 extraction septum dipole magnet was modified for compatibility with the new system.

E3.6.1 Perturbation/Spiller Magnet

The perturbation/spiller magnet produces magnetic fields that are conducive to slow, resonant extraction of the circulating ion beam over times of a second or so. The magnet has four separate circuits: a P1 perturbation circuit and an S1 spiller circuit for extracting high-energy ions, and a P2 perturbation circuit and an S2 spiller circuit for extracting low-energy ions. Previously, there were only one perturbation and one spiller circuit, both an integral part of the old M1 extraction magnet. The new arrangement is intended to give more efficient extraction of low energy ions.

The perturbation circuits are intended to produce an unstable fixed point adjacent to the beam so that the circulating ions near the inner radius are on the verge of spiraling inwards. The appropriate perturbation circuit is turned on approximately at the start of "flat-top" (after acceleration) with a current rise time of ~0.1 second.

The spiller circuits are intended to move the ion beam gradually across the unstable fixed point, thereby producing a steady stream of ions that spiral

inward in such a manner that most of the ions "jump" the septum of the M1 extraction magnet and are extracted. The current in the appropriate spiller circuit is programmed to provide steady extracted beam current. This requires the capability to change spiller current by 10 percent of full amplitude within one millisecond.

A typical cross section of the perturbation/spiller magnet is shown in Fig. E-23. The current in each slot produces a magnetic field that closely approximates that which would exist if the current were concentrated at the pole surface. The magnet gap accommodates the full beam stay-clear so the magnet does not need to plunge for each extraction cycle (as the M1 and M2 extraction magnets do). Since the injected beam passes through the magnet gap, it was necessary to reduce the residual field (at zero current) to a low value. The iron core also needed to have millisecond time response. These requirements were satisfied by making the magnet core from 0.6-mm-thick M22 fully-processed electrical silicon steel laminations which were stamped on a tape-controlled punching machine.

The magnet design was dominated by the need to simultaneously satisfy requirements for: (a) extremely low vacuum outgassing ($<10^{-6}$ Torr-liters/second), (b) millisecond time response of the magnetic field, and (c) the unusual conductor positions. Putting the magnet inside of a stainless steel "can" (as for the M1 and M2 magnets described hereafter) was considered and rejected because the can would either have been so thin (a few thousandths of an inch) as to be impractical, or would have required insulating seams or windows which again appeared impractical. If the magnet core were exposed to the vacuum, there would be $\sim 3 \times 10^6$ cm^2 of lamination surface area to outgas. At room temperature, the outgassing would be excessive, but outgassing rates typically are reduced by about factor of 10 for a 20°C reduction in temperature. Therefore, it was decided that the best solution to this difficult problem was to cool the magnet below ~170°K. The hollow copper conductors of the magnet are cooled by liquid nitrogen. The iron core is cooled to some extent by the conductors and is also cooled by radiation to the surrounding east tangent liner tank which is at ~80°K. The iron core reaches 170°K within a few days and continues down toward an equilibrium temperature near 80°K.

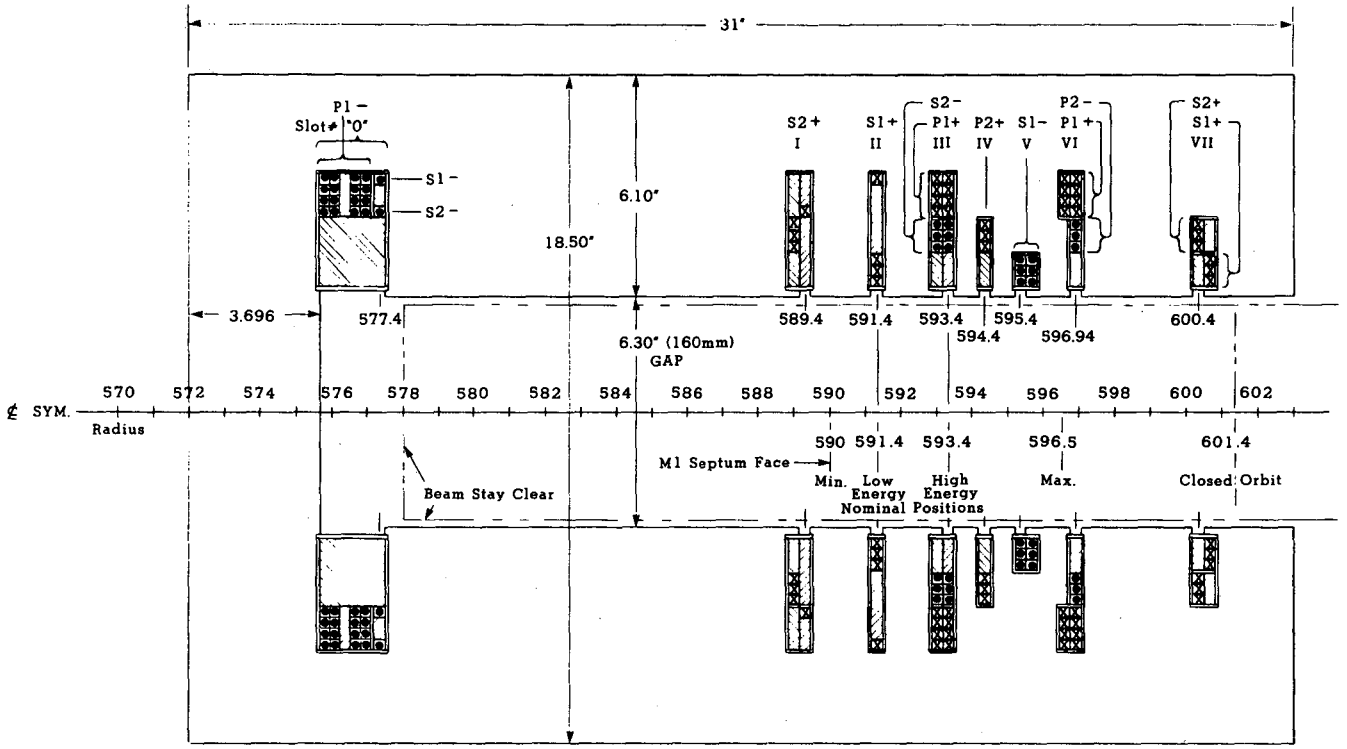

Figure E-23. Perturbation/spiller (P1) magnet typical cross section looking upstream. Positive (+) currents and "x" on conductors indicate current into the page. Negative (-) currents and dot (.) on conductor indicate current out of the page (XBL 827-10677).

The principal parameters for the perturbation/spiller magnet are:

Magnet:

Gap	160 mm
Iron Length	0.84 m
Effective length, measured	0.91 m
Lamination material	M22FP electrical steel
Lamination thickness	0.06 mm
Iron weight, calculated	1700 kg

Coils:

Circuit Designation:	P1	P2	S1	S2
Number of separate coils	8	2	6	6
Total number of turns	32	6	14	14
Calculated resistance at 80°K (excl. external cables), milliohms	6.0	1.1	2.6	2.7
Design current, amperes				
High Energy	394	0	420	0
Low Energy	184	98	0	233
Calculated average power at 80°K, watts				
High Energy (40 percent duty factor)	371	0	184	0
Low Energy (50 percent duty factor)	101	5	0	72
Conductor, copper	0.7 cm^2 x 0.5 cm diameter hole			

E3.6.2 Perturbation/Spiller Magnet Support

The perturbation/spiller magnet is supported on the end of a cantilevered 20-cm-diameter heavy-wall tube which passes through the wall of the cold-bore liner and through the main tangent tank wall to the outside. The penetration through the cold-bore wall incorporates a cryogenic seal with a 12°K surface to capture most of the gas that would otherwise pass through the penetration. The penetration through the main tangent tank wall has a

conventional elastomer seal. Outside, the support system provides for the magnet to be movable over a ±5 cm radial range by manual adjustment.

Forty-four LN-cooled magnet leads (two for each separate coil) pass through the support tube because it was felt imprudent to make LN joints in the ultra-vacuum region. It is difficult to design a completely tight vacuum sealing system for this many leads at cryogenic temperatures, so it was decided to incorporate a succession of six Teflon seal barriers with vacuum pumping at each interstage. The outermost interstage is a large evacuated box, mechanically pumped to a pressure of ~1 Torr, in which electrical and LN interconnections are made. The next two interstages are mechanically pumped to pressures of 10^{-1} and 10^{-2} Torr, respectively. The fourth interstage is open to, and pumped by the Bevatron guard vacuum of 10^{-6} Torr, while the fifth interstage is open to and pumped by the cryogenic shaft seal to a pressure of about 10^{-8} Torr.

E3.6.3 M1 Extraction Septum Magnet

After the perturbation/spiller magnet has caused most of the ions to continuously spill into the entrance of the M1 septum magnet (in the east), the magnetic field of this magnet deflects the beam inwards towards the M2 septum magnet in the south.

The three major differences between the new M1 septum magnet and its predecessor are: (a) the perturbation and spiller coils are no longer part of the M1 magnet assembly, (b) all of the magnet except for the septum is enclosed within a vacuum-tight stainless-steel welded can, and (c) there are no joints in any water circuit within the ultra-vacuum (although there are such joints in the guard vacuum). The interior of the can is at guard vacuum pressure. The septum consists of a stack of fourteen copper tubes which first have been squashed into a tall rectangular tubular shape and then have all been brazed into an integral unit with ceramic spacers between, all quite similar to the previous M1 septum magnet. There are individual electrical feedthroughs where each septum conductor enters and leaves the can. The return conductors are located within the guard vacuum region and are of conventional hollow square copper construction.

The magnet coils are water cooled. Interlocking has been provided so that, in the event of low water flow rate, the power supply is turned off and compressed air is used to blow down the magnet to prevent freezing of stagnant water.

The principal parameters of the M1 septum magnet are:

Magnet:

Magnet gap, nominal	11.25 cm
Clear gap height inside of can, nominal	11.07 cm
Iron length, nominal	84 cm
Effective magnetic length, measured	97 cm
Flux density, maximum	2.5 kG

Coils:

Septum thickness, nominal	3 mm
Number of turns	14
Current, maximum	1600 A
Current rise time (approximate)	~0.1 sec
Pulse duration, maximum on for 6-sec cycle	2.0 sec.
Duty factor, maximum	33 perent
Resistance, calculated (magnet only)	0.0365 ohms
Voltage, maximum	59 V
Average power, maximum	31 kW
Water flow (at 80 psid)	8.5 gpm
Temperature rise (at maximum average power)	15° C

E3.6.4 M1 Extraction Septum Magnet Support

Previously, the M1 magnet was hung directly from a carriage within the east tangent tank and was driven through a sliding seal by a large hydraulic ram located outside of the tangent tank. The new system retains the hydraulic ram, sliding seal, and parts of the carriage (in the guard vacuum). Instead of the M1 magnet hanging directly from the carriage, however, it is supported by a C-shaped frame in which the bottom leg of the C is a 30-cm-diameter hollow shaft which penetrates through the wall of the east tangent liner tank.

This penetration has a cryogenic seal of special design as shown in Fig. E-24. The chevrons not only function as an 80°K thermal shield between the shaft (which is near room temperature) and the 12°K cryopumping surfaces, but also as a series of orifices with differential pumping to provide a graded pressure along the length of the seal. The seal assembly has 3.5-mm diametral

clearance from the shaft so that during normal motion the shaft should not rub against the seal. The assembly includes a cryogenic face seal where the assembly is spring-loaded against the wall of the tangent liner tank. If, during cooldown or otherwise, the shaft should move toward the seal by more than the allowed clearance, it would bear against a Teflon ring which would cause the whole seal assembly to slip at the face seal to a new position. The weight of the seal assembly is carried by a spring so that the assembly weight will not bear against the shaft.

An enlarged doghouse on the tangent tank faceplate was required to accommodate the C-shaped support frame in the retracted position. This also required that the hydraulic ram assembly be moved a corresponding distance toward the center of the Bevatron.

The stroke of the hydraulic ram assembly was reduced to 52 cm. The plunged position of the outboard face of the septum can range from R = 14.99 m (590.1") to R = 15.15 m (596.4").

E3.6.5 M2 Extraction Septum Magnet

The existing spare M2 septum magnet was upgraded for use in the ultra-vacuum of the south tangent liner tank. The magnet was enclosed in a stainless-steel can to reduce vacuum outgassing; the can extends through the magnet gap and provides a clear aperture of 11.1 cm high by 15 cm wide for the extracted ions. The outboard face (nearest the circulating beam) and the entrance face of the can are AISI 430 magnetic stainless steel to provide magnetic shielding of the circulating beam, and the remainder of the can is AISI 304 non-magnetic stainless steel. The mounting frame on the magnet had to be modified to be compatible with the can. As for M1, the inside of the can is at guard-vacuum pressure.

The M2 magnet parameters are the same as they were before, so they are not repeated here. As for M1, the magnet coils are water cooled and are protected against freezing by interlocked blowdown of the water circuits in the event of low water flow.

E3.6.6 M2 Extraction Septum Magnet Support

Previously, the M2 magnet sat directly on top of a carriage within the south tangent tank and was driven through a sliding seal by a large hydraulic ram located outside of the tangent tank. The new system retains the hydraulic ram, sliding seal, and parts of the carriage (in the guard vacuum). Instead

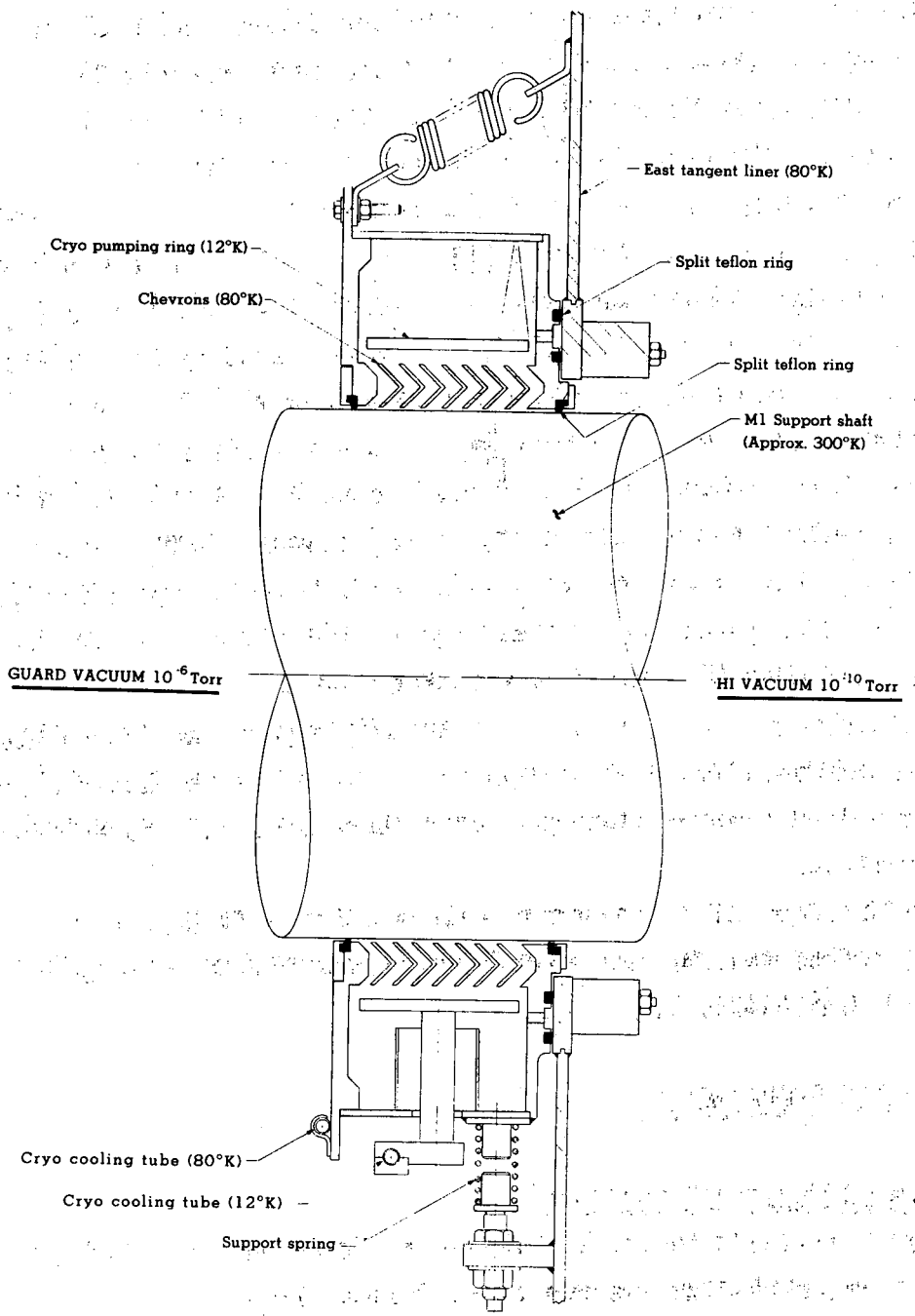

Figure E-24. Cryogenic seal arrangement for the M1 septum magnet support shaft. The arrangement for the M2 septum magnet support shaft is similar (XBL 827-10671).

of the M2 magnet sitting directly on the carriage, it is supported by a C-shaped structural frame in which the upper arm of the C is a 30-cm-diameter hollow shaft which penetrates through the wall of the south tangent liner tank. The carriage was strengthened to provide greater rigidity for the mounting of the C-frame. When initially installed, the rigidity of the support system appeared marginal, so both the C-frame and the carriage were stiffened further, particularly at the joints. After stiffening, the magnet had a natural mechanical oscillation frequency (analogous to a large tuning fork) of about 8 Hz. With the hydraulic ram system deliberately maladjusted to produce a significant jolt, the maximum deflection amplitude was observed to be 1.1 mm at the extreme end of the magnet, and 0.4 mm at the location of the cryogenic shaft seal. The oscillation damped to half-amplitude in about 1.0 second. This amount of motion is acceptable for beam extraction and should be significantly less when the hydraulic ram is functioning smoothly.

The penetration through the wall of the tangent liner tank is virtually identical to the one for the M1 magnet shown in Fig. E-24.

As for the M1 system, an enlarged doghouse on the tangent tank faceplate was required to accommodate the C-shaped support frame in the retracted position. Also, the hydraulic ram assembly was moved correspondingly toward the center of the Bevatron.

The stroke of the hydraulic ram assembly was reduced to 14 cm. The plunged position of the magnet gap center line can range from R = 14.85 m (584.6") to R = 15.0 m (590.5").

E4 CALCULATED SYSTEM PERFORMANCE

E4.1 Estimated Cryogenic Performance

The estimated heat loads on the 12°K helium refrigeration system and on the 80°K liquid nitrogen system are presented in Table E-1.

The estimated 12°K heat load is well within the capacity of the helium refrigeration system (Section E3.4), so refrigerant supply temperatures of less than 12°K are anticipated. The liquid nitrogen heat load of 8.5 kW corresponds to a liquid nitrogen consumption rate of ~190 liters/hours

TABLE E-1: ESTIMATED HEAT LOAD ON CRYOGENIC COOLING SYSTEMS

	Heat Load, Watts	
	Helium 12°K	LN 77°K
Quadrant Liner Tank (4)		
Through Superinsulation	60	300
Conduction by Supports	6	100
Eddy Currents	3	1
Louvered Pump Opening	10	2000
Radiation from Tangent Tank	7	--
Other Radiation Leaks	7	1000
Subtotal	93	3600
Tangent Tanks		
Through Superinsulation	--	200
Louvered Pump Opening	8	1700
Warm Magnets	--	1300
Supports	--	100
Other Radiation Losses	8	1700
Cryoseals	10	--
Subtotal	26	5000
Other Heat Loads		
Cold Box	7	--
Transfer Lines	6	--
Injection Cryotrap	5	--
Subtotal	18	00
Total	137	8500*

*Corresponds to 190 liter/hr or $365/day at $0.08/liter

Even though the new system has much more volume and surface area at cryogenic temperature than the previous Bevatron cryopumping system, heat loads are estimated to be only slightly greater than those formerly experienced at the Bevatron for the earlier cryopanels. This is because superinsulation is interposed between most 12°K and 80°K surfaces, and between most 80°K and 300°K surfaces, except at louvered pumps which are the principal 80°K heat loads. Since these louvered pumps have approximately the same pumping speed for the guard vacuum as the present cryopanels, they also have approximately the same heat load.

E4.2 Estimated Vacuum Performance

Estimates of gas loads, pumping speeds and resulting pressures (in the absence of ion beams) were presented in LBL Report PUB-5023 (revised November 1979), "High Intensity Uranium Beams; Preliminary Design Report and Technical Description." It was estimated that the pressure in the guard vacuum region would be comparable to that previously achieved (~10^{-6} Torr) in the Bevatron prior to this project, and that the azimuthally-averaged pressure within the new cold-bore liner should be less than 10^{-10} Torr. As the design for the new cold bore progressed, the assumptions behind these estimates were changed, but the conclusion still remained that pressures of the order of 10^{-10} Torr would be achievable.

E4.3 Ion Beam Considerations

The preceding section presented the anticipated vacuum performance in the absence of ion beams. Investigations of several possible, but unlikely, ion beam phenomena have also been made. Their effects on vacuum performance are discussed below.

E4.3.1 Primary-Ion Gas Desorption

Gas desorption from the interior surfaces of the new Bevatron cold bore caused by impingement of primary ions has been analyzed.

The most significant loss of primary ions will occur during injection into the Bevatron. To capture 10^{10} injected ions into the Bevatron orbit, it formerly was the practice that some 10^{11} additional ions from the injector were lost during the process. Some particles were injected early and some late, resulting in beam striking on the outer and inner beam aperture limits. Three

turns after injection, the injected beam focuses near the inflector location, and some particles are lost on the inflection septum. As part of this project, these injection losses have been reduced by improved timing and design of injection components.

An upper estimate of the number of gas molecules that might be desorbed due to injected ions lost on inner chamber surfaces is given in Table E-2. Two cases are shown, one for a Ne^{+10} beam and one for a U^{+70} beam. The calculations assume that the ions pass through one-hundred monolayers (probably an overestimate) of adsorbed nitrogen and then stop in a metal substrate. The estimate would be similar for adsorbed CO, H_2O or CO_2. It is assumed that all of the ion energy loss in traversing the N_2 monolayers is fully used to desorb molecules with an activation energy of 1.0 eV/molecule. It is also assumed that no energy is transferred from the metal substrate up to the gas monolayers to produce thermal desorption. This appears reasonable since heat from a thermal spike in the metal need travel transversely only a few tens of molecules to reduce the temperature rise to negligible values.

The roughly 50 m^3 interior volume of the new Bevatron cold bore contains 2×10^{14} molecules. If the upper estimate of 4×10^{14} molecules desorbed by Ne^{10+} (the more intense beam of the two examples) should all be released, the number of gas molecules, primarily H_2O, CO, H_2, O_2 and CO_2, in the beam path would triple. All but H_2 will refreeze on the 12°K inner wall after a transit time of ~7 ms from wall to wall. This is a very short portion of the full Bevatron acceleration cycle, but since most of the charge-exchange loss of accelerating ions occurs soon after injection (~50 percent loss in the first 50 ms), it still amounts to a time-averaged equivalent pressure rise of ~5 percent of the peak value or 6×10^{-11} Torr equivalent. Since the pressure in the absence of beam is very low by comparison, it is seen that even this upper-bound gas burst can be tolerated without exceeding the vacuum design goal.

During acceleration and extraction, some additional ions are lost onto the walls. However, the amount of gas desorption due to these losses is negligible by comparison because there are many fewer ions lost, and those that are, being of higher energy (lower dE/dx), each lose less energy while traversing the assumed one-hundred monolayers of adsorbed gas.

TABLE E-2: UPPER ESTIMATE FOR NUMBER OF GAS MOLECULES DESORBED BY PRIMARY IONS LOST DURING INJECTION INTO THE BEVATRON

Accelerator ion species	Ne^{10+}	U^{70+}
Particles per pulse accelerated in Bevatron (estimate)	10^{10}	10^{8}
Particles per pulse lost at injection (estimate)	3×10^{10}	3×10^{8}
Injection energy (MeV/A)	8.5	8.5
Total energy loss in traversing 100 monolayers of N_2 (MeV)	0.014	0.36
Upper bound on number of gas molecules desorbed per incident primary ion for activation energy of 1.0 eV/molecule	1.4×10^{4}	3.6×10^{5}
Upper bound on number of gas molecules desorbed per pulse	4×10^{14}	1×10^{14}
Time-averaged circumferentially-averaged equivalent pressure (293°K) in cold bore due to upper bound desorption (Torr)	6×10^{-11}	2×10^{-11}

Note: Based on normal entry of incident ions into 100 monolayers of frozen nitrogen on a metal substrate. Assumes all energy absorbed in N_2 goes into 1.0-eV gas desorption and no energy transfer from metal to nitrogen. (See text.)

E4.3.2 Secondary-Ion Gas Desorption

Gas desorption by secondary ions has become well known in proton storage rings such as the CERN Intersecting Storage Rings (ISE). In this mode, a stored circulating ion strikes a residual gas molecule and ionizes it. The stored circulating beam constitutes a positive potential well which accelerates the gas ion to the vacuum chamber wall. Under certain conditions, this can result in the desorption of many gas molecules per incident ion. Study has indicated that its occurrence is unlikely, primarily because the positive-potential well of the ion beam at the Bevatron is on the order of only a few volts, while that at the CERN ISR is on the order of a few kilovolts. Even if it were to be a problem, the walls of the cold bore function as an excellent pump for any gas molecules that might be desorbed.

E5 INITIAL PERFORMANCE RESULTS

This section sets forth the initial performance of the Bevatron Vacuum Improvement project that was observed during the first few months following installation. These results should be viewed as interim, since it is anticipated that the performance will continue to improve in the coming months. Emphasis has been placed on getting the Bevatron into prompt use for nuclear science and biomedical experiments, which has permitted measurement of only a few of the most important parameters.

E5.1 Vacuum Results

The first pump down of the new system commenced on December 17, 1981. On December 20, the cryogenic systems were turned on, and three days later the helium-cooled surfaces were at cryopumping temperatures (<20°K). Using the ion gauge readings in the north, east, and south tangent regions, combined with the presumption that the 12°K cold-bore sections were at very low pressure, led to the conclusion that the mean pressure around the Bevatron was about 4×10^{-10} Torr. Having achieved the technical goal of the project, the cryogenic systems were turned off for the holiday shutdown.

In early February, 1982, the Bevatron was again evacuated and cryogenically-cooled, and ion beams were accelerated. A definitive test to measure the effective vacuum in the Bevatron was undertaken as follows. Ions of C^{4+} are

known to charge exchange readily with residual gas, and their charge-exchange cross sections have been established at the SuperHILAC. Therefore, C^{4+} ions were injected and accelerated to the same energy as for the SuperHILAC experiments and then flat-topped at that energy to observe the rate of loss of ions. This test established that the average vacuum in the Bevatron at the time of this test was ~1×10^{-9} Torr. The ion gauge readings on the north, east and south regions accounted entirely for the 1×10^{-9} Torr average pressure, so the pressure in the 12°K cold-bore sections of the quadrants and the west tangent region must have been very low, likely below 10^{-11} Torr.

In early March, 1982, the Bevatron was evacuated and the cryogenic systems were cooled down preparatory for delivery of ion beams to experimental programs. The apparent pressure in the Bevatron was 2×10^{-10} Torr, which is entirely acceptable for accelerating all planned ions, including uranium.

E5.2 Cryogenic Results

It takes approximately three to four days to cool down the cryogenic circuits. The cryogenic heat load on the helium refrigeration circuits is well within the available refrigeration capacity. It has been established that, after cooldown, the helium refrigeration systems still function well when only four compressors and two refrigerators (one-half of installed capacity) are operating. In this mode, the helium supply and return temperatures are less than 8°K and 10°K respectively, which indicates that tje heat load is very small. It appears that it will be standard practice to operate with only half the units running and the remaining half on stand-by, available for use if the in- service units should need to be taken off-line for servicing.

E5.3 Ion Beam Results

In early February, 1982, ion beams of C^{6+} and C^{4+} were injected into the Bevatron and accelerated internally. The Bevatron then was shut down for adjustment of some of the components required for extraction.

Starting in early March, 1982, the Bevatron again was evacuated. Ion beams were not only accelerated but were also extracted for delivery to the experimental areas. On March 6, the Bevatron experimental program resumed with steady delivery of ion beams to a scheduled experiment. In the ensuing three weeks, beams were delivered for both biomedical and nuclear science research,

including delivery of ion beams of p^+, $^4He^{2+}$, $^{12}C^{4+}$, $^{12}C^{6+}$, $^{20}Ne^{10+}$, and $^{84}Kr^{33+}$. Acceleration of Kr was not possible prior to the vacuum improvements. Subsequent operation has produced beams of $^{93}Nb^{37+}$, $^{129}Xe^{45+}$, $^{197}Au^{61+}$, and $^{238}U^{68+}$ of intensities quite adequate for the experiments performed.

Tuning the heaviest beams has been facilitated by the use of tracer ions; i.e., lighter, partially stripped ions with Q/A's closely matching those of the desired heavy beams (e.g., $^{56}Fe^{16+}$ for $^{2348}U^{68+}$, and $^{55}Mn^{17+}$ for $^{197}Au^{61+}$). The heavy beams are stripped at the top of the transfer line so a broad range of charge states (and rigidities) is injected into the line making tuning very difficult. The tracer ion beams are not stripped at the end of the SuperHILAC, and therefore are quite clean. The transfer line, Bevatron injection, acceleration, and extraction are all tuned with the tracer so that when ions are switched at the SuperHILAC, the correct charge state of the heavy beam is automatically selected, and passes through the whole acceleration process with a minimum of additional tuning.

It is noteworthy that this tuning technique is made possible by the superb vacuum present in the Bevatron, since the electron cross sections for the unstripped tracers are substantially higher than those for the heavier stripped ions. Thus vacuum-induced beam losses are much more severe for the tracers. The fact that these tracers are accelerated with no visible beam attenuation is another tribute to the success of the project.

E5.4 Conclusions

The technical objective of 10^{-10}-Torr-range vacuum in the Bevatron has been attained ahead of schedule and within budget, and the Bevatron is now back in service delivering an unrestricted range of ion beams, from protons to uranium, to experimenters. Thus, the project has successfully achieved all of its goals.

This report was done with support from the Department of Energy. Any conclusions or opinions expressed in this report represent solely those of the author(s) and not necessarily those of The Regents of the University of California, the Lawrence Berkeley Laboratory or the Department of Energy.

Reference to a company or product name does not imply approval or recommendation of the product by the University of California or the U.S. Department of Energy to the exclusion of others that may be suitable.

TECHNICAL INFORMATION DEPARTMENT
LAWRENCE BERKELEY LABORATORY
UNIVERSITY OF CALIFORNIA
BERKELEY, CALIFORNIA 94720